UNIVERSITY OF NAIROBI

EVALUATION OF RESERVOIR PRODUCTION TRENDS IN OLKARIA GEOTHERMAL FIELD

BY

LUTI GEORGINA

I56/11563/2018

A Dissertation submitted in partial fulfilment of the Requirements for the award of the Degree of Master of Science in Geology of the University of Nairobi

2020

DECLARATION

I declare that this dissertation is my original work and has not been submitted elsewhere for examination, award of a degree or publication. Where other people's works, or my own work has been used, this has properly been acknowledged and referenced in accordance with the University of Nairobi's requirements.

Sign ……. Date ……

Luti Georgina

I56/11563/2018

Department of Geology

University of Nairobi

This dissertation is submitted with our approval as research supervisors.

	Sign	Date
Dr. Josphat Mulwa	….....	……..

Department of Geology,

University of Nairobi

P.O. Box 30197-00100

Nairobi, Kenya

jkmulwa@uonbi.ac.ke

	Sign	Date
Dr. Lydia Olaka	……	……..

Department of Geology,

University of Nairobi

P.O. Box 30197-00100

Nairobi, Kenya

lydiaolaka@gmail.com

DEDICATION

I would like to dedicate this dissertation to my mother and my late father who encouraged me to pursue my academics and to my family for their continuous and unwavering support.

I would also want to acknowledge all the assistance and well wishes from my friends and workmates.

ACKNOWLEDGEMENTS

I would like to thank the University of Nairobi for granting me a scholarship which enabled me to further my studies and to the Department of Geology staff for all the guidance and training opportunities they provided. The research was made possible by funds from the Volkswagen Foundation to L.O. Project 89369.

Special thanks to my supervisors, Dr. Josphat Mulwa and Dr. Lydia Olaka for their guidance and advice during the research and write up of the dissertation.

I am also grateful to Peter Ndirangu, Ruth Wamalwa, Urbanus Mbithi and Kennedy Mativo of the Kenya Electricity Generating Company (KenGen) Ltd for the geothermal training opportunity in Geology, Geochemistry and Geophysics and the production and geochemistry research data they provided.

ABSTRACT

Geothermal wells are requisites for monitoring changes within a geothermal reservoir. Some report an increment in production whereas majority have declined resulting in changes in chemistry, enthalpy and pressure, boiling and drying up of the reservoir and the destruction of production equipment which caused a drop in production and economic losses. The study area was the Olkaria Geothermal Field located in the Kenyan Rift Valley. Due to its location along the rift axis, it is associated with a high geothermal gradient with the heat source occurring below the volcanoes. Since 1981 when production wells were drilled in Olkaria, there has been decline in steam production which was managed by reinjection of brine and drilling of make-up wells. However, decline still occurs at a gradual rate due to the fact that the causes have not been well studied. Objectives included: assessment of trends of retired geothermal wells before their decline, determination of trends of production geothermal wells and identification of declining production wells and prediction of future fluid production of the production geothermal wells. Data from seven production and two retired geothermal wells from East and North-east fields (2005-2015, 1985-2000 and 1990-2005) were subjected to time series and trend curve analysis of geochemical as well as physical parameters, correlation and decline curve analysis using R Studio, Grapher, and MS Excel. Through the use of trend graphs, key reservoir parameters were monitored during the production history thus enabling the determination of the causes of the trends of these parameters and identification of mitigation measures to reduce the decline of production wells. Furthermore, the graphs also helped to narrow down potentially declining geothermal wells which were subjected to further study to determine their future performance. Retired geothermal wells trends displayed repeated cycles in all their parameters apart from Mg (stable with peaks). All the North-east production wells' trends displayed repeated cycles whereas the East production field wells had varying trends: Well Head Pressure (WHP)- rising; enthalpy- rising (26), declining (29) and repeated cycles (30); Cl- declining (26 and 30) and rising (29); SiO_2- repeated cycles and Mg- stable (26), declining (29) and repeated cycles (30). Changes in production wells were attributed to sub-surface processes such as boiling, influx of cool waters, adiabatic cooling, silica scaling and recharge of hot geothermal fluids. Relationships existing between chosen wells varied from weak to very strong but no two production wells were identical whereas parameters revealed moderate correlation between WHP and enthalpy and Enthalpy and Mg. Trends revealed one declining production well (OW-26) with an annual decline rate of 3.66% which is expected to reach its economic limit in 2047 whereas OW-709, 713, 720 and 728 had constant production and OW-29 and 30 had rising trends of production. Major challenges to production are mixing and silica scaling which can be mitigated through hot reinjected brine while its decline can be attributed to overproduction and the inflow of cooler waters. Decline curves are thus suitable for the prediction of the future production and rate of decline of the production wells through use of normalized steam flow rate and trend analysis.

TABLE OF CONTENTS

LIST OF SCHEMES/ FIGURES

LIST OF TABLES

LIST OF ABBREVIATIONS/ ACRONYMS AND SYMBOLS

a.s.l.: above sea level

D: Nominal decline rate

De: Effective monthly decline rate

ESIA: Environmental and Social Impact Assessment

GENZL: Geothermal New Zealand Limited

IFC: International Finance Corporation

KenGen: Kenya Generating Company Limited

MWe: Megawatt electric

Np: Cumulative production

P/Z: Pressure/ Gas deviation factor

Q: Production rate

Q_i: Initial production

R^2: Total number of squares over the sum total of squares

SDGs: Sustainable Development Goals

t: Time that has elapsed

TDS: Total Dissolved Solids

TS: Time Series

W: Rate of production

W_n: Normalized rate of production

WHP: Well Head Pressure

CHAPTER ONE: INTRODUCTION

1.1 Background Information

Geothermal energy is heat energy created and stored within the earth. Geothermal prospects are mapped in volcanic areas with the highest temperatures occurring along plate boundaries (IFC, 2013). Its popularity has been growing in recent years because it is a clean, readily available, affordable, renewable and indigenous source of energy that is not susceptible to adverse weather conditions (Mukeu and Langat, 2016) and hence can be utilized in electricity generation, recreational functions such as pool heating, green house operations and industrial purposes (Çakin, 2003).

This energy is utilized in over seventy countries and produced by twenty-four countries such as: United States, Indonesia, Philippines, Turkey, Mexico, Iceland and Kenya (Gehringer and Lokshav, 2012); some of which are described in the table that follows (Requejo, 1996; Truesdell et al, 1984; Regalado, 1981 and Ofwona, 2011).

Table 1.1 General characteristics of geothermal fields located around the globe

FIELD	TECTONIC SETTING	LITHOLOGY	GEOCHEMISTRY	TEMPERATURE
Bacon Manito, Philippines	Compressional	Basalts, andesites, breccias and limestones	Low amount of Non-Condensable Gases and neutral Chloride content	260-283°C
Cerro Prieto, Mexico	Extensional	Shales and sandstones	Varying levels of Chloride content	260-340°C
Reykjanes, Iceland	Extensional	Breccias, pillow lavas and basalts	Varying levels of salinity and high Calcite content	250-290°C
Olkaria, Kenya	Extensional	Trachytes, basalts, pyroclasts and comendite	Alkaline, Chloride rich and gas depleted	340°C

Monitoring geochemistry, temperature and flow measurements during exploration, development and utilization reveals any changes within the reservoir that could consequently affect operations and subsequently production. The chemistry of the fluids is dependent on temperature and the equilibrium that exists between the minerals and water hence any changes will cause a disequilibrium which occurs at a much faster rate with respect to chemistry as compared to the physical parameters (Gunnlaugsson, 2008). Exploitation and utilization of geothermal resources has resulted in some geothermal systems reporting an increase in production whereas others have experienced a decline.

Geothermal fields which have reported an increment in production during their operation history and the measures they undertook to increase production are as follows: Olkaria East field which used make-up wells and deepened existing production wells to 2200m from the initial 900m (Ofwona, 2011); Olafsfjordur field, North Iceland undertook pumping, deepening of production wells to 1169m and drilling of 1500m deep production wells (Shterev, 1994); Kamojang field, West Java drilled make up wells and used reinjection wells converted from unproductive geothermal wells (Sasradipoera et al, 2000); Geysers field, United States carried out infill drilling and expanded the feed to the power plant by using make-up wells (Ripperda and Bodvarsson, 1987) and Larderello field, Italy developed the shallow Calcium carbonate ($CaCO_3$) reservoir having wells 1000m deep, drilling deeper production wells and reinjecting condensed steam into the reservoir (Razzano and Cei, 2015).

The geothermal fields which underwent a decline in production are: Olkaria East from 45 to 31 MWe during 1981-1994 (Ofwona, 2011); Wayang Windu, Java from 30 to 17.5 MWe over 1998-2011 (Aditya and Jantiur, 2013) and Geysers field from 2000 to 850 MWe over 1989-2016 (Hidayat, 2016).

Decline of geothermal systems is caused by cooling, corrosion and scaling.

Cooling of the reservoir is attributed to reinjection due to cooler recharge (Mariaria, 2012), fluid mixing (Mwarania, 2014) or boiling which causes pressure and enthalpy/ temperatures to drop, the chemistry to change (Haizlip, 2016 and Gunnlaugsson, 2008) and corrosion and scaling to occur. Cooling caused a drop in: Chloride (Cl) concentration in Cerro Prieto (Truesdell et al, 1984) and Fluoride (F) and Silica (SiO_2) concentrations and temperature by 20°C in Reykjavik geothermal field, Iceland (Gunnlaugsson, 2008).

Corrosion eats away protective films and forms pits on equipment rendering them less effective in the supply and harnessing of geothermal energy (Stănășel, 1996 and Opondo, 2007). Corrosion is caused by water containing dissolved Oxygen (O_2), Carbon dioxide (CO_2) or high Cl concentration at a pH < 8.5 and temperatures < 100°C which indicates its temperature dependent. When a reservoir is subjected to continuous boiling, it dries up and the steam gains extremely high temperatures (Haizlip, 2016) with an increase in the concentration of salts that speeds up catalysis (Gunnlaugsson, 2008). Complete depletion of brine in Krafla, Iceland was characterized by a prominence of dissolved components in steam based on data collected from 1981. The steam underwent superheating and upon cooling and condensation, Hydrogen chloride (HCl) gas was deposited and ultimately caused corrosion (Truesdell et al, 1984) whereas corrosion in Reykjavik was caused by O_2 present in precipitation (Gunnlaugsson, 2008).

Scaling forms a coating within production equipment and limits the supply of fluid to the plants. It entails the precipitation of SiO_2 and $CaCO_3$ due to high rates of withdrawal which cause a decline in pressure and leads to boiling with the vapor phase forming in a liquid dominated reservoir. Scaling then occurs since the changes in temperature and pressure cause disequilibrium (Haizlip, 2016). Additionally, mixing of the reservoir fluid with cold water causes $CaCO_3$ to increase in concentration whereas SiO_2 remains in solution until its amorphous solution is attained and once this is attained, the concentration in the reservoir starts dropping (Gunnlaugsson, 2008). A production well in Cerro Prieto underwent scaling which resulted in its decline (Truesdell et al, 1984) whereas the geothermal field in West Java province reported a decline of 26% between 1987 and 1991 in some of its geothermal wells due to scaling (Sasradipoera et al, 2000 and GENZL, 1992).

The study area is the Olkaria Geothermal Field located in the Central sector of the Kenyan Rift Valley as shown in figure 1.1. It has more than two hundred geothermal wells, an associated production of 570 MWe and a capacity of 1500 MWe (Omenda and Simiyu, 2015). Decline has been observed since exploitation started with some of the associated problems being mitigated but conclusively, the field still reports a gradual decline (Ouma et al, 2016).

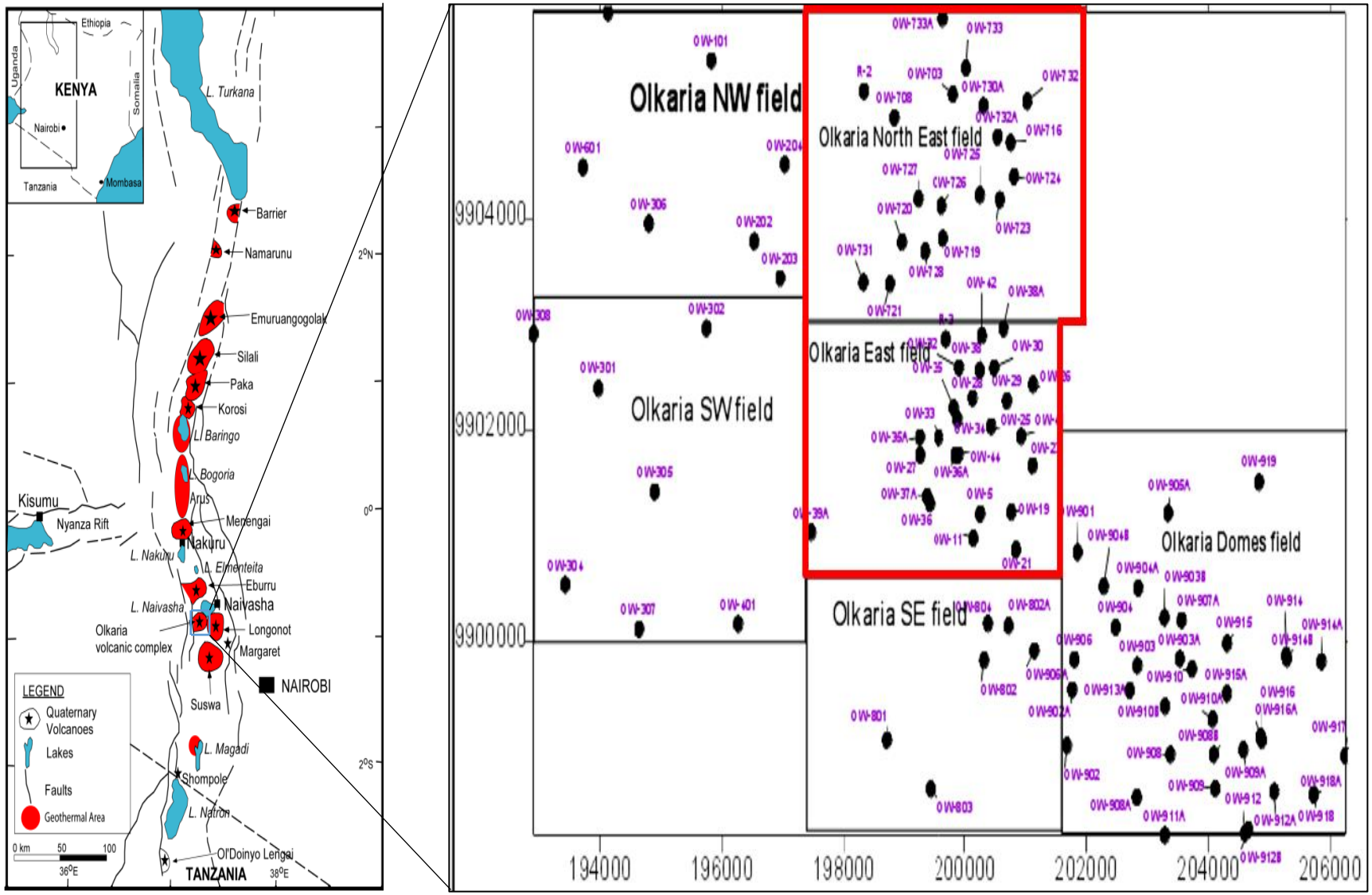

Figure 1.1 Location of Olkaria Geothermal Field with respect to Kenyan Rift Valley, its sectors and respective geothermal wells with the highlighted region indicating the study area- East and North-east fields (Okoo, 2013 and Wamalwa et al, 2016)

1.2 Problem Statement

The Olkaria geothermal field experiences decline in power and steam production just like other fields located all over the world (Aguilar et al, 2012; Aditya and Jantiur, 2013 and Hidayat, 2016). The first fields to undergo exploitation are the East and North-east sectors and they have undergone the most decline in pressure and hence production (Ofwona, 2011; Mariaria, 2012 and Ouma et al, 2016). This decline has been managed by injecting or reinjecting brine and condensed steam back to the reservoir but since most of the fluid being used is at a lower temperature, the production wells may actually experience an accelerated rate of decline due to corrosion, scaling and cooling caused by elements and compounds precipitating.

Other factors which had contributed to decline were the inclusions of the liquid-phase of the reservoir which is associated with lower enthalpies (Ofwona, 2002). As the geothermal wells began producing, decline rates of up to 5.5% were recorded but started to reduce over the years due to make up wells and reinjection. The cold reinjection has been limited due to its negative effects with hot injections being the preferred choice. Despite the decrease in steam decline (from 5.5% to less than 4%), steam decline rates increased to 4.6% in 1998 (Ouma, 2008).

The declining production wells had displayed a drop in both steam production and reservoir pressures with some of the production wells demonstrating brines' concentration increment yet low enthalpies were being recorded (Wamalwa, 2017). Conclusively, the decline in the geothermal field is gradual and it has been predicted by various models that used numerical simulations (Bodvarsson and Pruess, 1987; Ouma, 2008 and Axelsson et al, 2013). There are spatial differences in decline that are worth investigating and for planning the economic development of the field.

The research project aimed at comparing the physical and geochemical trends of two retired and seven production geothermal wells from the East and North-east production fields. The physical parameters used were Well Head Pressure (WHP) and enthalpy and geochemical parameters Cl, SiO_2 and Magnesium (Mg).

1.3 Aim and Objectives

Aim

To develop predictive trends for mitigating geothermal production decline in order to solve the decline of production of the reservoir and promote growth and production within the trachy-rhyolite dominated Olkaria geothermal field.

Objectives

i. To assess production and decline trends of retired geothermal wells over a period of fifteen years (1985-2000 and 1990-2005) before their decline.
ii. To determine the trends of production geothermal wells and identify those with declining trends.
iii. To predict the future fluid production of the declining production geothermal wells.

1.4 Justification and Significance of the Research

Geothermal energy is a readily available and reliable source of energy for the country that is required for both domestic and industrial purposes (Gehringer and Lokshav, 2012). As part of the Sustainable Development Goals (SDGs), goal number seven aims at providing clean and affordable energy; of which geothermal energy meets the criteria due to its inexpensive, renewable and non-toxic character during both extraction and utilization (Mukeu and Langat, 2016 and https://www.undp.org/content/undp/en/home/sustainable-development-goals/goal-7-affordable-and-clean-energy.html).

Fossil fuels are the most commonly used sources of energy but they produce greenhouse gases that cause global warming and in the mitigation of the production of these gases, reduction of fossil fuels' use is being encouraged (Çakin, 2003). This is only possible if there is an alternative clean source of energy such as geothermal energy that will aid in the mitigation of climate change (SDG goal number thirteen) and subsequently prevent the change and/or destruction of ecosystems (Johnson and Ogeya, 2018 and https://www.undp.org/content/undp/en/home/sustainable-development-goals/goal-13-climate-action.html).

It is important to monitor geothermal systems through the use of geochemical and physical parameters in order to reveal trends of the reservoir's behavior to exploitation and help infer about the processes occurring at depth (Gunnlaugsson, 2008 and Barragán et al, 2016). Probable causes

or challenges being experienced in the production wells and the reservoir can be identified and then addressed in order to subsequently boost the current production from the field and increase the production life of these geothermal wells (Ouma et al, 2016). This means that not only will there be production of clean affordable energy but also surplus production that will address the country's current energy needs and their growing demand (Mukeu and Langat, 2016).

1.5 Study Area

1.5.1 Location and Description

Olkaria Geothermal Field is located in the Central part of the Kenyan Rift Valley which extends from Northern Tanzania to Lake Turkana in a N-S trend. It is located north-west of Nairobi, west of Longonot, north of Mount Suswa and south of Lake Naivasha and Ol Doinyo Eburru complex. The geothermal field which is in Naivasha sub-county, Nakuru county is located between latitude 0°53'9"S and longitude 36°16'12"E and latitude 0°54'57"S and longitude 36°18'48"E (Mutia, 2010) at an elevation of 2000m above sea level (a.s.l.) (Wamalwa, 2017).

Olkaria occupies 204km^2; within it is the Olkaria geothermal field that covers about 140km^2 consisting of the area covered by the resource, its infrastructure and areas not under exploitation (Mariaria, 2012 and Wamalwa, 2017). For ease of development, the geothermal field has been subdivided into seven sub-sectors with respect to the Olkaria hill namely: Olkaria South-west, Olkaria North-west, Olkaria North-east, Olkaria East, Olkaria Central, Olkaria Domes and Olkaria South-east (Koech, 2011).

The geothermal field is located in Hells' Gate national park (Muchangi and Kagweni, 2014) as shown in figure 1.2 hence human population is limited in number for ecological and climatic reasons due to the intrusion and destruction caused by its activities. The main community occupying the area is the Maasai who are nomadic pastoralists (Karanja and Ngare, 2016).

The infrastructure of the area includes: Moi South lake road, four Olkaria plants and their rigs' sites, well pads, an airstrip and a railway line that is under development.

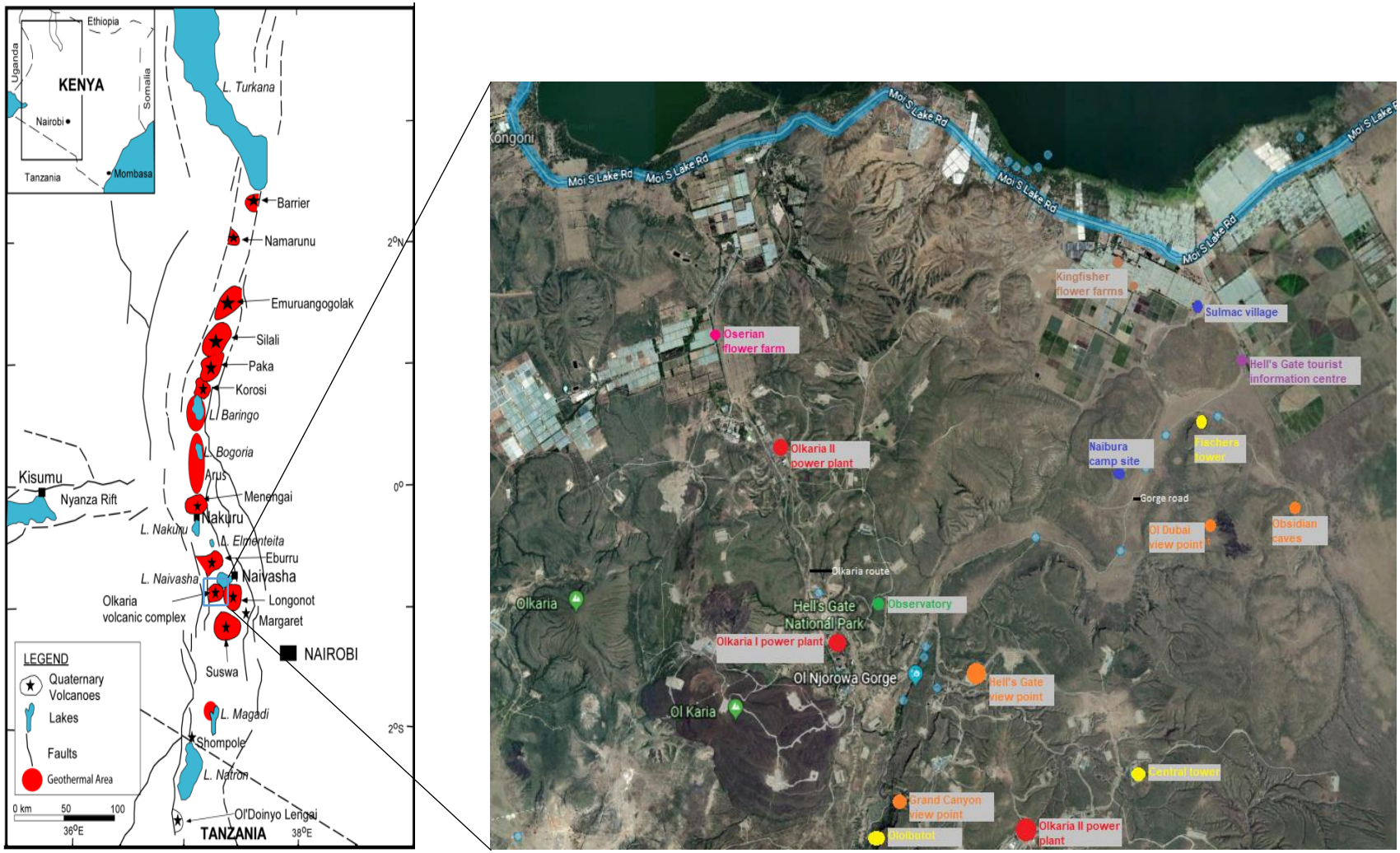

Figure 1.2 Kenyan Rift Valley displaying location of Olkaria Geothermal Field and its physiography, infrastructure and surroundings indicated by spots: red (power plants), yellow (physiography), orange (view points), green (observatory), blue (hotels), pink and brown (flower farms) and purple (tourist centers) (Okoo, 2013 and Google earth, Accessed: July, 2019)

1.5.2 Climate

Olkaria Geothermal Field's climate is under the influence of topography and altitude (Sombroek et al, 1982). The escarpments on either side of the rift act as barriers affecting the patterns of wind and rainfall with descending winds becoming warmer and denser whereas a rise in altitude is characterized by a drop in temperature and pressure.

High temperatures are experienced with the maximum ranging from 24.6 to 28.3°C while minimum temperatures of up to 9°C have been encountered. February records the highest temperature whereas July records the coolest with mean monthly temperatures ranging from 18 to 19.4°C (Wamalwa, 2017). Rainfall depends on the movement of Inter-Tropical Convergence Zone (ITCZ) with long rains occurring from March to May and short rains in the October-November season (Sombroek et al, 1982). The average annual rainfall received is 634mm due to the shadowing effect by escarpments (Kollikho and Kubo, 2001). Humidity is less than 75% and the rate of evaporation exceeds that of precipitation by a factor of 2 or 3 every month apart from April (Muga, 2012). Winds are weak and quite prevalent during August and October with no particular flow direction (Ogola, 2004).

Conclusively, Olkaria Geothermal Field is warm and dry and classifies as semi-arid or Agro-climatic Zone V (Sombroek et al, 1982).

1.5.3 Vegetation

The vegetation is dominated by *Acacia drepanolobium* which occurs in a canopy that has an average height of 20m, bushes and grass species such as *Pennisetum clandestinum* and *Themeda triandra* with the latter being the dominant variety according to an Environmental and Social Impact Assessment (ESIA) conducted in 2009. Additionally, a sage referred to as *Fimbristylis exilis* is also present together with an invasory indigenous species referred to as *Tarconanthus camphoratus*. Due to its semi-arid nature, cactus and euphorbia are also observed whereas papyrus and a weed *Silvania molesta* are characteristic around and within the lake (Ogola, 2004).

1.5.4 Land Use and Land Resources

Olkaria has a wide diversity of uses for its land and resources. The surrounding areas are used for floriculture as represented by greenhouses shown in figure 1.2 whereas the lake hosts a large variety of wildlife and hence acts as a tourist attraction popular for sailing, swimming and boat

rides whilst providing water for the municipality, geothermal fields, irrigation and wildlife (Muga, 2012).

1.5.5 Physiography and Drainage

Olkaria Geothermal Field has a wide variety of physiographical and drainage features as shown in Figure 1.2. It appears to be uneven due to piles of volcanic rocks with the elevation ranging from 2400m at Olkaria hill to 1600m at Akiira ranch (Muga, 2012).

The physiographical features include: a caldera complex of which the field is a remnant part of (Naylor, 1972), Quaternary volcanoes such as Olkaria hill and Hobley's, rhyolitic volcanic plugs such as Central tower and Fisher's tower and at least eighty volcanic cones/centers located along Ololbutot fault, Gorge farm fault, the ring structure and Olkaria hill (Clarke et al, 1990 and Marshall et al, 1998).

There are also rhyolitic and pumiceous domes (Ofwona, 2011) which have steep sides composed of lava and pyroclasts either occurring as isolated or conjoined to form ridges with Olenguruoni hills, Gilgil plateau, Mau and Kinangop escarpments, Kinangop plains, Hells' gate gorge and fumaroles next to Hobley's volcano also characterizing the area. Hydroclastic craters are located north of the Domes and associated with explosions in the subsided country (Clarke et al, 1990; Mungania, 1999 and Mabwa, 2010) whereas the valleys such as Kedong are responsible for draining slopes and run off.

The drainage features of the area include: hot springs, boreholes such as Mai Mahiu, Florensis and Jikaze and steam jets along Ol'Njorowa gorge, Maiella and east of Olkaria with the sulphurous kind being found west of Olkaria hill (Karanja and Ngare, 2016 and Onacha, 1989). Additional drainage features located in the surroundings of the study area include: permanent rivers Gilgil and Malewa whose source is the Nyandarua Mountains, seasonal rivers which include Karati and a papyrus swamp located around Lake Naivasha (Muga, 2012).

1.5.6 Geology and Structures

The geology of the area is dominated by trachytes, rhyolites, pyroclasts and basalt (Clarke et al, 1990) as shown in Figure 1.3. The tuffs in the area are either lithic or vitric with the former containing trachyte or basalt fragments and deposits of $CaCO_3$ whereas the latter contain pumice, glass and secondary SiO_2 infilling. The rhyolites furthermore have a low percentage of

phenocrysts, are glassy and their flow banding occurs at a low angle whereas the basalts contain phenocrysts of olivine and plagioclase within a matrix of plagioclase (Wamalwa, 2017).

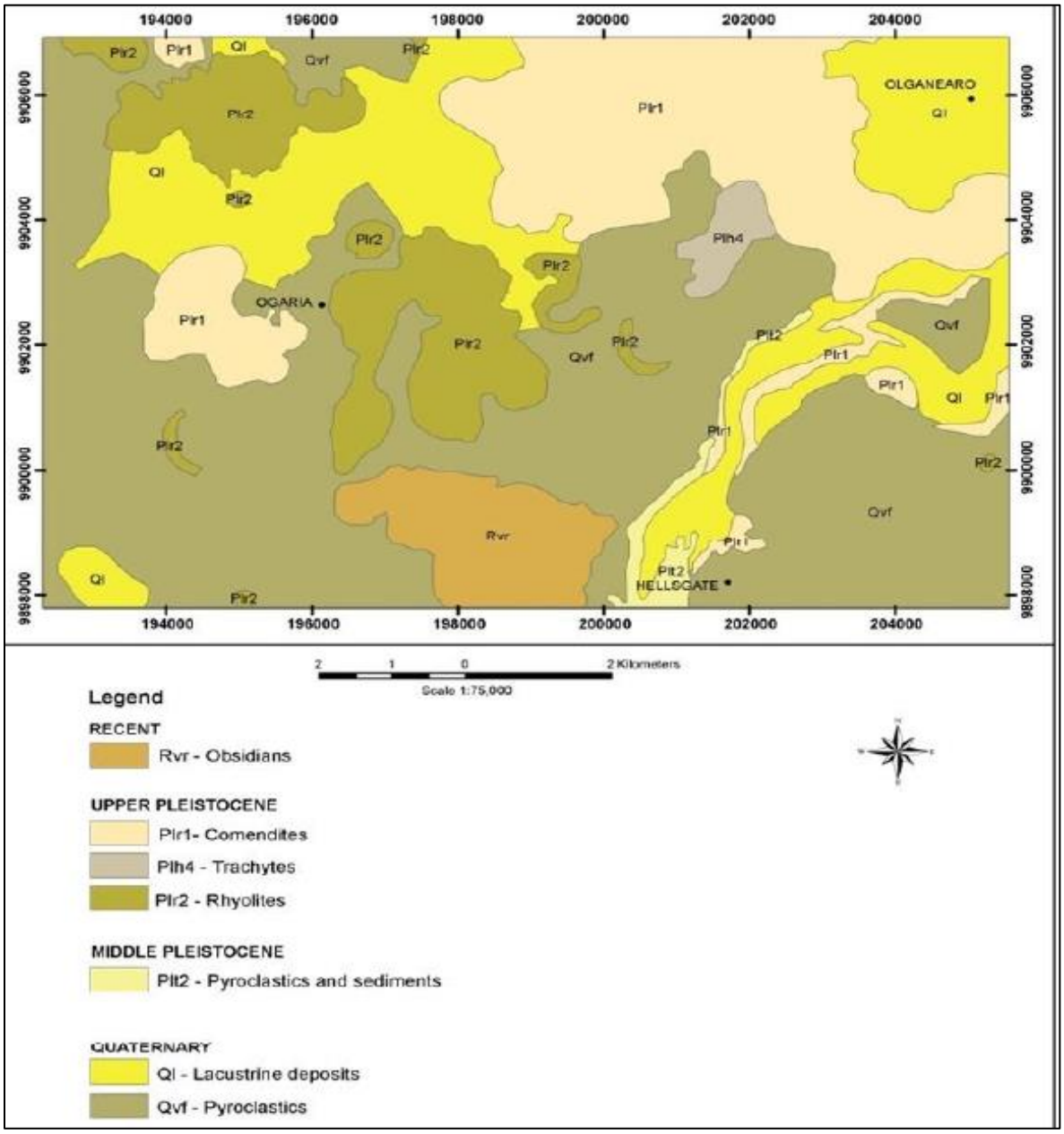

Figure 1.3 The general geology of Olkaria Geothermal Field (Wamalwa, 2017)

The lithological units are classified based on tectonics, age and stratigraphy (Karingithi, 2000) from the lowest to the highest as follows:

Basement: Mozambique mobile belt schists and amphibolites (Shackleton, 1986) with an age > 590Ma and a depth of 5-6km (Simiyu et al, 1995). The basement is cut through by intrusions

ranging from syenite, granite to basalt (Baker and Wohlenberg, 1971) which have been dated to late Pleistocene-Holocene (<1.8Ma). An unconformity which overlies the basement is followed by the Pre-Mau formation.

Pre-Mau formation: visible on the scarps of the southern sector of the rift (Omenda, 2000) and composed of basalts, trachytes, ignimbrites and phonolites. This formation is dated < 10Ma.

Mau tuffs: occur west of the Olkaria hill due to a normal fault with a high angle and a dip in the eastern direction (Omenda, 1994). They are characterized by an ignimbrite to consolidated texture and consist of trachytes, basalts and rhyolites dated 4.5-3.4Ma which were followed by faulting and graben formation.

Plateau trachytes: occur at 1-2.6km depth east of the hill (Ogoso-Odongo, 1986) with an age of 2.1-1.8Ma and consist of tuffs, basalts and rhyolites.

Olkaria basalts: composed of basalts, trachytes and pyroclasts (Clarke et al, 1990) with 100-500m thickness and serve as the cap rock (Haukwa, 1984). This was followed by a magmatic hiatus due to grid faulting in the rift valley. The basalts are dated < 1.65Ma.

Upper Olkaria volcanics: occurred in six stages (Baker et al, 1971) which were characterized by caldera collapse, eruptions, extrusions and formation of ring domes. They consist of comendite, pyroclasts, limited trachytes, basalt and ash from Longonot and Suswa (Omenda, 1998) from the surface to a depth of 500m with the youngest being the Ololbutot comendite 180±50yr. BP (Clarke et al, 1990) whereas the other rocks are dated 0.95Ma.

The stratigraphy in the geothermal field is demonstrated in Figure 1.4.

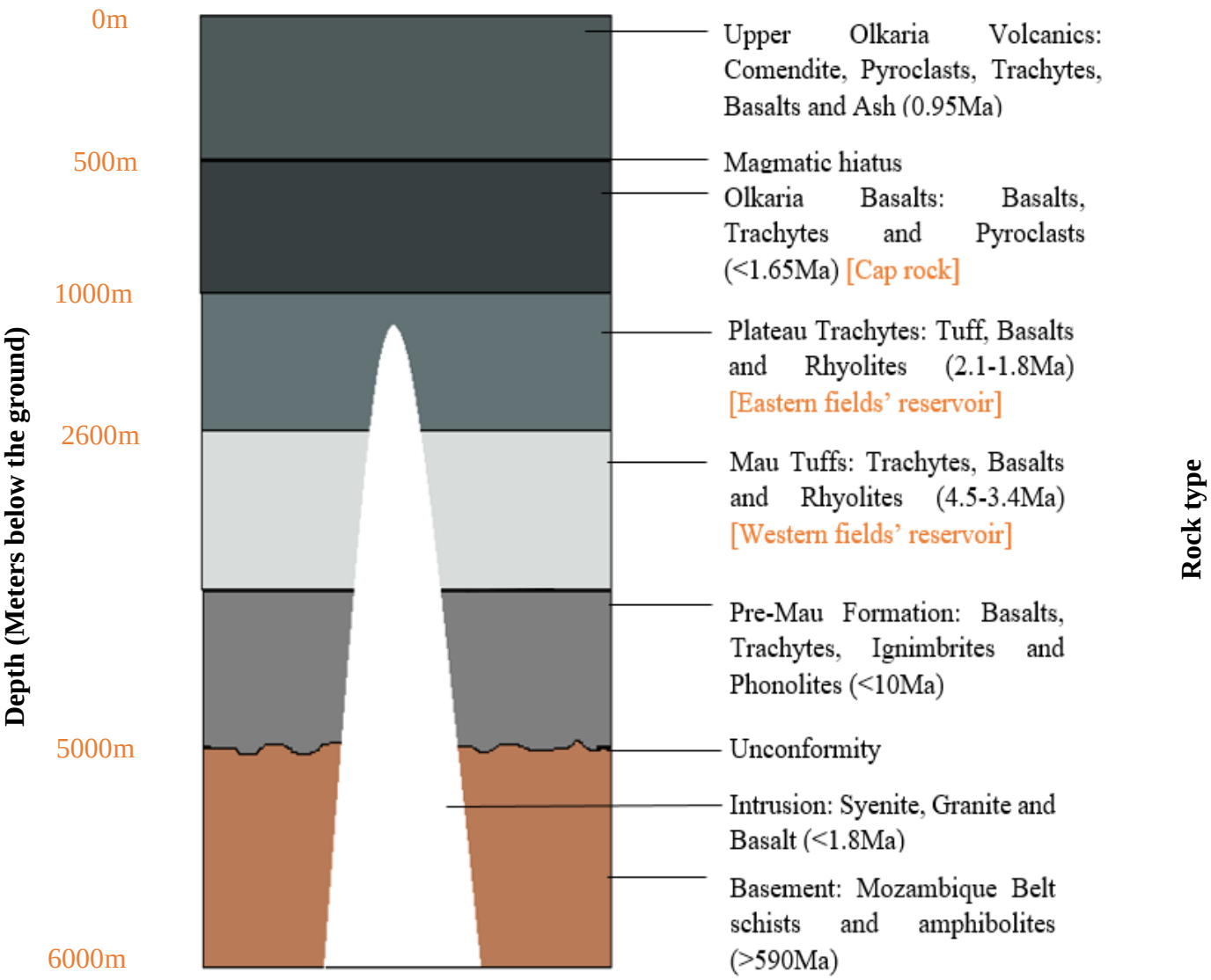

Figure 1.4 A stratigraphic profile of Olkaria Geothermal Field

Dominant structures in Olkaria Geothermal Field include: faults, ring structure, fissures and fractures as shown in figure 1.5.

The faults which are all normal trend: N-S, NE-SW, E-W, ENE-WSW, NW-SE, NNE-SSW, WNW-ESE and NNW-SSE. NW-SE and WNW-ESE trending faults are the oldest and associated with graben formation whereas the rest are younger and affect flows in Holocene (Lagat, 2004). The faults are observed in the North-east, East and West fields and limited in the Domes due to the thick pyroclasts cover (Muchemi, 2000). Some of the faults include: Ololbutot fault (associated with obsidian and rhyolite flows, has a N-S trend and separates Eastern and Western fields), Ol'Njorowa gorge (bounds Olkaria Domes to the west), Gorge farm fault (bounds the North-

eastern field up to the Domes and may extend to Lake Naivasha (Lagat, 1995)) and the Olkaria fault (ENE-WSW trend which transects the most productive fields namely Western and North-eastern).

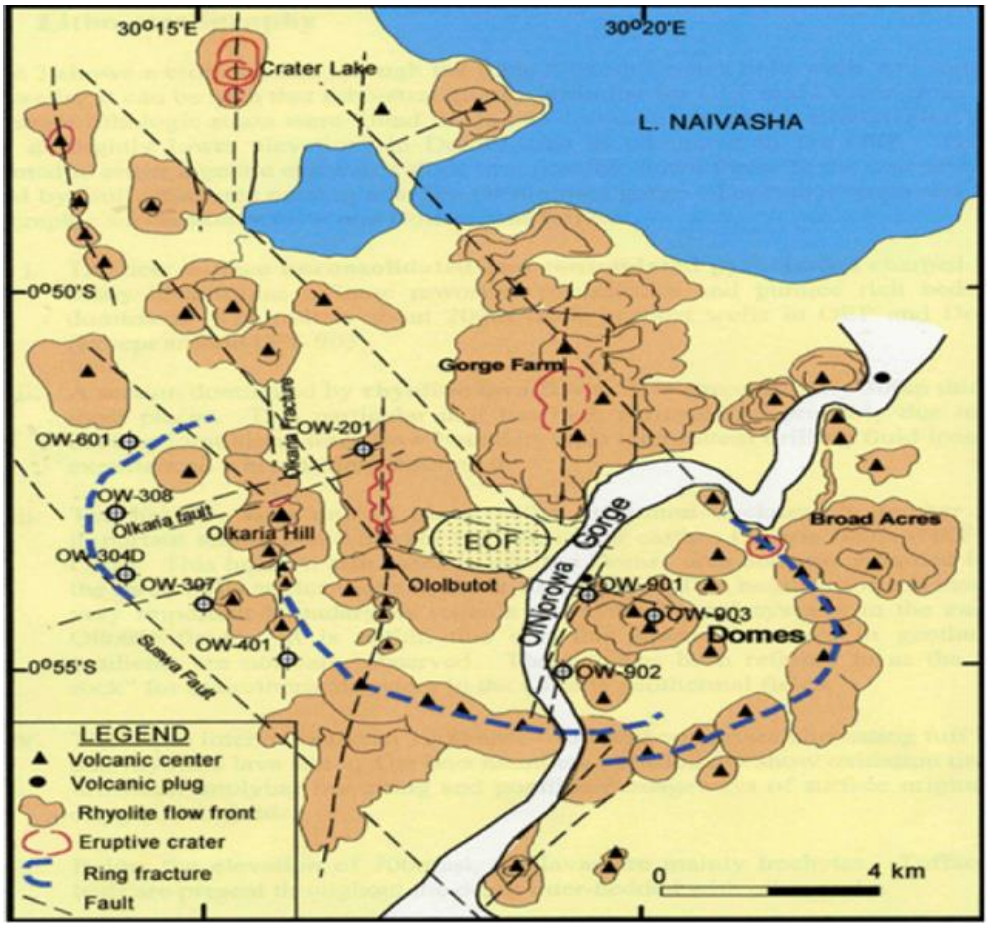

Figure 1.5 A structural map of Olkaria Geothermal Field with some geological context (Okoo, 2013)

There also include: fractures such as Olkaria, fissures and dikes which occur in swarms along Ol'Njorowa gorge up to a depth of 2000m with a NNE trend and the ring structure which is composed of arcuate faults that surround the reservoir (Koech, 2011).

Hydrogeology is influenced by faults, fractures and porous volcanic rocks on the rift flanks and axis with the grid faults being responsible for the transport of water from the scarps to the axis before the water travels deeper (Ofwona, 2002). Recharge is by rift shoulders which have greater elevation (Abebe, 2000) with the dominant structures being Olkaria and Ololbutot faults and Olkaria fracture. Boreholes have shallow water tables at the lake but deepen southwards indicating

that the hydrological gradient causes water to flow north-south; parallel to the axis (Clarke et al, 1990; Onacha, 1989 and Ouma, 2008).

1.5.7 Soils

Olkaria Geothermal Field is dominated by volcanic soils which are porous. These soils come from volcanic rocks such as basalts and rhyolites with ashes having pumiceous fragments originating from Suswa and Longonot (Clarke et al, 1990). These ashes form an unconformity with conglomerates as a result of erosion by seasonal streams in the area. The soils are characterized by good drainage, limited depths, dark brown color with ferrous content, high $CaCO_3$ amounts and form either clay or loam. They are hence classified as lithosols with calcic xerosols (Atkilt, 2001).

Additionally, the surface is also covered by sands, pebbles, gravels and boulders of pumice and comendite obtained from Ol'Njorowa. The sand is located on plains and comes from the gullies due to fluviatile action whereas lacustrine sediments are observed near the lake and result from the reworking of ashes. These soils which occur in layers become loose in the dry season and become susceptible to erosion (Muga, 2012).

1.5.8 Surface and Ground Water Resources

Surface water

Lake Naivasha which is prominent in the area covers an area of 145km^2, Oloiden- 5.5 km^2, Crescent island- 2.1 km^2 and Sonachi- 0.6 km^2. Lake Naivasha which is a fresh water lake with no surface outlet and a depth of 8m has its water levels depending on the amount of precipitation whereas the Crescent Island is at a depth of 18m hence qualifying as the deepest section of the Lake Naivasha basin (GIBB Africa Ltd, 2014 and Muga, 2012). Rivers Gilgil and Malewa are both perennial and account for input into the lake by 20% and 80% respectively (Lukman, 2003). The latter is the dominant river of the area whereas the seasonal streams are usually responsible for the gully erosion observed on hill slopes.

Geothermal groundwater resources

Groundwater in Olkaria Geothermal Field uses grid faults as its conduits because they aid axial and lateral flow. These faults are classified as being open due to their high activity (Allen et al, 1989) with water travelling to great depths (1000m) evidenced by the presence of Boron (B) (Clarke et al, 1990). The groundwater resources of the area include:

The geothermal reservoir is widest in the south and narrows northwards. It is two-phase in the southern section with a steam cap and one phase in the northern section (Ambusso and Ouma, 1991) and the water level ranges from 400-700m. It is dated to 0.9-1.65Ma and highly fractured with hot up flow occurring in Olkaria East, North-east and West fields, north-west of Domes and the ring structure. Steam is lost along Ololbutot fault between geothermal wells where cold inflow also takes place with no flow occurring south of Olkaria East field (Ouma, 2008). The reservoir occurs in plateau trachytes in Olkaria East and Mau tuffs in Olkaria West (Omenda, 1994) and its water may originate from Lake Naivasha through leaking in the sub-surface (Sikes, 1935) accounting for two thirds whereas the rest is from precipitation.

An aquifer exists and it is connected to the geothermal field through NE-SW structures at a depth of 1050-1400m a.s.l. within tuff and trachy-rhyolites and it subdivides into three zones based on stratigraphy: 1050-1350m a.s.l., 200-250m a.s.l. and 50-120m below sea level (b.s.l.) (Agonga, 1992).

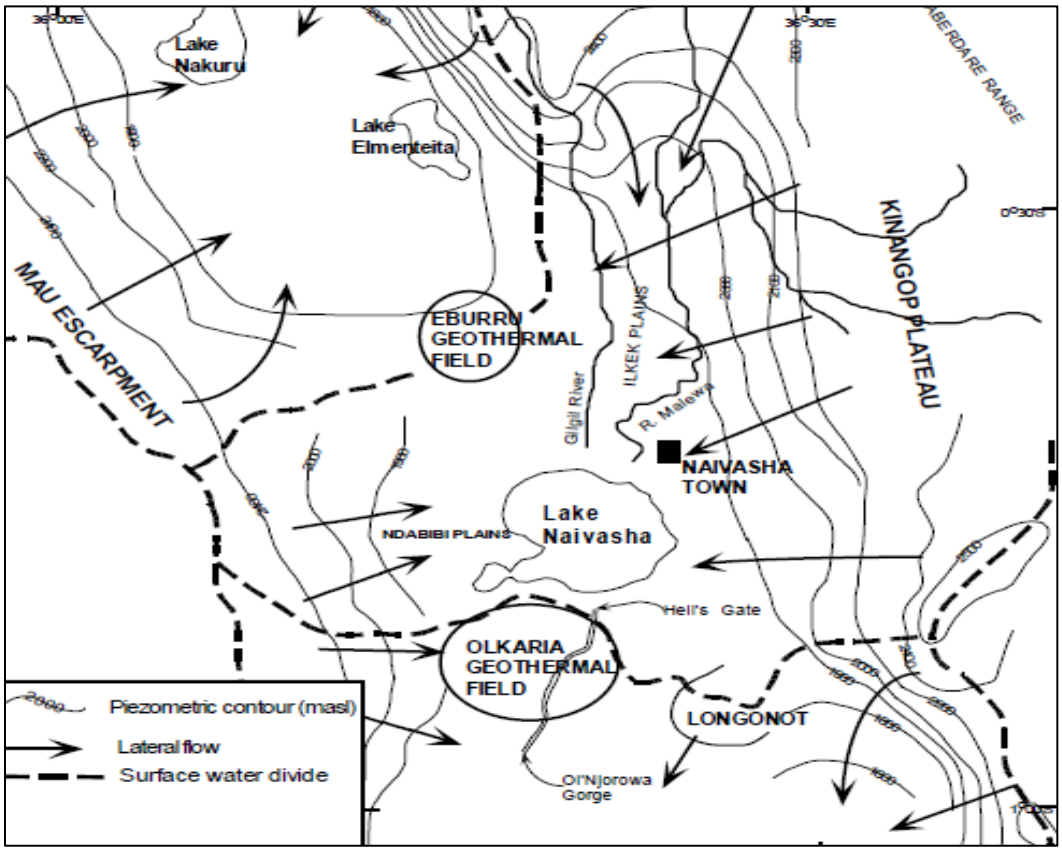

Figure 1.6 A piezometric map of the area demonstrating groundwater flow patterns (Clarke et al, 1990)

CHAPTER TWO: LITERATURE REVIEW

The literature reviewed pertained to Olkaria Geothermal Field's Geology focusing on its Rock types, Structures and Features and Stratigraphy; Geochemistry and Characteristics of its Geothermal Resource.

2.1 Geology

2.1.1 Rock types

The geology of the Geothermal Field is characterized by peralkaline extrusive volcanic rocks such as trachytes, rhyolites, basalts and volcanic ejecta (Clarke et al, 1990) and warm, altered grounds. These rocks occur in a belt with a N-S trend (Lagat, 1995) and originate from volcanic centers dating back to the Quaternary with magmatism having commenced in Late Pleistocene extending up to recent times (Okoo, 2013). Despite the mapping of centers in Olkaria, more information is required with respect to the actual sources of these volcanic materials and the processes involved in their formation.

Observed outcrops are comenditic in nature but lack good representation due to coverage by pyroclasts (Muchemi, 1982) which occur in strata and are overlaid by ash and pumice (Okoo, 2013).Trachytes which tend to undergo slight alteration occur mostly at great depths with sanidine phenocrysts and a mafic content of amphiboles and pyroxenes within a microlite groundmass (Lagat, 1995). The trachytes grade in texture with the shallow ones being coarser and the deeper ones being the finest (Agonga, 1992) while the rhyolites appear from 44m depth up to 1122m whilst alternating with other lithologies. They also display a grading mechanism opposite that of trachytes (Lagat, 1995), a resistance to alteration and a prominent occurrence of fluorite phenocrysts which mark a depletion and enrichment of various trace elements. Six of the volcanic groups have these phenocrysts which occupy up to 16% of the lava with Light Rare Earth Elements (LREEs) being more abundant than Heavy Rare Earth Elements (HREEs) (Marshall et al, 1998). Further research is required to account for the significant depletions and enrichments of trace elements within the rhyolites and the high ratios of water to Fluoride.

The basalts occur within the 480-576m interval and contain phenocrysts, secondary depositions, a limited number of vesicles and varying levels of alteration; mostly prominent along olivine phenocryst cracks whereas the tuffs occur in thin layers within volcanic rocks apart from 638-840m depth where they occur as a massive formation and are susceptible to alteration which varies

with the depth in which they occur (Lagat, 1995). The acidic tuffs occur at shallower depths relative to the basalts (Wambugu, 1996) while the 44m thick oxidized pyroclasts consist of pumice and discontinuous glass laminations due to welding.

Apart from volcanic rocks, Olkaria is also associated with some lacustrine sediments that were deposited during minimal to no volcanic activity (Mariita, 1986). Due to the location of Olkaria in an active geothermal system, hydrothermal activity and hence alteration is quite common. The 550m depth is marked with hydrothermal alteration whereas above it, oxidation dominates apart from fumarole and fracture zones. Chlorites are common in basalts which contain $CaCO_3$ and epidote indicating possible reversals of temperatures due to the presence of the latter below its stability temperatures or epidote making up the lithology of basalts (Muchemi, 1982). The reversals need validation so as to determine whether the reservoir has undergone/ is undergoing a major change or whether epidote makes up the lithology of basalts in Olkaria Geothermal Field.

2.1.2 Structures and features

Magmatic and tectonic activity occur in a NE trend along the rift floor (Lagat, 1995) hence characterizing the geothermal field with a variety of structures and features. These include: normal faults, ring structure, gorge, aquifers, caldera, vents, craters, intrusions and veins.

Some of the faults include: Suswa lineament, Gorge farm fault, ENE-WSW and N-S trending faults, NNW-SSE and NW-SE dipping faults. The Suswa lineament has a NW-SE trend and transects the Ol'Njorowa gorge (Odongo, 1993) while the Gorge farm fault trends WNW-ESE (Wamalwa, 2017). The Olkaria fault trends ENE-WSW as evidenced by shallow seismicity and fumarole activity (Agonga, 1992) and a branch of it controls temperatures in the middle of the geothermal field which is associated with hot water up flow which then flows laterally. This up flow leads to boiling and forms a zone of steam which is restricted at 1400m a.s.l. by a cap rock (Ouma, 1992).

The N-S faults which are located on the floor of the rift have undergone reactivation and are responsible for hydrogeological flow along the axis and shallow recharge with bounding faults controlling flow to greater depths. Additionally, they are associated with volcanism that led to the formation of an underlying network of dykes (Karingithi, 2000), geothermal manifestations (Wamalwa, 2017) and pumice and rhyolite flows observed in Ol'Njorowa gorge as they traverse

the remainder of the caldera (Naylor, 1972). An example of these faults is the Ololbutot which has been associated with shallow seismic activity (Simiyu and Keller, 2000).

The NNW-SSE and NW-SE dipping faults are rift faults located on the Mau escarpment and they control hydrogeology with some reported as being active (Karingithi, 2000) with seismicity associated with these faults occurring on either side of Ololbutot (Simiyu and Keller, 2000) whereas the ring structure has been linked with the swarm of dykes underlying the caldera (Karingithi, 2000) and infer to the presence of the latter (Odongo, 1993). This structure is also involved in hydrogeological control and considered a zone of permeability based on fumarole activity along its faults (Agonga, 1992).

The Ol'Njorowa gorge started forming through faulting and down cutting due to overflow from Lake Naivasha and is characterized by plugs and dykes (Okoo, 2013). Olkaria Geothermal Field is located in a tectonically active region hence further investigation is required to determine which of the faults in the area and surroundings are still active or are prone to reactivation. Additionally, the area has sub-surface faults which also require mapping since they affect hydrogeology of the area.

The prominence of fracture and faults systems and piles of volcanic rocks (Ouma, 1992) encourage the development of aquifers with minor aquifers occurring at 950, 1500, 1800, 2250 and 2750m depths, the intermediate aquifers at 750 and 1100m depths and the major aquifer at 2100m depth (Okoo, 2013). Various studies reveal different number of aquifers in the geothermal field hence an accurate investigation of the actual number of aquifers present should be carried out and incorporate the use of geophysical surveys to determine causes of circulation losses.

The Olkaria Geothermal Field is said to occur within an inferred caldera (Wambugu, 1996) supported by the presence of ignimbrite and the chemistry of lavas and domes forming at its points of weakness (Okoo, 2013). Furthermore, the geothermal field is said to be a remainder of this caldera (Naylor, 1972) with the eastern side of the caldera having vents arranged in a concentric manner to form a ring structure whereas the western side has hills forming depressions (Mertz and McLellan-Virkir, 1979). Inference to the presence of a caldera has been debated thus geological and geophysical mapping is required to conclusively determine whether the caldera actually exists.

Vents are present in the area along the ring structure and N-S faults (Wamalwa, 2017) and associated with the observed craters. The craters are hydroclastic and linked to eruptions in the subsided country and act as trace of caldera rim (Okoo, 2013). Additionally, intrusions which are most likely dykes occur as swarms. They include: rhyolite at 1674m, syenite at 2170m, basalt at 2252, 2504 and 2914m and granite at 2992m depths (Okoo, 2013). The prominence of the volcanic activity indicates the magmatic nature of the rift but further study needs to be carried out to determine the size and extent of the magma chamber(s) responsible for the volcanic rocks present in the area.

Veins are also key features in the area due to the volcanic activity and they have a wide range of thicknesses occurring in proximity to fissure zones, trachytes and basalts with more than one mineral occurring within a vein such as calcite, epidote and quartz (Lagat, 1995).

2.1.3 Stratigraphy

The stratigraphy of Olkaria Geothermal Field is sub-divided into the basement and overlying volcanic rocks which are 3.5km thick. In general, there is a dominance of lavas with pyroclasts at and near the surface followed by trachytes, basalts and rhyolites and their respective tuffs to 1122m depth with the trachytes and their tuffs dominating the rest of the underlying stratigraphy (Lagat, 1995). Layers appear successive but their thickness is non-uniform throughout the field (Ouma, 1992).

From the surface to 500m depth, the Quaternary pantellerites, comendites and the Suswa and Longonot pyroclasts dominate dating back to 250±100 yr. BP and are referred to as the Upper Olkaria volcanics (Wambugu, 1996). They are sub-divided into: 0-14m pyroclasts, 14-208m rhyolite tuffs and flows, 232-368m rhyolite tuffs, 374-414m basalt tuff and flows and 400-500m trachytes. The underlying Olkaria basalts include: 500-700m basalts, tuffs and trachytes and 700-1000m trachyte, rhyolite and basalt flows and basalt tuffs.

The Plateau trachytes are the Eastern fields' reservoir (Okoo, 2013) and consist of:1000-1200m rhyolite and basalt and trachyte tuff, 1200-1500m trachytes and rhyolite intervals, 1550-1602m basalt tuff and flow, 1628-1674m trachytes, 1692-2054m basalt and trachyte and tuff, 2066-2148m trachytes and 2240-2600m trachyte with intrusions of basalt whereas the Mau tuffs act as the Western fields' reservoir (Okoo, 2013) and overlie the Pre-Mau formation with the bottom most unit being the basement (Agonga, 1992; Mwangi, 1982 and Okoo, 2013).

The stratigraphic units cannot be directly correlated from one location to another due to down throwing hence further investigation should be carried out on the sub-surface faults and the missing gaps in stratigraphy. Additionally, the stratigraphy clearly outlines the formations but detailed elaboration is required on the various components making up each of the formations, their thicknesses and respective ages.

Apart from lithology, stratigraphy can also be expressed in terms of alteration zones which are four in number (Lagat, 1995). They include: the smectite-zeolite zone with zeolite and smectite from 0-202m and temperatures less than 200°C, mixed layer clays zone with both clays and chlorite at 202-518m and temperatures of 200-230°C, illite-chlorite zone with chlorite and illite at 518-616m and temperatures from 230 to 250°C and chlorite-epidote zone having chlorite and epidote and temperatures exceeding 250°C (Okoo, 2013). The first alteration zone has low resistivity (Mariita, 1986) whereas the rest of the zones are marked with high resistance due to chlorite and epidote presence (Lichoro, 2009).

2.2 Geochemistry

The geochemistry of the Olkaria Geothermal Field fluids especially the North-east and East fields are characterized by Sodium Chloride (Na-Cl) waters. These waters are classified as being mature and indicate the existence of a water-mineral equilibrium with Cl values of 350-500 ppm and Na values of 330-400 ppm (Wambugu, 1996). Over time, the Cl concentrations have been declining with the North-east field recording the highest decline followed by the East field with values ranging 300-550 ppm and 170-700 ppm respectively. The East production field hosts the highest Cl concentrations in the area with both the North-east and East production fields having high Cl values due to deep hot up flowing brine with the latter also including boiling processes caused by contact with heated rocks. Despite the associated high Cl values, the geothermal field still ranks rather low as compared to other similar geothermal fields (Karingithi, 2000).

The decline in Cl concentration has been linked to drops in temperature but initially, the concentrations had risen due to reservoir boiling and deepening of production wells while decline was probably caused by a shift in zones of production and influx from the top and lateral directions of the reservoir (Wamalwa, 2017). Much of the focus has been on Cl values to indicate the change in reservoir conditions however, additional parameters are needed to validate the mentioned findings and the causes for the reported decline. The Cl values trend SE possibly due to dilution

similar to the trends in temperature and the faults (Wamalwa, 2015 and Wamalwa et al, 2016) with trend graphs needed to clearly display the changes in concentration for each of the fields over time based on their respective initial conditions.

The geothermal wells in the East and West production fields record high Chloride/ Boron (Cl/B) ratios due to the origin of the water being distant and the partitioning of B whereas low values occur near the reservoir rock representative of its fluids (Wambugu, 1996). High bicarbonate (HCO_3) content of 90-13000 ppm is observed and caused by the supply of CO_2 and carbonic acid (H_2CO_3)-mineral reactions (Karingithi, 2000). The high values of the gas are associated with proximity to the gas source; possibly the magma source and indicates the area has good permeability (Wambugu, 1996) yet the values tend to vary between the East, North-east and Domes field (Wamalwa, 2017) with the reasons behind it still unknown. Conclusively, the boundaries of the reservoir are characterized by the mixing of both Na-Cl and Na-HCO_3 waters (Ouma, 1992).

Hydrogen sulphide (H_2S) is also abundant due to its closeness to the magma chamber with limited conversion to sulphate ions (SO_4^{2-}) through oxidation whereas the nitrogen (N_2) abundance has been linked to atmospheric interference (Wambugu, 1996) but the interference can be confirmed by investigating the presence of O_2. Other explanations state that the gas occurrence is due to water external to the system recharging along Ol'Njorowa mixing with the brine (Wamalwa, 2017) with the trend being opposite that of Cl (Wamalwa, 2015). Conclusively, the quality of steam is good with 0.3% occupancy of gas (Ouma, 1992) which is highest in the domes trending towards the North-east then East production fields. The gases initially rose before dropping as a result of boiling processes (Wamalwa, 2017). The trend in gases follows a certain direction which requires further investigation to determine if it is based on the source or structural influences.

The fluid has moderate alkalinity, a pH of 8.1-9.9 (Karingithi, 2000) with the center of the field having the highest concentrations due to boiling resulting in a low steam content which mixes with other cooler fluids during up flow to condense and cause low Total Dissolved Solids (TDS) (Wambugu, 1996) and this makes corrosion unlikely to occur (Ouma, 1992). Olkaria Geothermal Field has an abundance of Oxygen-18 (^{18}O) and Deuterium (D) as compared to the rainfall received with a close proximity to the local meteoric line because of evaporation that occurs before the water infiltrates the geothermal system's bedrock (Karingithi, 2000). The field is also recharged

by Lake Naivasha based on isotopic studies with variations occurring with respect to the geothermal fluid due to the dissolution of minerals.

2.3 Resource characteristics

The capacity of the resource in Olkaria Geothermal Field is 80km^2 (Ouma, 2008) and is characterized by two-phase system production zones which are located at 600-800m (steam) and 800-900 and 1000-1100m (brine) and reservoir temperatures of 240-300°C (Wambugu, 1996). The segregation of phases in the aquifer has caused a surplus of enthalpy in the brine (Karingithi, 2000) yet only steam is used in electricity generation meaning a large component of energy remains untapped (Ouma, 2008).The trachytic reservoir is enclosed by arcuate faults that form the caldera (Ouma, 1992) which contains intrusions inferring the presence of a heat source. The general shape widens southwards and the pressure, temperature and hydrological gradient decrease southwards (Ouma, 2008) yet the causes for its shape and trends having not yet been identified. This reservoir contains multiple feed zones but most of the geothermal wells are shallow hence they risk a drop in temperatures and scaling by SiO_2 if the production wells undergo boiling (Wamalwa, 2017) whereas its two zones of up flow of hot fluid have a loss of steam as they move through fractures and faults. The static water level rests at 400-700m with its upper level in contact with a cap rock that is overlaid by saline water (Ouma, 1992).

Production is carried out in six of the sub-sectors. The Olkaria East field (Olkaria I) with temperatures of 102°C at 1000m depth has an associated production of 45 MWe: 15 MWe unit in 1981, 15 MWe unit in 1982 and a 15 MWe unit in 1986 (Ouma, 1992). It has a surplus steam potential of 25 MWe (Ouma, 2008) which is being tapped by two Additional Units of 70 MWe (Mbithi, 2011) whereas the North-east field (Olkaria II) has chemistry similar to that of the East field (Ouma, 2008), reservoir temperatures of 250°C and an up flow zone (Wamalwa, 2017). Total production of the field is 105 MWe (Mbithi, 2011): a 70 MWe condensing plant established in 2003, a 2.5 MWe binary plant in 2004 and in 2010, the field's 28 MWe and Olkaria East's surplus were simultaneously combined to be harnessed by a 35 MWe unit. Olkaria South-west (Olkaria III) has a production of 48 MWe: a 12 MWe binary plant in 2000 and 36 MWe in 2009 (Mbithi, 2011) whereas the Domes field produces 140 MWe with very high temperatures exceeding 300°C, a production of 2 MWe in Olkaria North-west (Oserian) and a 48 MWe plant in Olkaria West whose up flow system is separate from the others and contains abundant CO_2 (Ouma, 2008). The

East, North-east and South-west production fields qualify as the most explored in the Geothermal Field with the former two and the Domes sharing a connection which requires a scheme in order to maximize their efficient exploitation (Ouma, 2008).

Olkaria Geothermal Field has an abundant number of geothermal wells distributed throughout the sub-sectors. The Olkaria East field had forty-one geothermal wells by 2016 (Wamalwa et al, 2016): twenty-five production and two reinjection wells in 1982 (Wamalwa, 2017), twenty-seven production wells in 1992 (Ouma, 1992) and in 2016, twenty-two production and nine retired geothermal wells- two of which are used for hot reinjection with ten additional geothermal wells being drilled. Olkaria North-east field had a total of twenty-eight geothermal wells: twenty production, four hot reinjection (100%) and four monitoring (Wamalwa et al, 2016). Olkaria East's western and central section geothermal wells have been reported to being almost dry and the southern section is experiencing inversions of temperature due to influx of cold fluids (Ouma, 2008) which is also observed in Olkaria Central that is associated with medium enthalpy classifying it as a zone of outflow and hence used for reinjecting cold water. Despite the extensive development, better quantification of the resource and the potential of the fields need to be carried out.

Since exploitation commenced, pressure drops annually by 1 bar and its steam production decline together with that of TDS has been attributed to mixing with cooler waters (Wamalwa, 2017) occurring as follows: 1981-1988 by 5.5%, 1988-1992 by 4% and 1998 by 4.6%. In 1993-1998, there was rise in production and no decline due to connection of make-up wells, 1999-2000- steam supply increased by 1%, 2001- increase in steam production by 3-7% and 2002-2004- constant steam supply (Ouma, 2008). The decline seemed to be reducing yet it suddenly rose in 1998 prompting the inquiry as to the probable cause for this behavior. In 1992-2004, the enthalpy dropped due to drop in pressures which resulted in drying caused by boiling in production wells at the center of the field which were marked with an increase in TDS whereas the geothermal wells at the edge had a drop in enthalpy resulting from cold influx (reinjection) with a drop to stable concentration. Over the years, some of the production wells have recovered evidenced by an increase in Cl because of increasing the depths of the production wells (Wamalwa, 2017).

CHAPTER THREE: MATERIALS AND METHODS

3.1 Desktop Studies

Desktop studies entailed organization of geochemical (Cl, SiO_2 and Mg) and physical parameter data (enthalpy and WHP) of geothermal wells into their respective excel sheets to ease analysis and retrieval. Statistical analysis was undertaken to determine available parameters and completeness of the data sets, frequency of data collection and identification of gaps within the data set. From the gaps in the data set, areas that required additional data for analysis were identified.

Parameters and time periods for analysis were chosen followed by time series analysis using Impute Time Series (Impute TS) package to fill the gaps, trend curve analysis of retired and production geothermal wells using Grapher software and determination of the rates of change, statistical analysis for each parameter in all the geothermal wells and the extent of the similarity between the production wells using Microsoft Excel. Upon interpretations, the declining production wells underwent decline analysis using Excel Trend line tests and Arps formula and their future performance predicted.

3.2 Data

Secondary data obtained from KenGen's database was used consisting of data sets for two retired and seven production geothermal wells in the East and North-east sectors as highlighted in figure 3.1. All the geothermal wells chosen for the study were vertical wells which are characterized by lower productivity and shallower depth than the directional production wells which are inclined by certain angles in order to intercept zones of permeability such as faults and fractures that supply hot geothermal brine into the reservoir. The vertical geothermal wells hence cannot access zones of permeability especially if they are located in remote regions.

The data consisted of geochemical and physical parameters collected two to three times a year. The geochemistry data analyzed included: Cl, SiO_2 and Mg whereas the physical parameters were enthalpy and WHP.

The two retired Olkaria geothermal wells are located in the East production field and the productive data period chosen for each spanned fifteen years before they ceased production (1985-

2000 and 1990-2005) whereas the Production geothermal wells located in the East and North-east production fields were studied during the 2005-2015 period.

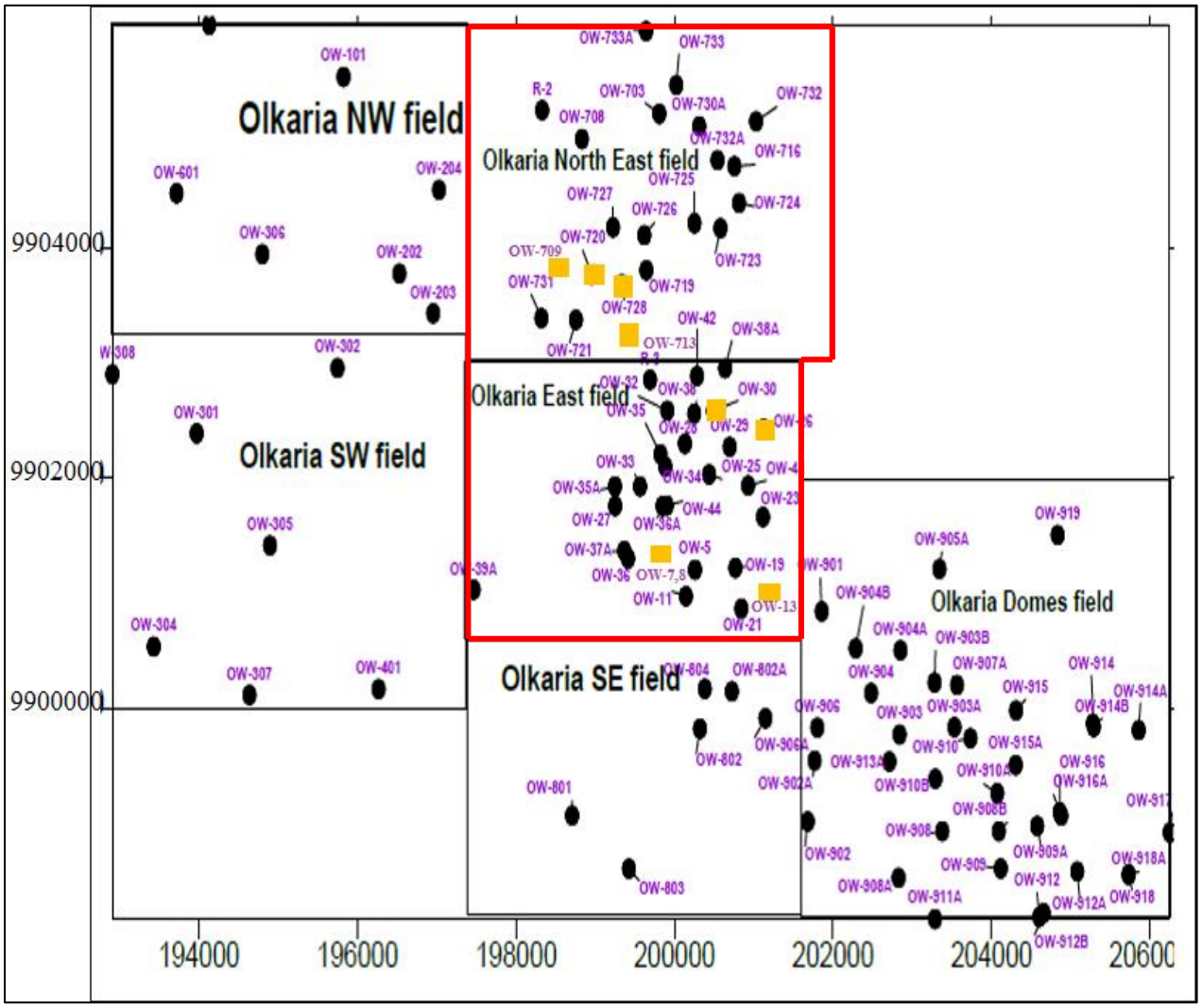

Figure 3.1 Highlighted study area with square shaped spots indicating the chosen geothermal production wells for study (Wamalwa et al, 2016 and Ofwona, 2005)

3.3 Data Analysis

3.3.1 Time Series Analysis

Time series analysis was carried out using Time series Imputation whereby gaps in the datasets of the physical and geochemical parameters over chosen study periods were filled. Data was entered into R script to create a time series in form of a vector using the code:

$$x < -ts(c(\,\boldsymbol{data\ values}), \boldsymbol{start} = \boldsymbol{c}(\,), \boldsymbol{frequency} =))\ldots\ldots\ldots \textit{Equation 3.1}$$

Where x is the name of the file, ts stands for time series, start represents when the data was first collected and frequency- number of times collection was done in the year. After creating the time series, interpolation was executed using Impute TS through linear interpolation. Results displayed all the values inclusive of those that were missing. It used the code:

$$\boldsymbol{na\_interpolation(x)}\text{.....}\ \textbf{\textit{Equation 3.2}}$$

Some of the examples are as shown below:

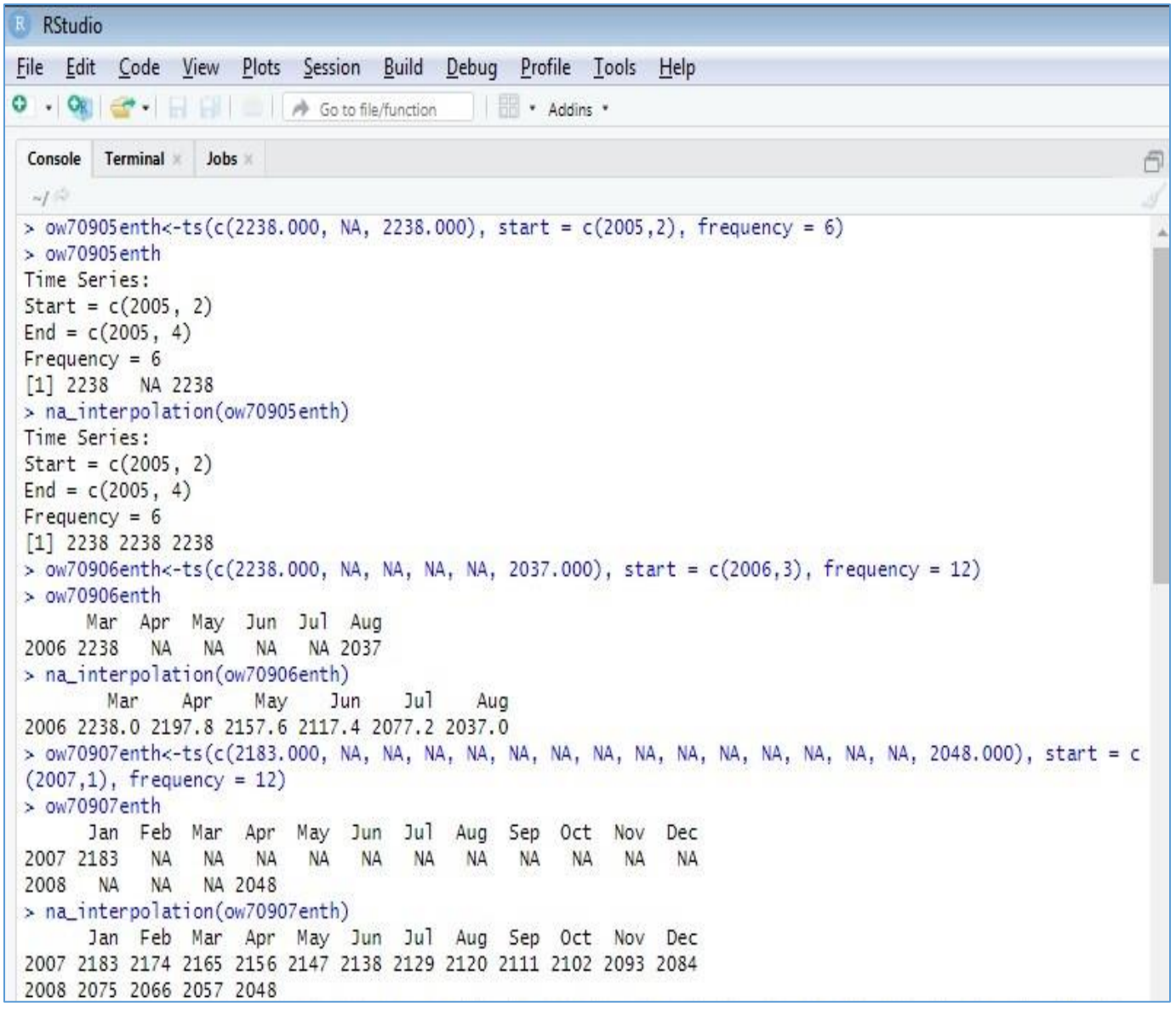

Figure 3.2 Time Series Analysis and Imputation for OW-709's enthalpy for the years 2005-2008

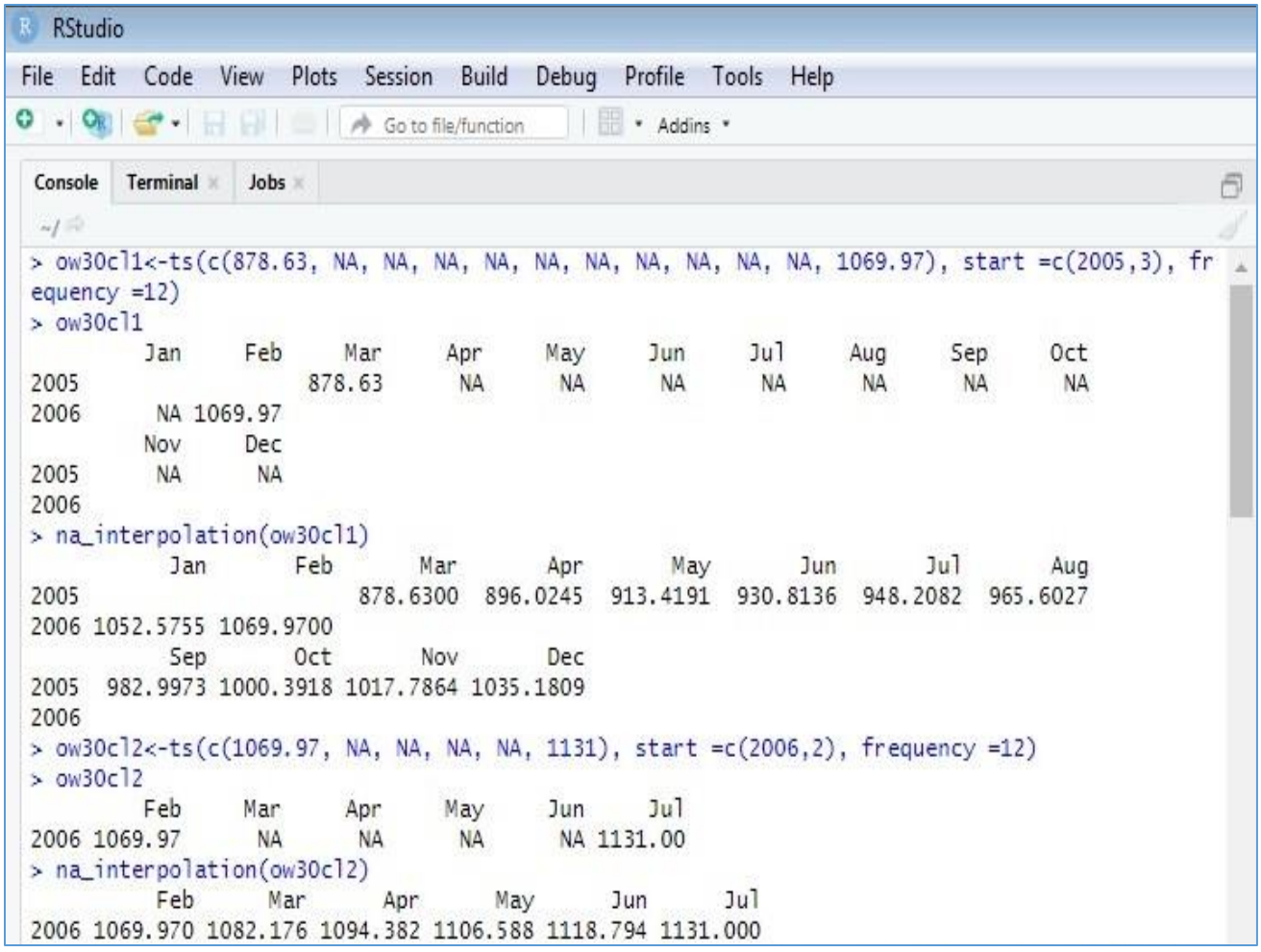

Figure 3.3 Time Series Analysis and Imputation for OW-30's Chloride concentration for the years 2005-2006

Impute TS was used on a univariate time series with linear interpolation suitable for single non-continuous gaps in data sets that lacked a strong trend and seasonality (Coghlan, 2018).

3.3.2 Trend curve analysis

Grapher (Golden software) was used to carry out trend analysis. The template consists of four windows: worksheet, plot, excel worksheet and grid. The worksheet modifies data files, excel sheets are obtained in the excel window, the grid window is used for grids while the type of graph plotted is displayed in the plot window.

In order to plot, the type of graph was chosen followed by selection of the file and plotting of the graph which was later modified with respect to title, axis and legend among others. Data was displayed on a Cartesian plot with parameter values accorded y-values with the time period along

the x-axis. Multiple production wells were plotted on one graph using different colors hence easing comparison such as in geochemistry which is very sensitive to changes.

Trends revealed the behavior of geothermal wells and reservoir to exploitation over time, performance of retired geothermal wells before they stopped production, rates of change and conditions in which the production wells were no longer suitable for production. Additionally, they assisted in comparison among production wells and retired geothermal wells and to each other based on their rates and trends with declining production wells being identified.

Trend analysis requires a minimum time period of five years. Grapher software uses various assumptions (linearity and independence) but sometimes it is observed that one or more of the variables may not fit into the predetermined assumptions.

3.3.3 Correlation analysis

The Data analysis sub-menu command of the Microsoft Excel package was used to compute correlation coefficients. This entailed quantifying the relationship for each production well with respect to the rest of the production wells for each parameter individually and for the relationships that exist between the individual parameters. For each parameter and production well, all the data spanning the ten-year period for each production well was incorporated into the same excel sheet. Using the DATA menu command, the DATA ANALYSIS sub-menu was selected and the CORRELATION tool used. The input range was then selected and the output range displayed on a separate worksheet.

The correlation coefficients are displayed as values and in order to identify closely correlated production wells and parameters, conditional formatting was used that entailed selection of a suitable range that would highlight the strongly correlated production wells and parameters.

The challenge associated with this method is that every parameter requires selection of a new range depending on the values generated during correlation with some parameters displaying very high coefficients or having values that are in close proximity to each other hence complicating the range for analysis.

3.3.4 Decline curves analysis

The Impute TS package, Grapher software and Microsoft Excel were used to evaluate the production and physical parameters and plot the trend of declining geothermal wells based on their

past and current performance and extrapolate their future values. The decline curves are used in geothermal monitoring and provide rates of decline of geothermal wells and fields with respect to pressure drawdown through the use of type curves. The prediction feeds into the most suitable formula such as: Arps, Fetkovich, Gentry and McCray, Influence functions, Slider's, P/Z versus Q and Linearized free surface-Green's function. The Arps method which is the most commonly used is based on a non-linear least squares method and calculates R^2 with $R^2 > 0.65$ enhancing confidence in extrapolated values (Requejo, 1996).

Once the declining production wells were identified, their production data was subjected to a time series analysis using the Impute TS package to fill in gaps for the chosen intervals in the study period. The data was then plotted using Grapher in order to validate the decline of the identified production wells. Based on the production and physical parameter plots of the declining production wells, data was selected on a 1-month interval for a period of a year targeting the end of the study period (2014-2015) where the decline in production history was observed. Normalization of production was executed using the following formulae:

$$W_n = \frac{(P^2 - Pstd^2)W}{P^2 - Pf^2}$$ (Reyes et al, 2006)……. ***Equation 3.3***

Whereby W_n: Normalized rate of production

P: Static/ Shut-in pressure

P_{std}: Standard flowing WHP

W: Rate of production

P_f: Standard flowing pressure

In order to determine the model for the decline of a production well, both harmonic and exponential curves were examined based on their linearity and R^2 values. After identification of a suitable model, the production data was converted from its hourly rate by multiplying with a factor of 720 (24 hours in a day * 30 days in a month). The data was then subjected to a moving average analysis over an interval of three months and the Loss Ratio calculated using the Arps formulae:

$$Loss\ Ratio = \frac{Q}{\Delta Q}$$……. ***Equation 3.4***

Where Q is the Current production and

ΔQ: Change in production

To determine the effective monthly decline rate (De), the following formulae was used:

$$\boldsymbol{De = \frac{1}{Loss\ ratio} \times 100\%} \text{ ..... } \textbf{\textit{Equation 3.5}}$$

Afterwards, the effective monthly decline rate was used to determine the monthly nominal decline rate (D) which would be used for prediction purposes.

$$\boldsymbol{D = (-Ln\,(1 - De)) \times 100\%} \text{ ..... } \textbf{\textit{Equation 3.6}}$$

In the prediction of when a geothermal well would cease production, the universal average economic limit (10 t/hr) was converted from its hourly rate to a monthly value by multiplying with a factor of 720 giving a monthly rate of 7200 tons per month.

Using the nominal decline rate (D), the future production of the declining production wells was calculated using:

$$\boldsymbol{Q = Q_i e^{-Dt}} \text{ ..... } \textbf{\textit{Equation 3.7}}$$

Where Q_i: Initial production

t: Elapsed time

These curves determine when to drill make up wells hence manage a geothermal field, estimate its future production and identify the relationship of pressure drawdown to the decline of the production well and other parameters.

For predictions to be carried out, initial data is required and it is only applicable to production wells with a smooth decline. They cannot operate in the absence of a theoretical background especially when predicting for systems which have been subjected to management change. Additionally, use of too many parameters causes the trends to cross and overlie each other and may be difficult to analyze.

CHAPTER FOUR: RESULTS AND DISCUSSION

This section presents the results and discussions of the analysis of the trends of physical and geochemical parameters of two retired geothermal wells (located in the East production field) and seven production geothermal wells (located in the North-east and East production fields). The North-east field was represented by four production wells while the East field was represented by three production wells as shown in figure 3.1.

Trends of the WHP and enthalpy values (physical parameters) and Cl, SiO_2 and Mg concentrations (geochemical parameters) were presented and compared in graphs for each of the chosen retired and production wells which enabled the identification of the types and rate of change for each parameter in all the geothermal wells and the sub-surface processes associated with the observed trends. Correlation studies were also carried out and helped identify the relationships and extent of similarities between the production wells and the parameters. Subsequently, the trends were used to identify declining production wells and their future performance.

4.1 Results

4.1.1 Trends of Retired Geothermal Wells

OW-7+8 and OW-13 are retired geothermal wells located in Olkaria east. OW-7+8 are located to the south of the field and share a separator and on ceasing production, they were converted to a monitoring well (Ofwona, 2011) whereas OW-13 is located to the south east of the field and when it stopped production, it was converted to a hot reinjection well (Bodvarsson and Pruess, 1987). Based on the data, the two geothermal wells had different fifteen year operational periods before they ceased production: OW-7+8: 1985-2000 and OW-13: 1990-2005. The physical parameters of the retired geothermal wells are presented below:

4.1.1.1 *Well Head Pressures*

The trends of the retired geothermal wells displayed repeated cycles with WHPs ranging from 4.8 to 11.8 bars with a mean range of 5.101-6.513 bars/yr. The retired geothermal well with the highest WHP was OW-7+8 (11.8 bars in 2000 and lowest value of 5 bars in 1991-1992 and 1997) with OW-13 recording its highest value of 5.8 bars in 2005 and lowest value of 4.8 bars in 1994.

Generally, the lowest WHP values of OW-7+8 represented the average WHP values recorded for OW-13 with the only exception in 1997 as shown in figure 4.1. Additionally, OW-13 had more

phases of changing trends. Both geothermal wells recorded the same WHP values in 1991 with the highest values recorded at the point when the geothermal wells ceased production. In 1992-1993 and 1994-1995, both showed an increase in pressure with a stop in production being preceded by constant pressure and a rise.

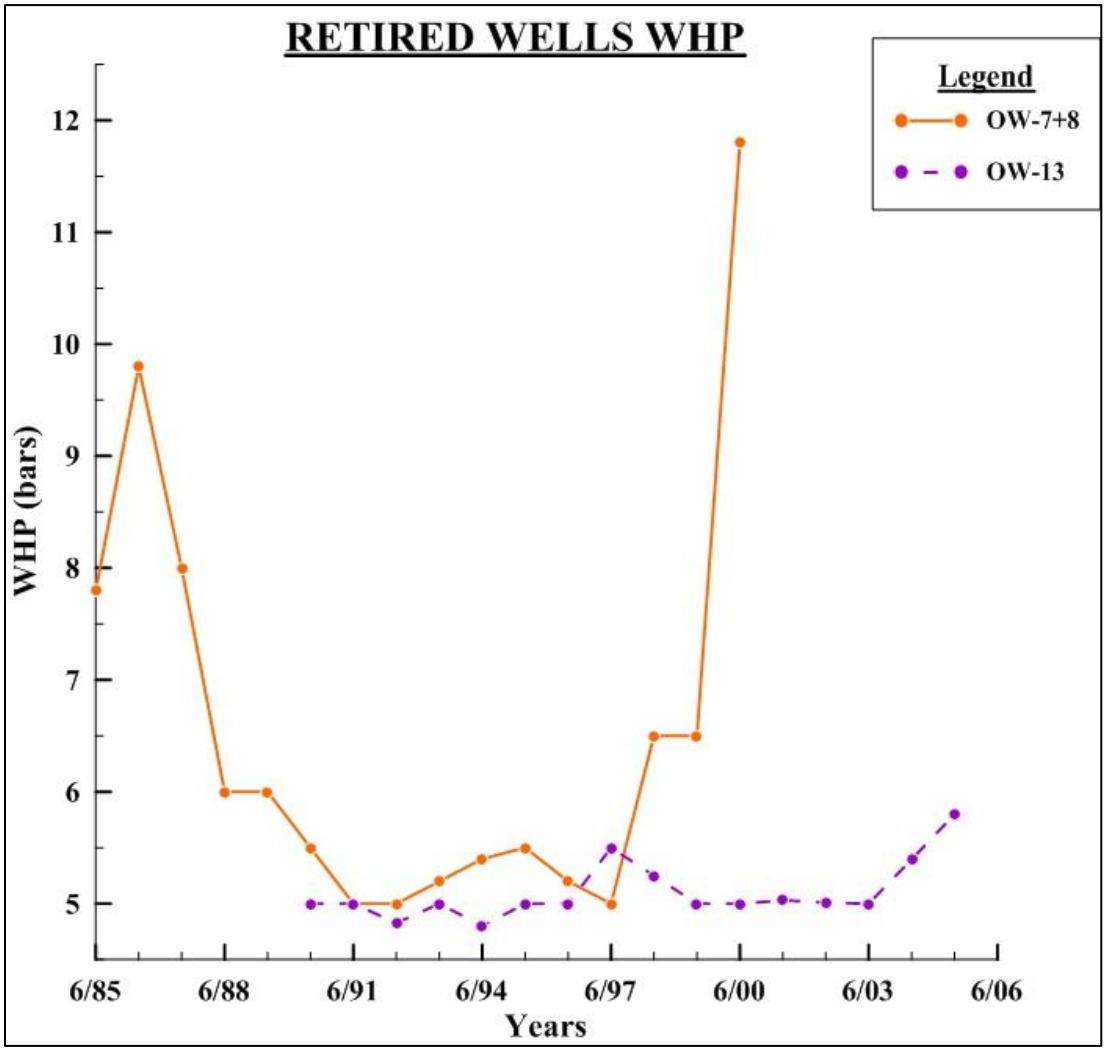

Figure 4.1 WHPs of Retired geothermal wells (OW-7+8 and 13)

OW-7+8's WHP increased by 2 bars from 1985 to 1986 before declining at a rate of 1.9 bars/yr until 1988. Pressure remained constant in the 1988-1989 period followed by a 0.5 bars/yr decline rate until 1991. Stability was observed between 1991 and 1992 with a rise at a rate of 0.167 bars/yr from 1992 to 1995. The pressures declined from 1995 to 1997 at a rate of 0.25 bars/yr before rising until 2000 in a series of three steps: 1.5 bars rise from 1997 to 1998, constant pressure in 1998-1999 and a rise of 5.3 bars over 1999-2000.

WHP in OW-13 commenced with a phase of stability from 1990 to 1991 then declined in 1991-1992 by 0.173 bars before the pressure rose by 0.173 bars in 1992-1993. Pressure declined in 1993-1994 by 0.2 bars before rising by 0.2 bars in 1994-1995 and maintaining a constant pressure until 1996. It continued to increase from 1996 to 1997 by 0.5 bars followed by a decline to 1999 at a rate of 0.25 bars/yr. Pressure remained stable until 2003 before increasing to 2005 at a rate of 0.4 bars/yr.

The rates of decline of WHP for OW-7+8 decreased whereas its rates of increment started with a reduction before rising over successive phases with both initial phases (increment: 1985-1986 and decline: 1986-1988) having almost similar rates of change whereas OW-13's constant WHPs seemed to occur at 5.0 bars. Its rates of increase and decline increased over time with similar rates of decline and increment occurring in 1991-1992/ 1992-1993 and 1993-1994/ 1994-1995.

4.1.1.2 Enthalpy

The trends present in the graph (Figure 4.2) also displayed repeated cycles with enthalpy values ranging 1283-2662 kJ/kg and mean values ranging in 2101.938-2221.531 kJ/kg/yr. The highest enthalpy was recorded in OW-13 (2662 kJ/kg in 1995 and lowest value of 1433 kJ/kg in 2000) with OW-7+8 recording its highest value of 2649 kJ/kg in 1994 and lowest value of 1283 kJ/kg in 2000. The higher enthalpy values of OW-13 correlated with the lower recorded WHPs and displayed more phases of changing trends.

The geothermal wells displayed a peak before their decline with the lowest enthalpy for both geothermal wells being recorded in 2000. Both geothermal wells started with a rise in enthalpy and displayed similar trends of increment in their fifth year and decline in eighth, tenth, fourteenth and fifteenth years. Additionally, they had the same trends in 1990-1994, 1995-1996 and 1998-2000 with no phases of stability.

Enthalpy in OW-7+8 commenced with an increment of 107 kJ/kg from 1985 to 1986 followed by a decline in 1986-1987 of 54 kJ/kg then a rise of 13 kJ/kg until 1988. In 1988-1989, the enthalpy dropped by 27 kJ/kg followed by an increase over the 1989-1992 period at a rate of 27.33 kJ/kg/yr. A decline of 23 kJ/kg was observed in 1992-1993 followed by an increment in 1993-1994 of 276 kJ/kg and then a drop at a rate of 568.5 kJ/kg/yr until 1996. The rise in enthalpy from 1996-1998 was marked by two steps: 1996-1997 by 92 kJ/kg and 1997-1998 by 742 kJ/kg before declining at a rate of 531.5 kJ/kg/yr until 2000.

OW-13's enthalpy started with an increment from 1990 to 1992 at a rate of 22 kJ/kg/yr followed by a drop of 129 kJ/kg over 1992-1993 then a rise at a rate of 65 kJ/kg/yr in 1993-1995 period. The decline in enthalpy occurred in 1995-2000 in three steps: 1995-1997 at rate of 266.5 kJ/kg/yr, 1997-1999 at a rate of 66 kJ/kg/yr and 1999-2000 by 564 kJ/kg then increased by 758 kJ/kg in 2000-2001 period before finally declining over 2001-2005 in two steps: 2001-2002 by 12 kJ/kg and 2002-2005 at a rate of 223 kJ/kg/yr.

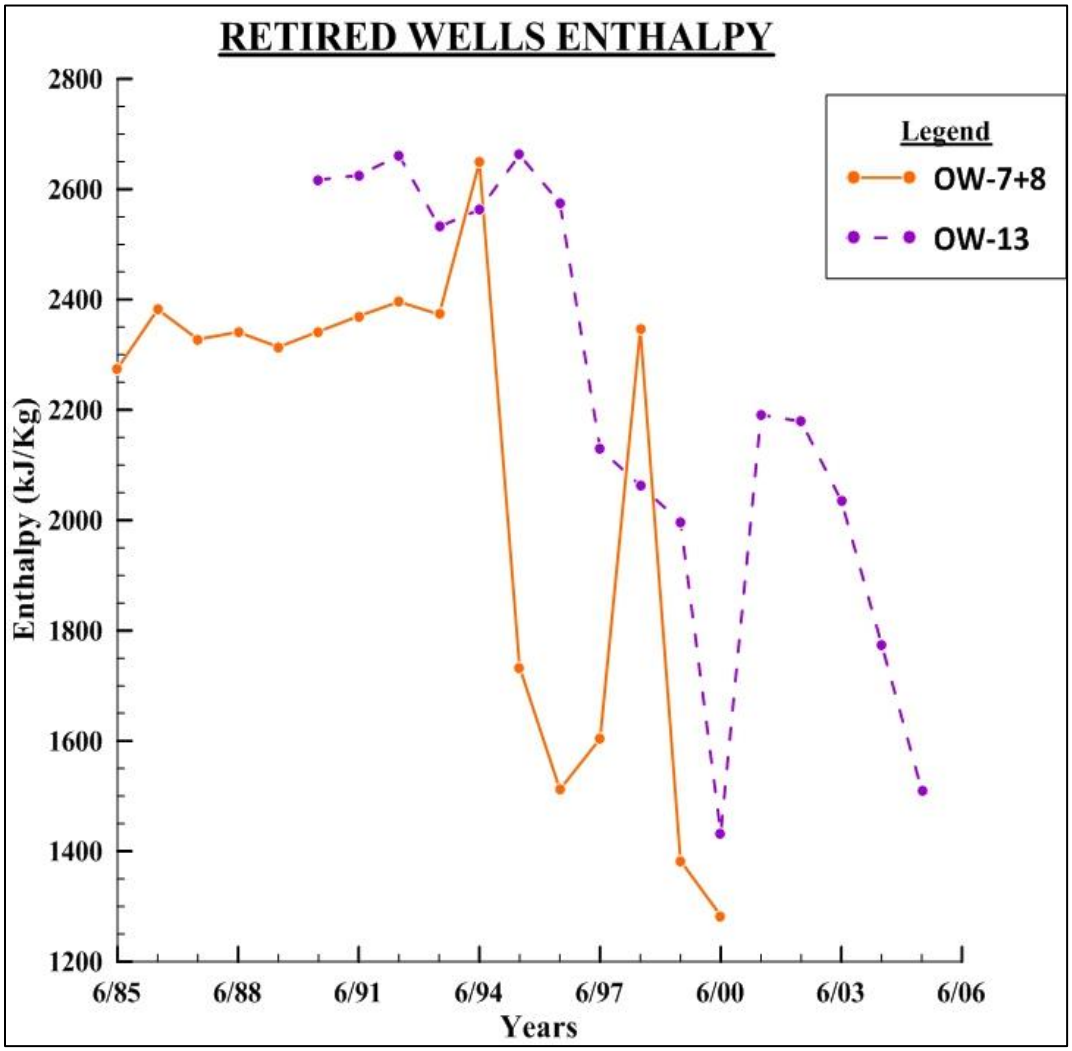

Figure 4.2 Enthalpy of Retired geothermal wells (OW-7+8 and 13)

OW-7+8's enthalpy had rates of increment and decline starting with a decrement then a rise and a drop. Similar rates of decline and increment were observed in 1988-1989/ 1989-1992 whereas OW-13's rates of decline in enthalpy dropped over successive phases and its rates of increment rose, dropped, rose again, fell then rose.

4.1.2 Geochemical parameters of Retired geothermal wells

Geochemical parameters tend to react faster to changes in the reservoir as compared to the physical parameters. The changes are brought about by a disequilibrium between the fluid-mineral/rock interaction caused by natural processes such as recharge or anthropogenic activities such as production.

4.1.2.1 Chloride Concentrations

The Cl concentration displayed repeated cycles ranging between 302.3-1934 ppm with a mean range of 723.965-846.941 ppm/yr. The highest Cl value was observed in OW-13 (1934 ppm in 1992 and lowest value of 302.3 ppm in 1997) with OW-7+8 recording its highest value of 895.66 ppm in 1993 and lowest value of 338.23 ppm in 1985. OW-13 had more phases of changing trend whereas OW-7+8's lowest Cl concentration was observed at the start of the chosen period.

Both displayed similar trends in increment in the second, eighth, tenth and thirteenth year and decline in third, eleventh and fourteenth years of the chosen periods. The same trends were observed in decline in 1993-1994 and 1996-1997 and increment in 1997-1998 and 1999-2000.

OW-7+8's Cl values had an increment at a rate of 212.535 ppm/yr from 1985 to 1987 followed by a decline of 90.17 ppm in 1987-1988 and a rise of 66.54 ppm over 1988-1989. Concentration remained relatively constant in 1989-1992 before rising by 164.77 ppm in 1992-1993 and then declining in 1993-1994 by 166.37 ppm. An increment of 53 ppm took place in 1994-1995 before dropping at a rate of 54.68 ppm/yr in 1995-1997. A rise in concentration by 118.19 ppm occurred in 1997-1998 before dropping by 116.05 ppm in 1998-1999 only to rise by 185.7 ppm in 2000.

Cl concentrations in OW-13 started with a decline from 1990 to 1991 by 297.51 ppm then rose by 946.51 ppm in 1991-1992 and declined in 1992-1995 at a rate of 379.42 ppm/yr. The concentration rose over 1995-1996 period by 33.31 ppm before dropping by 526.75 ppm in 1996-1997. An increment rate of 106.05 ppm/yr occurred over 1997-2000 before declining by 264.5 ppm in 2000-2001 followed by increment rate of 460.655 ppm/yr over 2001-2003 then declined in 2003-2005 at a rate of 216.575 ppm/yr.

OW-7+8's Cl rates of increment started with a drop then rose then dropped to finally rise whereas the rates of decline started with a rise then dropped then rose again while OW-13's Cl increment

rates dropped then finally rose whereas the decline rates started with a rise then continued declining.

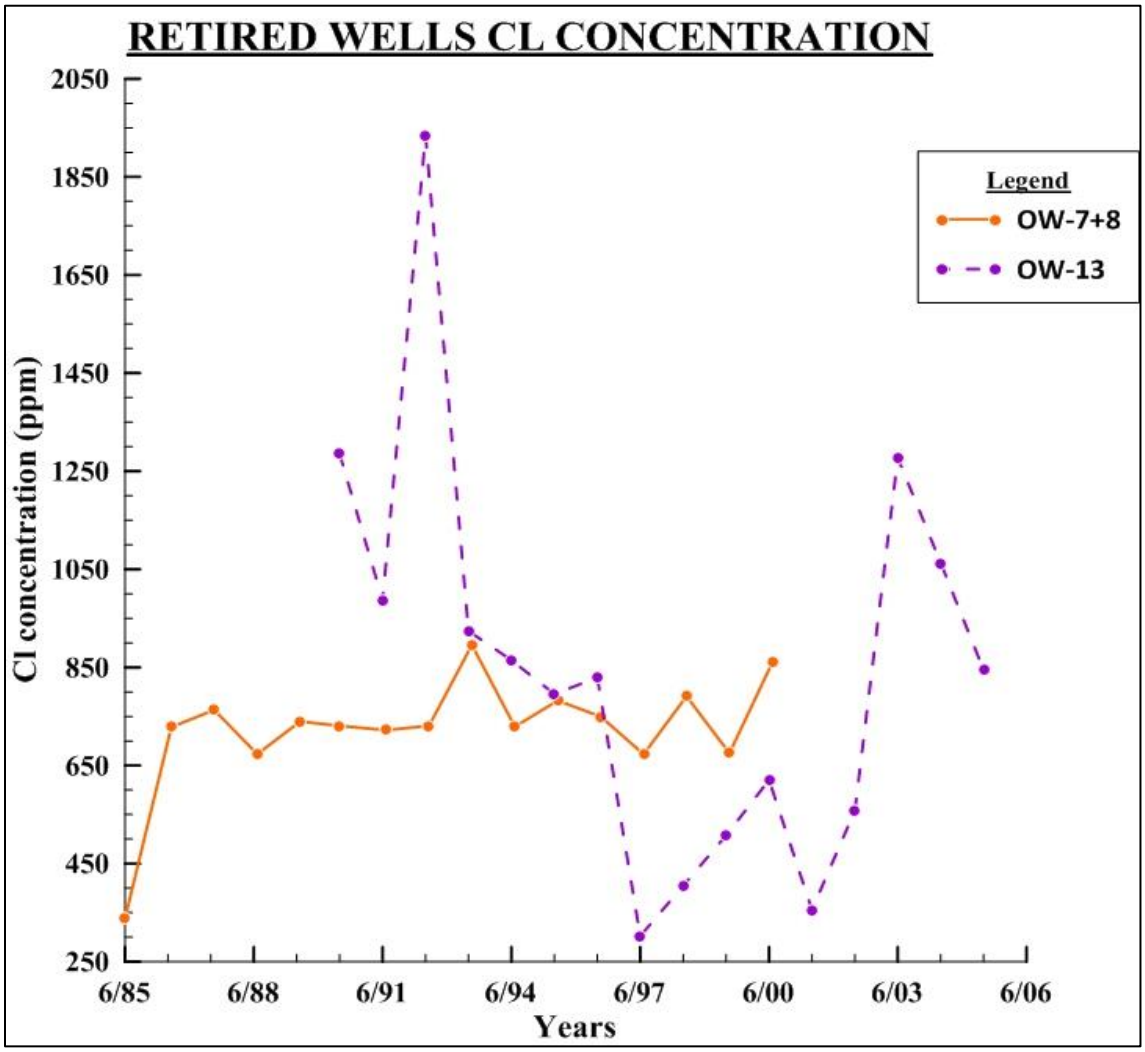

Figure 4.3 Chloride concentrations of Retired geothermal wells (OW-7+8 and 13)

4.1.2.2 Silica Concentrations

The repeated cycles of the trend operated at a range of 207.65-1454.6 ppm with a mean average of 589.966-601.58 ppm/yr. The highest concentration was observed in OW-13 (1454.6 ppm in 1992 and lowest value of 207.65 ppm in 1995) with OW-7+8 recording its highest value of 748.11 ppm in 2000 (end of the study period) and lowest value of 315.31 ppm in 1991.

Both geothermal wells appeared to have the same SiO_2 concentrations apart from peaks observed in 1992 and 1994 in well OW-13 which had more phases of change. Both geothermal wells had similar trends of decline in the first, third, fifth, ninth years and fourteenth years and increment in

the second, seventh and thirteenth years. The same trend of decline was observed in the years 1990-1991, 1994-1995 and 1998-1999 and increment in 1991-1992, 1995-1997 and 1999-2000.

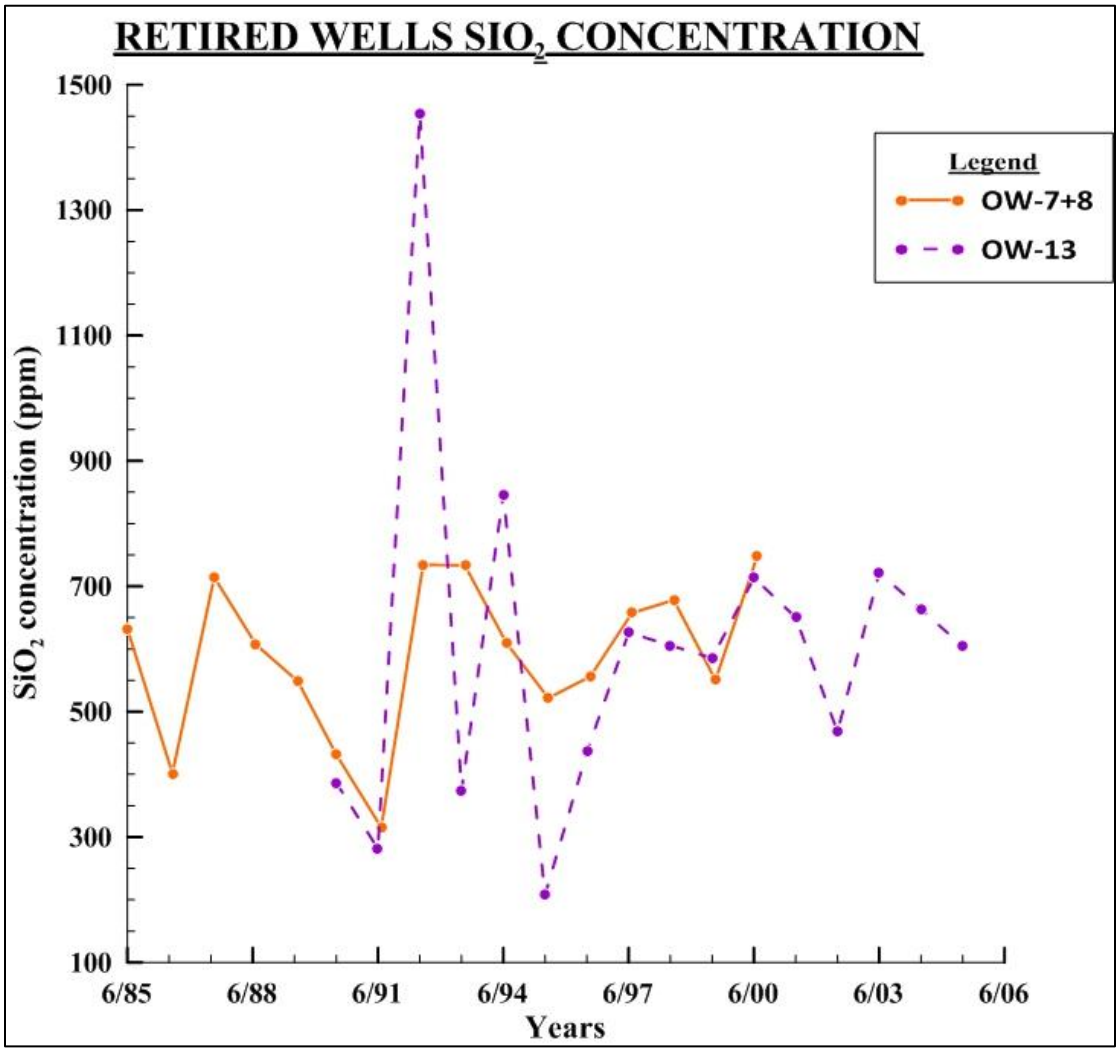

Figure 4.4 Silica concentrations of Retired geothermal wells (OW-7+8 and 13)

OW-7+8's SiO_2 declined by 230.89 ppm in 1985-1986 then rose by 313.08 ppm in 1986-1987 followed by a decline rate of 99.7875 ppm/yr in 1987-1991 and an increment of 419.01 ppm in 1991-1992. Concentration remained constant over 1992-1993 before declining at a rate of 105.85 ppm/yr over 1993-1995. Concentration then rose at a rate of 52.093 ppm/yr in 1995-1998 followed by a decline of 127.61 ppm in 1998-1999 then rising by 197.63 ppm in 2000.

OW-13's SiO_2 declined by 105.51 ppm in 1990-1991 then increased in 1991-1992 by 1173.31 ppm followed by a drop of 1080.72 ppm in 1992-1993 before rising by 472.67 ppm over 1993-1994. Decline occurred by a value of 638.9 ppm in 1994-1995 then an increment rate of 209.24

ppm/yr over 1995-1997 and a decline rate of 20.375 ppm/yr in 1997-1999. Concentration rose in 1999-2000 by 128.17 ppm then dropped at a rate of 122.775 ppm/yr in 2000-2002 followed by an increment of 253.57 ppm in 2002-2003 and a decline of 2003-2005 at a rate of 58.785 ppm/yr.

OW-7+8's SiO_2 decline rates dropped then rose whereas the increment rates rose then dropped then rose again. OW-13's SiO_2 decline rates rose then dropped then rose followed by a drop while the increment rates dropped then rose.

4.1.2.3 Magnesium Concentrations

The trend appeared to be rather stable with occasional peaking in values. The range was 0-0.130 ppm with a mean range of 0.006-0.036 ppm/yr. The highest Mg value was observed in OW-7+8 (0.13 ppm in 1987 and lowest value of 0 ppm in 1991-1999) with OW-13 recording a high value of 0.1 ppm in 1995 and lowest value of 0 ppm in 1990-1994, 1996-1999 and 2001-2005. Both geothermal wells had the same lowest value of 0 ppm with the highest values being almost the same value.

Both geothermal wells had the same number of phases of changing trends with OW-7+8 had three peaks covering 1985, 1990 and 2000 while OW-13 peaked twice in 1995 and 2000. Both geothermal wells had the same trends in decline observed in the sixth year, increment in 1999-2000 and constant concentration in the seventh-ninth and twelfth-fourteenth years. The same concentration was observed in 1991-1994 and 1996-1999 with all stable phases occurring at 0 ppm concentration.

Mg in OW-7+8 declined by 0.01 ppm in 1985-1986 before rising in 1986-1987 by 0.05 ppm then dropped in 1987-1988 by 0.09 ppm. An increment in concentration occurred over 1988-1989 by 0.06 ppm before dropping at a rate of 0.05 ppm/yr in 1989-1991. Concentration remained constant at 0 ppm from 1991-1999 before rising in 1999-2000 by 0.078 ppm.

OW-13's Mg maintained its concentration at 0 ppm from 1990-1994 before rising by 0.1 ppm in 1994-1995 then dropped by 0.1 ppm in 1995-1996. Stable concentration was acquired from 1996-1999 then rose by 0.002 ppm in 1999-2000 before declining by 0.002 ppm in 2000-2001 then maintaining a stable concentration until production ceased.

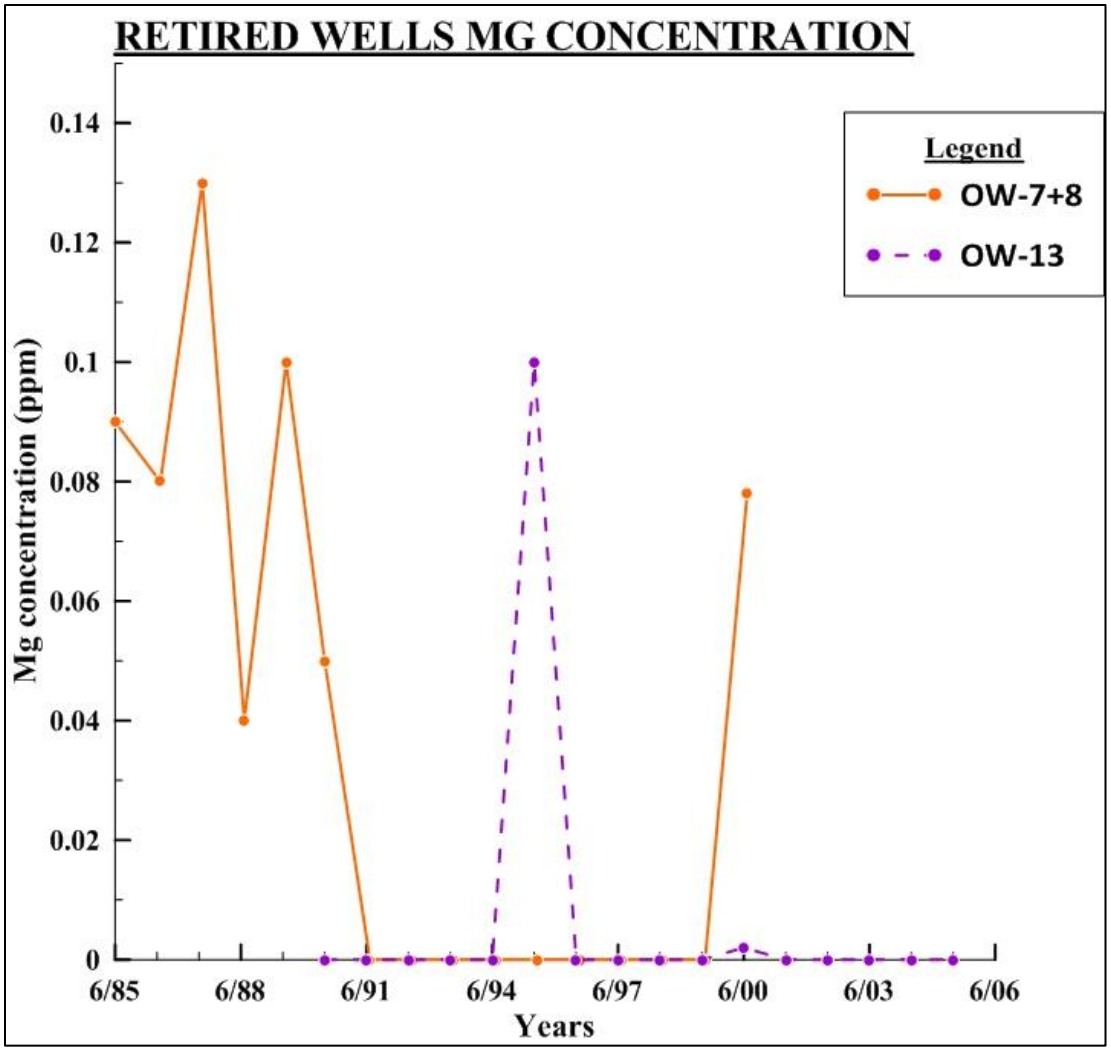

Figure 4.5 Magnesium concentrations of Retired geothermal wells (OW-7+8 and 13)

Magnesium concentration in OW-7+8 displayed rates of decline that rose then dropped and its rates of increment rose in successive phases with OW-13's having similar rates of increment and decline in 1994-1995/1995-1996 and 1999-2000/2000-200 with both rates declining over successive phases. Conclusively, the trends of the geothermal wells displayed similarity at the start of the period with a rise in enthalpy and a drop in SiO_2 and the end of production with a rise in WHP and a drop in enthalpy.

4.1.3 Trends of Production Geothermal Wells

North-East Production Field

The North-east field has twenty-eight geothermal wells; twenty of which are production wells (Wamalwa et al, 2016). The chosen production wells for study included: OW-709, 713, 720 and

728 with OW-713 being located south of the field and the remaining three production wells located to the south-west of the field. The production wells OW-720 and 728 share a separator. OW-709, 720 and 728 are located in areas identified as up flow zones for fluids in the Olkaria geothermal reservoir (Ofwona, 2002). The physical parameters of the production geothermal wells are presented below:

4.1.3.1 Well Head Pressures

The WHPs for the four production wells did not display an inclining or declining trend but repeated cycles over the study period. The WHPs ranged from 4.5 to 7.75 bars with the mean WHP ranging between 5.2-6.5 bars/yr. OW-720 recorded the highest WHP value (7.75 bars in 2008 and its lowest value of 5.23 bars in 2010) followed by well OW-728 (highest value of 7 bars in 2015 and lowest value of 5.091 bars in 2005). The production well with the third highest WHP values was OW-713 (highest value of 6.2 bars in 2011 and lowest value of 5.050 bars in 2005) and lastly, well OW-709 (highest value of 5.5 bars in 2009, 2012 and 2015 and lowest value of 4.5 bars in 2013). Hence, the order of production wells of decreasing WHP was as follows: 720>728>713>709.

It was also observed that OW-713 and 728 recorded their lowest WHP in 2005 and OW-709 and 728 recorded their highest WHP in 2015. As shown in figure 4.6, all the production wells commenced with an increment in WHP apart from OW-720 with all four production wells displaying a rise over 2006-2007 and 2010-2011 and all declined in WHP in 2009-2010 and 2012-2013. Additionally, OW-713 and 728 displayed a similar trend from 2005-2007 and recorded the same WHP values in 2007 whereas OW-709 and 713 recorded the same WHP in 2015.

WHP in OW-709 commenced with an increment from 2005 to 2007 at a rate of 0.304 bars/yr before stabilizing at 5.35 bars for one year. OW-709's WHP continuously rose by 0.15 bars between 2008 and 2009 then declined by 0.417 bars in the following year. Over the 2010-2012 period, a rise of pressure at a rate of 0.208 bars/yr occurred but in the 2012-2013 interval, there was a 1 bar drop which preceded an increment rate of 0.5 bars/yr between 2013 and 2015.

WHP in OW-713 also started with a rise of 0.317 bars/yr over 2005-2008 period then declined from 2008 to 2010 at a rate of 0.3 bars/yr. Between 2010 and 2011, a 0.8 bar rise occurred followed by a drop from 2011 to 2013 at a rate of 0.35 bars/yr and the maintenance of a constant pressure of 5.5 bars over 2013-2015.

WHP in OW-720 alternatively had a decline from 2005 to 2006 by 0.446 bars before rising at a rate of 0.755 bars/yr over 2006-2008. Afterwards between 2008 and 2010, WHP dropped at a rate of 1.26 bars/yr then increased at a rate of 0.835 bars/yr over the 2010-2012 period only to decline by 0.9 bars in the following year. The pressure subsequently rose by 0.25 bars from 2013 to the end of the study period.

WHP in OW-728 had an increase of 0.227 bars/yr over 2005-2009 period before it dropped by 0.5 bars from 2009 to 2010. A 0.5 bar rise marked the 2010-2011 interval before maintaining a stable phase of 6 bars between 2011 and 2012. The WHP later declined at a rate of 0.375 bars/yr over 2012-2014 period followed by an increment rate of 1.75 bars/yr from 2012 to 2015.

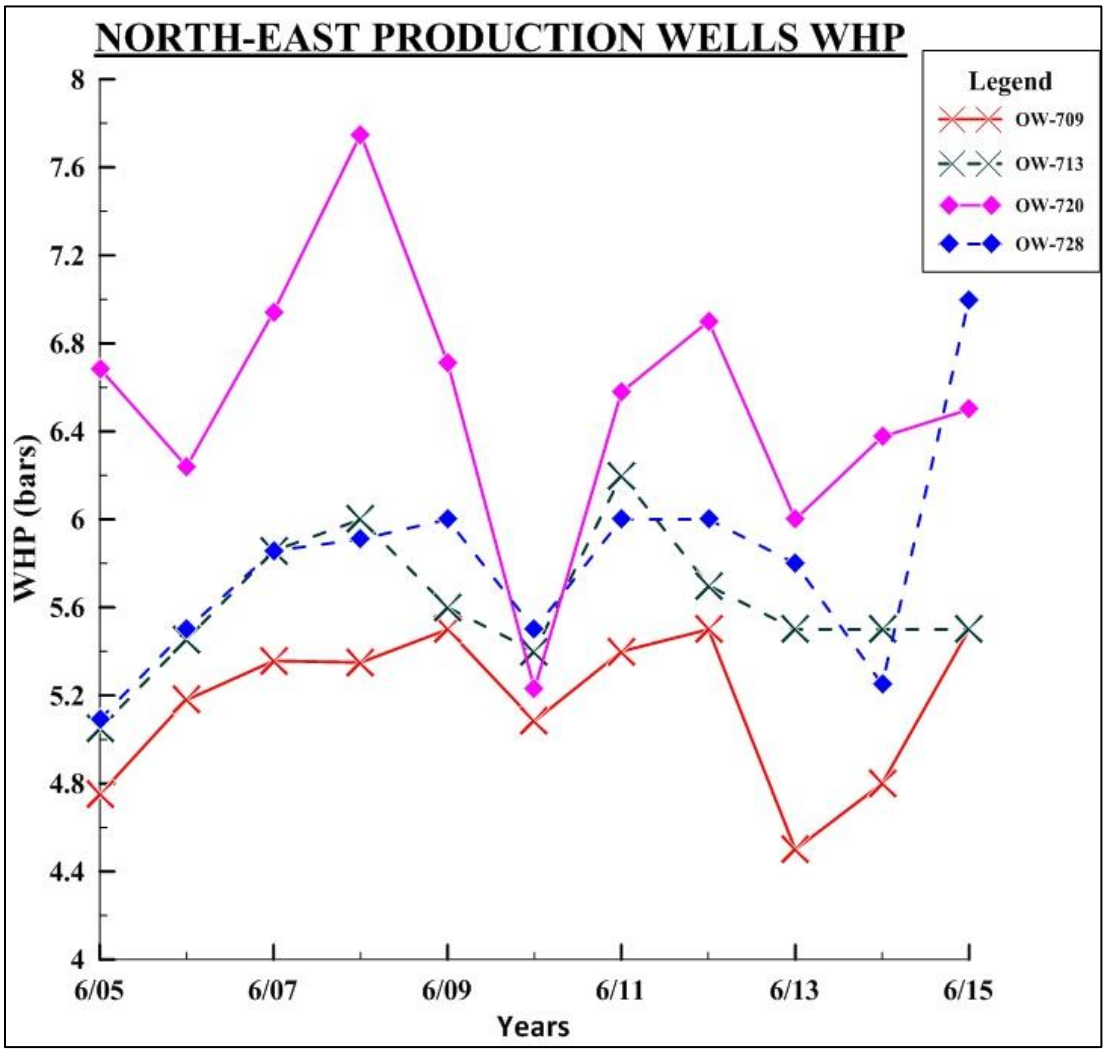

Figure 4.6 WHPs of NE production geothermal wells (OW-709, 713, 720 and 728)

WHP rates of increment for OW-709 initially dropped before finally rising whereas its decline rates continuously rose while rates of increment and decline of WHP for OW-713 both increased and recorded the same rates in 2005-2008 and 2008-2010 respectively. The increment and decline rates of WHP for OW-720 both rose before subsequently dropping whereas OW-728's WHP had rates of increment rising whereas the decline rates decreased over time. The same rate of increment and decline was observed in 2009-2010 and 2010-2011 respectively.

4.1.3.2 Enthalpy

As seen in the WHP plot, the production wells displayed repeated cycles apart from OW-713 which displayed a declining trend from 2008 to 2014. The enthalpy values for this period ranged from 1752 to 2441.512 kJ/kg with the mean enthalpy values of the area ranging between 2037-2302 kJ/kg/yr. The highest enthalpy value was observed in OW-713 (2441.512 kJ/kg in 2008 and the lowest value of 1752 kJ/kg in 2005) followed by well OW-720 (highest value of 2304.447 kJ/kg in 2012 and lowest value of 1959.16 kJ/kg in 2005). The production well with the third highest enthalpy value was OW-709 (highest value of 2238 kJ/kg in 2005 and the lowest value of 2052.64 kJ/kg in 2008) and lastly, well OW-728's enthalpy (highest value of 2170.207 kJ/kg in 2012 and lowest value of 1927.875 kJ/kg in 2014). Hence, the order of production wells of decreasing enthalpy was as follows: 713>720>709>728.

Both OW-720 and 728's enthalpy appeared to peak in 2012 while OW-713 and 720 recorded their lowest enthalpy in 2005. OW-709 and 728's enthalpy started with a decline while the rest of the production wells' enthalpy rose. The enthalpy rose in all production wells in 2007-2008 and declined in 2008-2009 apart from OW-709's enthalpy. The enthalpy values also appear to have risen in 2009-2010 apart from OW-713 with all the production wells' enthalpy values declining from 2012-2014 excluding OW-709.

Enthalpy values of OW-709 started with a decrease in enthalpy by 120.6 kJ/kg from 2005 to 2006 before increasing in the following year by 20.6 kJ/kg. Over 2007-2008 period, a decline of 85.360 kJ/kg took place preceding a rise at a rate of 25.073 kJ/kg/yr between 2008 and 2010. The enthalpy dropped from 2010 to 2012 at a rate 22.741 kJ/kg/yr, increased at a rate of 56.611 kJ/kg/yr over the 2012-2014 interval followed by a decline of 106.947 kJ/kg between 2014 and 2015.

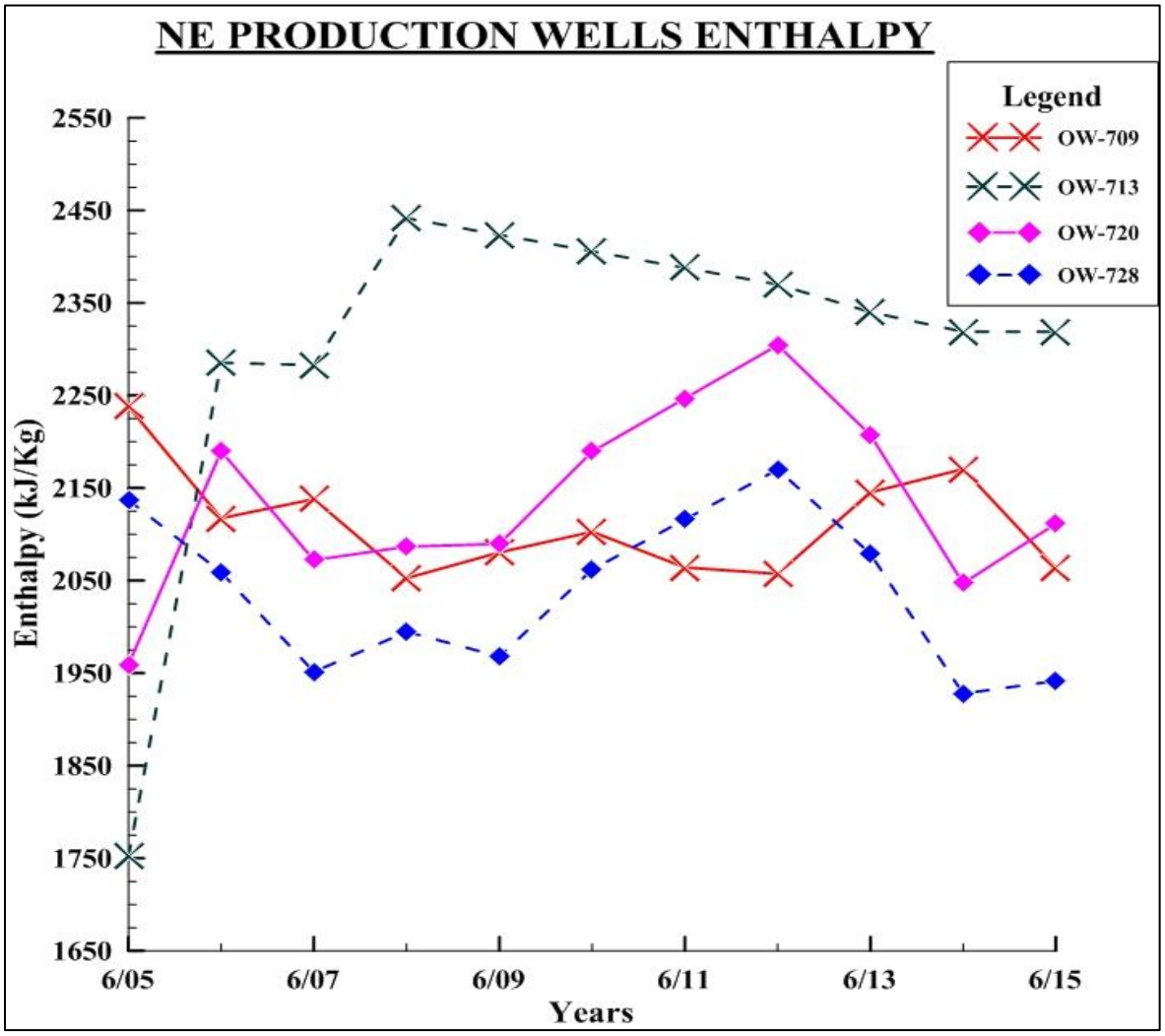

Figure 4.7 Enthalpy of NE production geothermal wells (OW-709, 713, 720 and 728)

OW-713's enthalpy values displayed an increment of 533.5 kJ/kg in 2005-2006 interval before maintaining a constant value of 2283 kJ/kg from 2006 to 2007. The enthalpy rose again between 2007 and 2008 by 158.798 kJ/kg then declined at a rate of 20.419 kJ/kg/yr and ended with a stable phase of 2319 kJ/kg over 2014-2015 period.

The initial increment values recorded for OW-720's enthalpy values were 230.62 kJ/kg from 2005 to 2006. The following year, a drop valued at 117.649 kJ/kg took place before rising at a rate of 46.463 kJ/kg/yr between 2007 and 2012. A decline rate of 128.661 kJ/kg/yr then characterized the 2012-2014 interval before ending with a rise of 64.375 kJ/kg.

OW-728's enthalpy commenced with a decline at a rate of 92.788 kJ/kg/yr from 2005 to 2007 before increasing by 43.331 kJ/kg over 2007 to 2008. Another drop was observed between 2008 and 2009 by 26.774 kJ/kg followed by an increment rate of 67.409 kJ/kg/yr in the 2009-2012 interval, a decrease in enthalpy from 2012 to 2014 at a rate of 121.166 kJ/kg/yr and a rise of 13.742 kJ/kg in the year that followed.

The enthalpy values for OW-709 displayed an increase in rates of increment but a decrease in decline rates before their drastic rise whereas OW-713's enthalpy increment rates continuously dropped while its decline rates rose then dropped. OW-720's enthalpy had rates of increment decreasing before they rose while its rates of decline increased whereas increment and decline rates of enthalpy in OW-728 rose then dropped and dropped then rose respectively.

The similarity observed between the two physical parameters revealed that OW-709 had the lowest range of values with all geothermal wells apart from OW-709 rising between 2007 and 2008. Additionally, a similar trend occurred for both parameters in the 2005-2006 interval for OW-709 and 720.

4.1.4 Geochemical Parameters of North-east field production geothermal wells

4.1.4.1 Chloride Concentrations

The Cl trends for the four production wells over the study period displayed decaying repeated cycles. The Cl values ranged from 13.064 to 1730.032 ppm with a mean concentration range of 372-907 ppm/yr. The highest Cl concentration was observed in OW-709 (1730.032 ppm in 2006 and lowest value of 315 ppm in 2014) followed by well OW-728 (highest value of 1187.12 ppm in 2006 and lowest value of 453.83 ppm in 2010). The third highest Cl concentration was observed in OW-713 (highest value of 1059.062 ppm in 2005 and lowest value of 199.78 ppm in 2011) and lastly, well OW-720 (highest value of 909.581 ppm in 2006 and lowest value of 13.064 ppm in 2010). Hence, the order of production wells of decreasing Cl concentration was as follows: 709>728>713>720.

OW-709, 720 and 728 Cl concentrations peaked in 2006 with OW-713 Cl values peaking in 2005 and OW-709 and 720 Cl values appeared to reduce by almost half after peaking. OW-720 and 728 recorded their lowest Cl concentrations in 2010. All geothermal wells appeared to decline in Cl concentration over 2009-2010 and 2012-2013 periods and rise in 2011-2012 interval. The same

concentrations in Cl were observed in OW-713 and 728 in 2010, 2013 and 2014, OW-709 and 720 in 2014 and OW-709 and 728 in 2015. Cl values increased in all production wells in 2005-2006 apart from OW-713, 2008-2009 apart from OW-728, 2010-2011 apart from OW-713, 2013-2014 apart from OW-709 and 2014-2015 apart from OW-728. All Cl values appeared to decline in all production wells in 2006-2007 apart from OW-713.

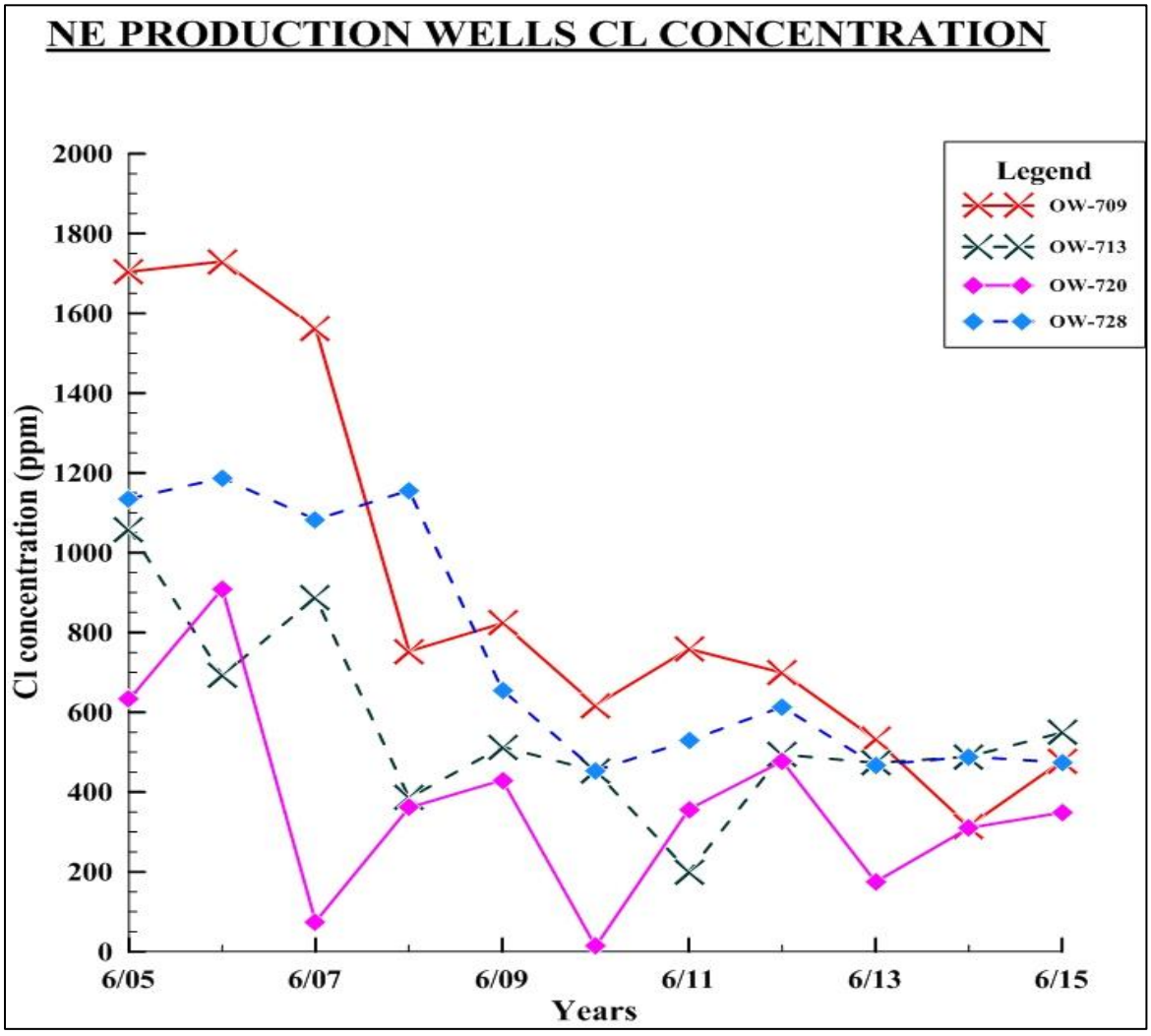

Figure 4.8 Chloride concentrations of NE production geothermal wells (OW-709, 713, 720 and 728)

Cl concentration in OW-709 rose from 2005 to 2006 by 25.732 ppm followed by a decline rate of 488.525 ppm/yr between 2006 and 2008 and an increment in the following year by 70.391 ppm. The concentration decreased by 205.609 ppm in 2009-2010 period but increased afterwards from

2010 to 2011 by 141.056 ppm. Another decline phase which had a rate of 147.94 ppm/yr occurred between 2011 and 2014 before ultimately rising by 163.22 ppm.

Cl concentration in OW-713 dropped from 2005 to 2006 by 367.296 ppm then rose by 196.063 ppm in 2006-2007 interval before dropping again by 502.255 ppm over 2007-2008 period. This was followed by an increase in 2008 to 2009 by 127.918 ppm, a decline rate of 156.856 ppm/yr from 2009 to 2011 and an increment of 294.71 ppm between 2011 and 2012. The decrease in concentration was observed over 2012-2013 period by 21.44 ppm and subsequently rose at a rate of 38.14 ppm/yr in the 2013-2015 interval.

An increase in Cl concentration by 277.578 ppm in OW-720 marked the start of the study period spanning 2005 to 2006 followed by a decline of 834.265 ppm between 2006 and 2007 and another rise in concentrations at a rate of 177.355 ppm/yr over the 2007-2009 period. The concentration dropped again in the following year by 416.962 ppm then increased at a rate of 232.188 ppm/yr in the 2010-2012 interval. A decline between 2012 and 2013 was observed by a value of 302.46 ppm before ending with an increment at a rate of 86.96 ppm/yr.

OW-728's Cl concentration increased from 2005 to 2006 by 51.929 ppm before decreasing in 2006-2007 interval by 104.269 ppm. The concentration rose by 73.487 ppm over 2007 to 2008, dropped between 2008 and 2010 at a rate of 351.254 ppm/yr then rose again at a rate of 80.01 ppm/yr in the 2010-2012 interval. A drop in Cl concentration occurred in 2012 to 2013 by 146.3 ppm but rose by 21.31 ppm the following year only to end in 2014-2015 interval with a decline of 14.76 ppm.

The Cl concentration for OW-709 had its rates of increment rising while its rates of decline dropping whereas OW-713's Cl concentration increment rates decreased then increased then decreased again while its decline rates increased then decreased. OW-720's Cl rates of increment also dropped at first then rose then dropped again whereas its decline rates dropped while the Cl increment and decline rates of OW-728 increased then eventually decreased.

4.1.4.2 Silica Concentrations

The SiO_2 concentrations for the four production wells displayed repeated cycles. The SiO_2 concentration ranged between 64-1030.857 ppm with a mean range of 487-559 ppm/yr.

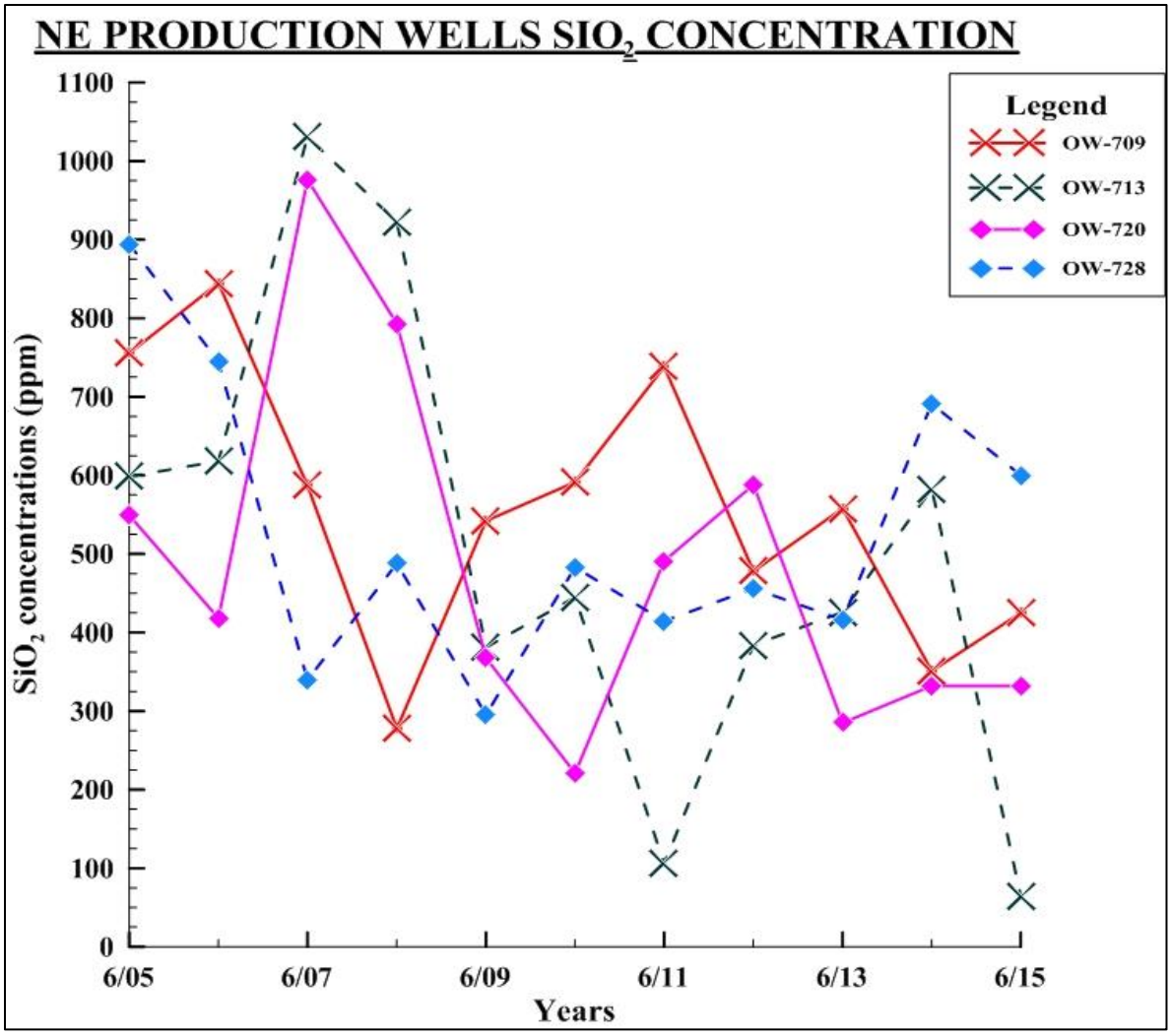

Figure 4.9 Silica concentrations of NE production geothermal wells (OW-709, 713, 720 and 728)

The highest SiO_2 concentration was observed in OW-713 (1030.857 ppm in 2007 and the lowest value of 64 ppm in 2015) followed by well OW-720 (highest value of 976.5 ppm in 2007 and lowest value of 221 ppm in 2010). The third highest SiO_2 concentration was observed in OW-728 (highest value of 894.498 ppm in 2005 and lowest value of 295.3 ppm in 2009) and lastly, well OW-709 (highest value of 848.36 ppm in 2006 and lowest value of 277.875 ppm in 2008). Hence, the order of production wells of decreasing SiO_2 concentration was as follows: 713>720>728>709.

OW-713 and 720 peaked in their SiO_2 concentrations in 2007. All SiO_2 concentrations increased in all the production wells in 2009-2010 apart from OW-720 and 2011-2012 apart from OW-709

whereas its values declined in all production wells in 2007-2008 apart from OW-728 and 2008-2009 apart from OW-709.

SiO_2 concentration in OW-709 commenced with an increment of 89.336 ppm in 2005-2006 interval then declined at a rate of 283.481 ppm/yr over 2006-2008 period. An increment rate of 153.375 ppm/yr was observed from 2008 to 2011 before the concentration dropped a year later by 260 ppm. Over 2012-2013, the SiO_2 rose by 80 ppm but declined by 207 ppm in the 2013-2014 interval before finally rising by 74 ppm.

SiO_2 concentration of OW-713 started with a rise at a rate of 216.179 ppm/yr from 2005 to 2007 but dropped between 2007 and 2009 at a rate of 324.929 ppm/yr. The concentration then increased by 64 ppm the following year but decreased over 2010-2011 by 339 ppm and increased by 159 ppm/yr in 2011-2014 interval only to drop afterwards by 519 ppm.

OW-720's SiO_2 concentration dropped between 2005 and 2006 by 130.903 ppm before increasing with a value of 558.26 ppm in 2006-2007 interval. The concentration declined at a rate of 251.833 ppm/yr over 2007-2010 period but an increment rate of 183.5 ppm/yr followed after from 2010 to 2012. A decrease of 303 ppm was observed in 2012-2013 interval before rising by 47 ppm in 2013-2014 then ended with a stable concentration of 332 ppm.

SiO_2 concentration in OW-728 declined at a rate of 277.499 ppm/yr from 2005 to 2007 before rising by 148.5 ppm the following year then decreasing over 2008-2009 by 192.7 ppm. The rise in concentration occurred in the 2009-2010 period by 187.7 ppm with a drop of 68.5 ppm between 2010 and 2011. 41.5 ppm rise in concentration in the 2011-2012 period was followed by a decline phase valued at 40 ppm in 2012-2013, an increment of 275 ppm over 2013-2014 and drop of 91 ppm between 2014 and 2015.

SiO_2 concentrations for OW-709 had increment rates rising then dropping whereas the decline rates dropped while the OW-713's SiO_2 values had increment rates decreasing then rising whereas decline rates increased. OW-720's SiO_2 increment rates dropped whereas decline rates rose while OW-728's SiO_2 rates of increment rose before dropping then rose again whereas the rates of decline decreased before increasing again.

4.1.4.3 Magnesium Concentrations

The Mg concentrations for the four production wells displayed repeated cycles with a range in concentration of 0-0.226 ppm and a mean value range of 0.03-0.06 ppm/yr. The highest Mg concentration was observed in OW-720 (0.226 ppm in 2006 and lowest value of 0 ppm in 2015) followed by well OW-713 (highest value of 0.188 ppm in 2006 and lowest value of 0.004 in 2013). The production well with the third highest concentration of Mg was OW-728 (highest value of 0.09 ppm in 2012 and lowest value of 0 in 2005, 2006 and 2013) and lastly, well OW-709 (highest value of 0.085 ppm in 2005 and lowest value of 0 in 2006 and 2015). Hence, the order of production wells of decreasing Mg concentration was as follows: 720>713>728>709.

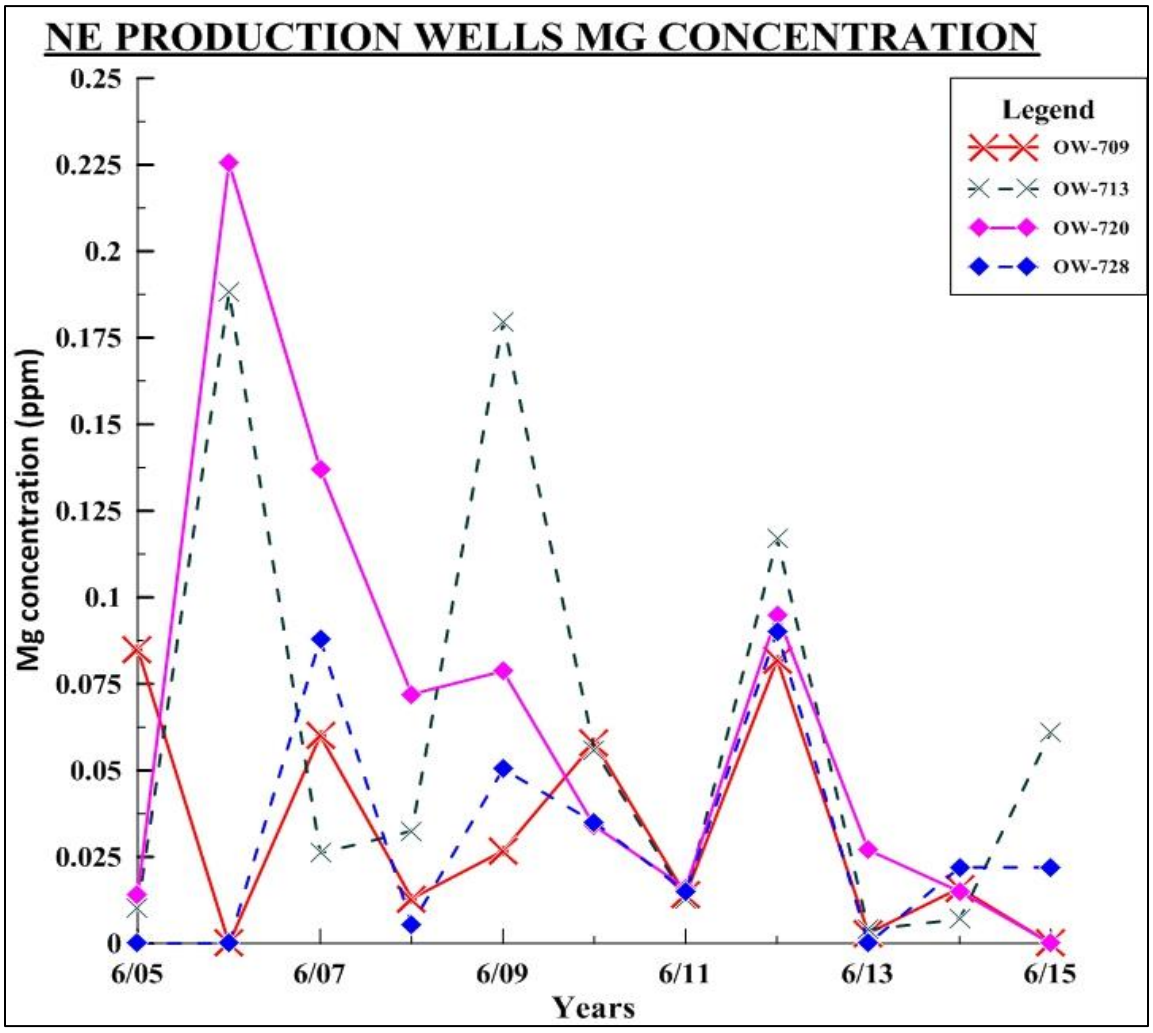

Figure 4.10 Magnesium concentrations of NE production geothermal wells (OW-709, 713, 720 and 728)

OW-713 and 720 Mg values peaked in 2006 with OW-709, 720 and 728 recording 0 ppm as their lowest values- OW-709 and 728 in 2006 and OW-709 and 720 in 2015. A similar trend was observed in 2005-2006 in Mg concentrations in OW-713 and 720. Mg concentrations declined in all the production wells in 2007-2008 apart from OW-713, 2009-2010 apart from OW-709 and 2010-2011 and increased in all the production wells in 2008-2009 and 2013-2014 apart from OW-720. In 2010-2011, Mg concentrations in OW-709 and 713 and OW-720 and 728 displayed similar trends with all four production wells recording the same value in 2011. A similar Mg trend was displayed in all four production wells from 2011 to 2013 with OW-709 and 720 having the same value in 2014 and same trend in 2014-2015.

Mg concentration in OW-709 declined by 0.085 ppm from 2005-2006 followed by an increase of 0.06 ppm the following year. A drop of 0.047 occurred between 2007 and 2008 then rose at a rate of 0.023 ppm/yr over 2008-2010 period before dropping again by 0.044 ppm in the 2010-2011 interval. Mg rose in 2011-2012 by 0.068 ppm followed by decline of 0.079 ppm in the 2012-2013 interval, an increment of 0.013 ppm in 2013-2014 and a drop of 0.016 ppm over 2014-2015 period.

Mg concentration rose in OW-713 from 2005 to 2006 by 0.178 ppm before dropping between 2006 and 2007 by 0.162 ppm. An increment at a rate of 0.077 ppm/yr was observed over 2007-2009 period with a later drop at a rate of 0.083 ppm/yr in the 2009-2011 interval. The concentration rose again from 2011 to 2012 by 0.104 ppm then decreased the following year by 0.113 ppm before rising again in 2014-2015 interval at a rate of 0.029 ppm/yr.

Mg concentration in OW-720 commenced with an increase of 0.211 ppm in 2005-2006 before declining at a rate of 0.077 ppm/yr over 2006-2008 and rising again in 2008-2009 interval by 0.007 ppm. The concentration dropped at a rate of 0.032 ppm/yr between 2009 and 2011 then increased by 0.079 ppm the following year and ultimately declined at a rate of 0.032 ppm/yr from 2012 to 2015.

Mg concentration in OW-728 maintained a constant concentration of 0 ppm between 2005 and 2006 then rose by 0.088 pm the year that followed. A decline phase was observed from 2007 to 2008 characterized by a value of 0.083 ppm with the concentration increasing by 0.044 ppm over 2008-2009 period and decreasing in 2009-2011 interval at a rate of 0.018 ppm/yr. Mg values increased from 2011 to 2012 by 0.075 ppm followed by a decrease of 0.09 ppm in 2012-2013, a

rise between 2012 and 2014 at a rate of 0.022 ppm/yr before ending with a stable phase with a concentration of 0.022 ppm.

OW-709's Mg concentration showed that the rates of increment and decline dropped then rose then dropped while OW-713's Mg increment rates decreased, increased then decreased again whereas decline rates dropped then rose. OW-720's Mg rates of increment and decline decreased then increased while OW-728's Mg increment rates decreased then rose then dropped whereas decline rates dropped then increased. Similar rates of increment and decline were observed in 2006-2007 and 2007-2008 respectively. The similarity observed among the three geochemical parameters included an increment in 2008-2009 for OW-709, 2011-2012 for OW-713, 720 and 728 and 2013-2014 for OW-713 and 728 and a decline in 2007-2008 for OW-709, 2010-2011 for OW-713 and 2012-2013 for OW-720 and 728.

East Production Field

The East production field has forty-one geothermal wells; twenty-two which are production wells. The chosen production wells for study were OW-26, 29 and 30 which are located in the north-eastern section of Olkaria East production field (Wamalwa et al, 2016) with OW-29 and 30 sharing a common separator. An up flow zone is located at OW-30 which is usually characterized by boiling and steam cap formation whereas OW-26 has been associated with some cold inflow (Ofwona, 2002).

4.1.5 Physical Parameters of East field production geothermal wells

4.1.5.1 Well Head Pressures

As shown in figure 4.11, the plot displayed a general rising trend with the WHP ranging between 6.209-9.546 bars and the mean WHP range was from 7.570 to 7.886 bars/yr. The production well with the highest WHP value was OW-30 (9.546 bars in 2013 and lowest value of 6.4 bars in 2006). The production well with the second highest value was OW-29 (9.058 bars in 2015 and lowest value of 6.274 bars in 2005) and lastly, well OW-26 (8.898 bars in 2012 and lowest value of 6.209 bars in 2005). Hence, the order of production wells of decreasing WHP was as follows: 30>29>26.

The lowest values for the production wells were recorded over the 2005-2006 interval. All production wells recorded the same pressure in 2007 and rose in 2008-2010 with the stable phases

each occurring at 8.5 bars for OW-26 and 30 for a period of a year. OW-29 and 30 displayed the same trend in 2007-2009 and recorded the same WHP in 2008 and 2011.

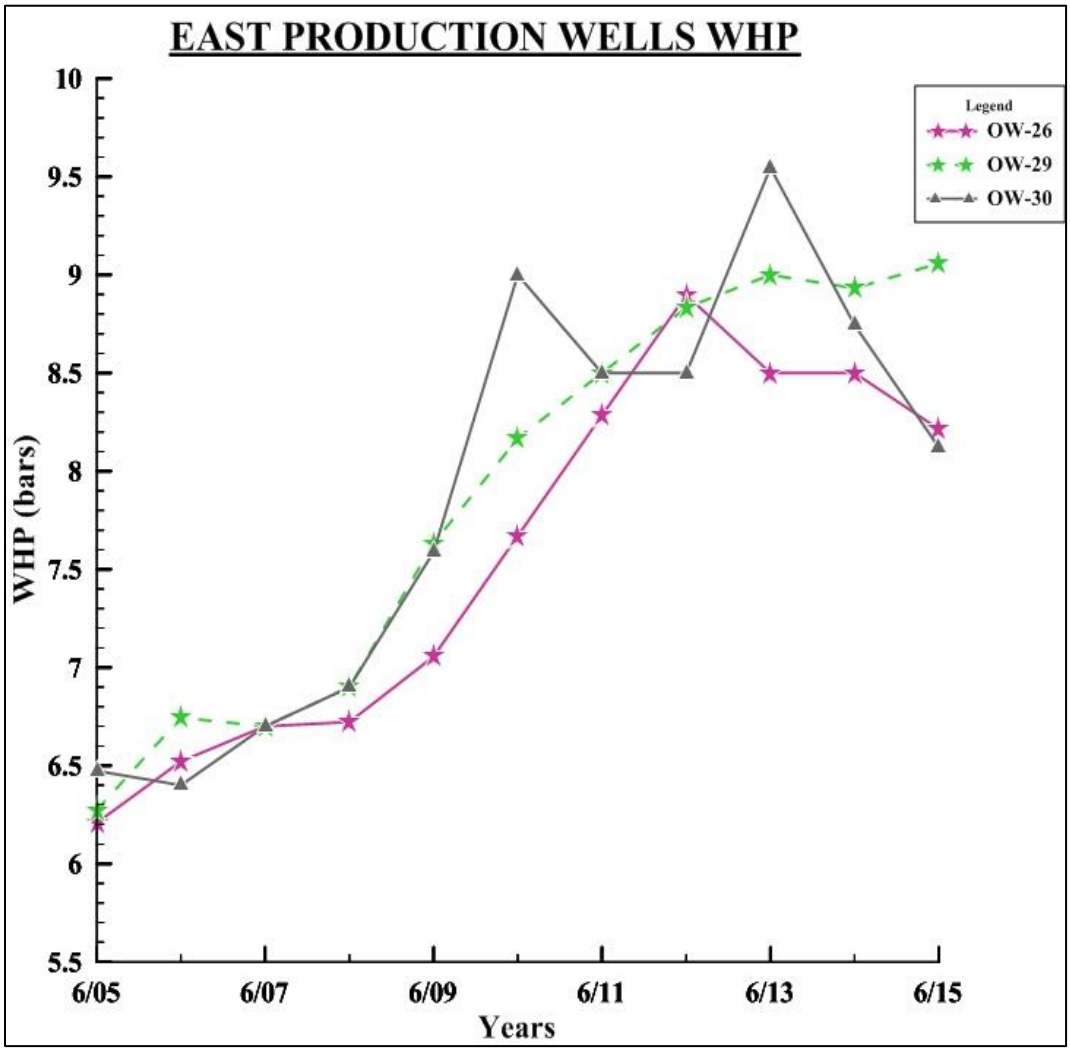

Figure 4.11 WHPs of East field production wells (OW-26, 29 and 30)

WHP in OW-26 commenced with an increment at a rate of 0.246 bars/yr between 2005 and 2007 before retaining a stable pressure of 6.7 bars in the following year. Another increase in WHP occurred over the 2008-2012 interval at a rate of 0.544 bars/yr followed by a 0.398 bars decline in the subsequent year and attainment of a stable phase at a pressure of 8.5 bars in 2013-2014 period. The end of the study period was marked by a decline of 0.286 bars in WHP.

OW-29's WHP increased over 2005-2006 by 0.47 bars followed by a decline of 0.044 bars the following year before rising again in the 2007-2013 interval by 0.383 bars/yr in two phases. A

0.068 bar drop in WHP occurred over the 2013-2014 period with pressure rising by 0.126 bars between 2014 and 2015.

WHP values in OW-30 dropped by 0.073 bars between 2005 and 2006 followed by a two-phase increment over the 2006-2010 period at a rate of 0.65 bars/yr before dropping 0.5 bars in pressure the following year. The pressure became stable at 8.5 bars during 2011-2012 interval only to rise between 2012 and 2013 by 1.046 bars and ultimately drop over the 2013-2015 period at a rate of 0.712 bars/yr.

OW-26's WHP was characterized by two stable phases each lasting a year with its increment rates rising and its decline rates dropping whereas OW-29's WHP increment rates dropped and decline rates rose and OW-30's decline and increment rates rose.

4.1.5.2 Enthalpy

Figure 4.12 does not display any uniformity in the trends of enthalpy for the involved production wells: OW-26 had a rising trend, OW-29 had a stable trend before declining whereas OW-30 displayed repeated cycles. The range of enthalpy was 1836-2775.5 kJ/kg with a mean range of 2265.503-2720.695 kJ/kg/yr. OW-29 recorded the highest enthalpy (2775.7 kJ/kg in 2010-2013 and its lowest value of 2642.925 kJ/kg in 2014) with OW-30 being the production well with the second highest enthalpy (2774.7 kJ/kg in 2009-2012 and lowest value of 2462.925 kJ/kg in 2014) followed by OW-26 (2767.143 kJ/kg in 2014 and lowest value of 1836 kJ/kg in 2005). Hence, the order of production wells of decreasing enthalpy was as follows: 29>30>26.

OW-29 and 30 both recorded their highest value in 2010-2012 period and their lowest values in 2014; recording the same value and the same trends in 2009-2012 and 2014-2015.

Enthalpy values of OW-26 started with a two-phase increase in 2005-2007 interval at a rate of 83.084 kJ/kg/yr only to attain a stable value of 2022 kJ/kg the following year before declining by 30.222 kJ/kg over 2008-2009 period. A two-phase increment whose rate of 159.029 kJ/kg/yr occurred between 2009 and 2014 and was succeeded by a drop of 366.286 kJ/kg in the 2014-2015 interval.

OW-29's enthalpy remained stable at 2775 kJ/kg between 2005 and 2013. It dropped by 312.575 kJ/kg the following year before rising by 26.3 kJ/kg over 2014-2015 period.

Enthalpy in OW-30 commenced with a decline of 10.563 kJ/kg in 2005-2006 followed by a rise at a rate of 97.865 kJ/kg/yr between 2006 and 2009 and a stable phase of 2774.7 kJ/kg in the 2009-2012 interval. The enthalpy dropped over 2012-2014 at a rate of 112.155 kJ/kg/yr then rose afterwards by 26.3 kJ/kg the following year.

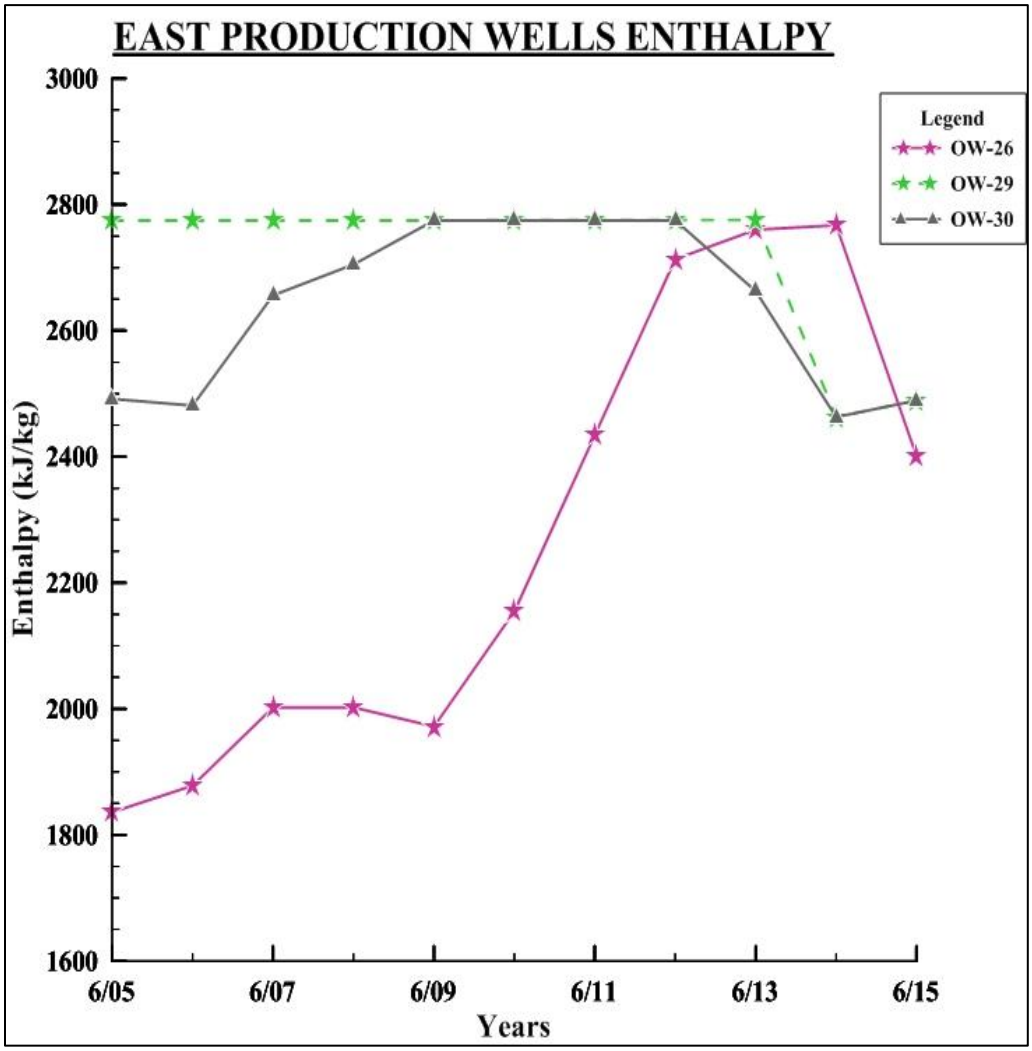

Figure 4.12 Enthalpy of East production wells enthalpy (OW-26, 29 and 30)

OW-26's increment and decline rates increased while OW-30's rates of decline rose and its rates of increment dropped.

Based on the two physical parameters, OW-26 recorded the third highest values and recorded its lowest values in both parameters in 2005. Rising trends in WHP and enthalpy were observed in OW-26 in 2005-2007 and 2009-2012, OW-29 in 2014-2015 and in OW-30 in 2006-2009. Stable

phases occurred in OW-26 in 2007-2008 and OW-30 in 2011-2012 whereas declining trends were present in OW-26 in 2014-2015, OW-29 in 2013-2014 and OW-30 in 2013-2014.

4.1.6 Geochemical Parameters of East field production geothermal wells

4.1.6.1 Chloride Concentrations

The graph shows a dominant declining trend for all the production wells excluding OW-29 which was rising. The range of Cl concentrations was 206.861- 1250 ppm with a mean concentration of 611.215-1025.358 ppm/yr.

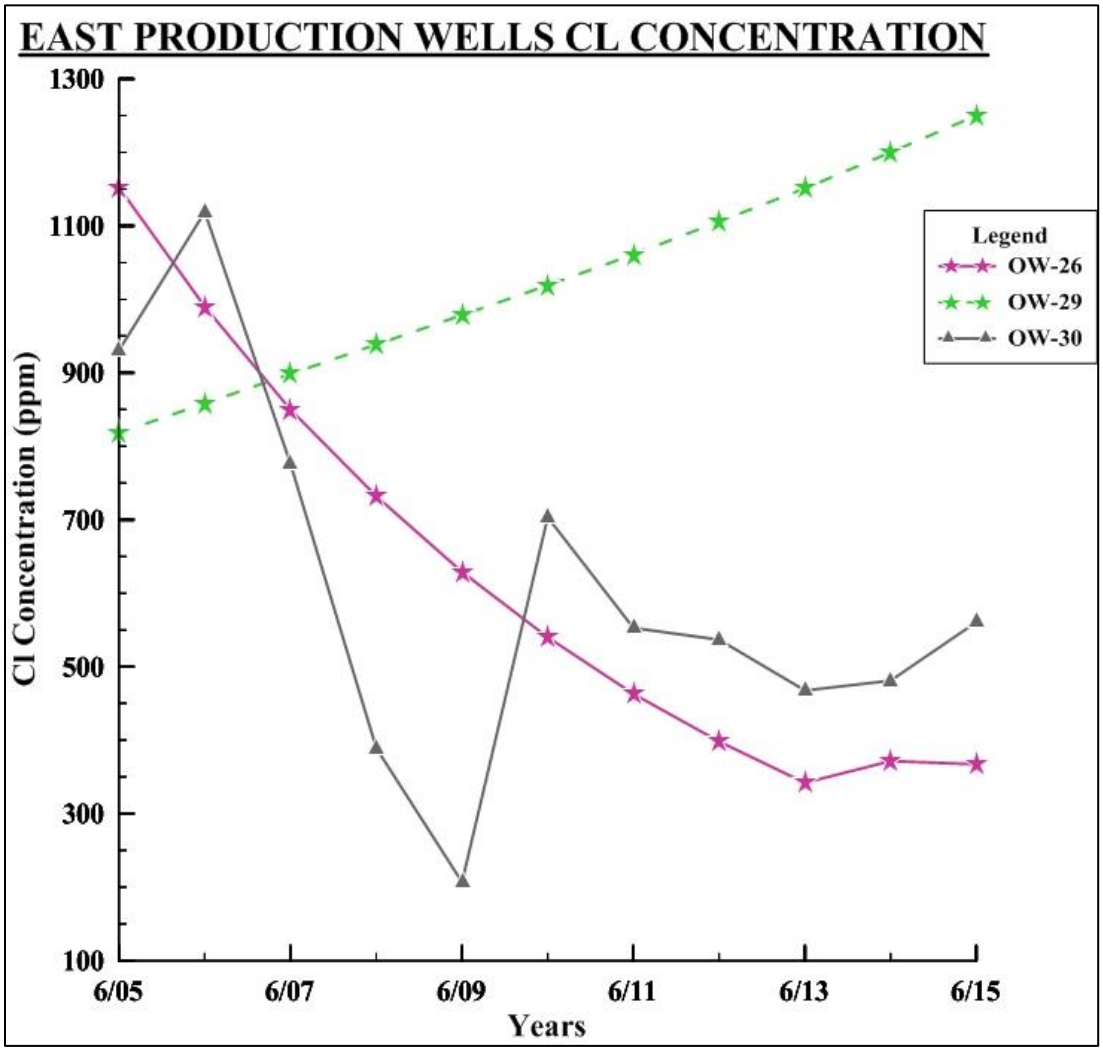

Figure 4.13 Chloride concentrations of East field production wells (OW-26, 29 and 30)

The highest concentration was observed in OW-29 (1250 ppm in 2015 and lowest value of 818.264 in 2005) followed by well OW-26 (1152 ppm in 2005 and lowest value of 341.9 ppm in 2013) and

lastly, well OW-30 (1118.794 ppm in 2006 and lowest value of 206.861 ppm in 2009). Hence, the order of production wells of decreasing Cl concentration was as follows: 29>26>30.

OW-26 and 30 recorded their highest values over the 2005-2006 interval with all three production wells recording the same value around February 2007 and rising in 2013-2014.

OW-26's Cl concentration declined at a rate of 135.017 ppm/yr between 2005 and 2013 then the value rose by 29.661 ppm the following year before ultimately declining by 4.443 ppm in 2014-2015.

Cl concentration in OW-29 was characterized by an increment throughout the entire period at an average rate of 43.1736 ppm/yr.

Cl concentrations in OW-30 commenced with an increment of 187.98 ppm between 2005 and 2006 then a two-phase decline occurred over the 2006-2009 period at a rate of 303.978 ppm/yr only for it to rise the following year by 496.465 ppm. In the 2010-2013 interval, a three-decline phase at a rate of 78.566 ppm/yr characterized this period before finally rising in two phases at a rate of 46.485 ppm/yr towards the end of the study period.

OW-26's decline rates decreased whereas OW-30's increment rates rose then dropped and its decline rates dropped. Hence, both OW-26 and 30's decline rates appeared to drop. From the plot, the trends appear different despite the fact that the production wells occur in the same area and have the same geology. This could be attributed to OW-26 suffering from cold inflow, OW-29 undergoing extensive boiling and overproduction during the production period and OW-30 having frequent influx of cooler fluids and episodes of adiabatic cooling.

4.1.6.2 Silica concentrations

The plot displayed repeated cycles for the three production wells with a range of 230-758.236 ppm and mean range of 401.025-462.070 ppm/yr. The highest SiO_2 concentration was recorded in OW-30 with its highest value of 758.236 ppm in 2005 and lowest value of 230 ppm in 2009. It was followed by well OW-26 (658 ppm in 2013 and lowest value of 262 ppm in 2005) and finally, well OW-29 (542.525 ppm in 2005 and lowest value of 292.865 ppm in 2010). The order of production wells of decreasing SiO_2 concentration was as follows: 30>26>29.

OW-29 and 30 recorded their highest values in 2005 and their lowest values in the 2009-2010 interval. The production wells appear to record the same concentration around April 2008 with OW-26 and 29 having the same value in 2008. All the three production wells concentration rose in 2010-2012.

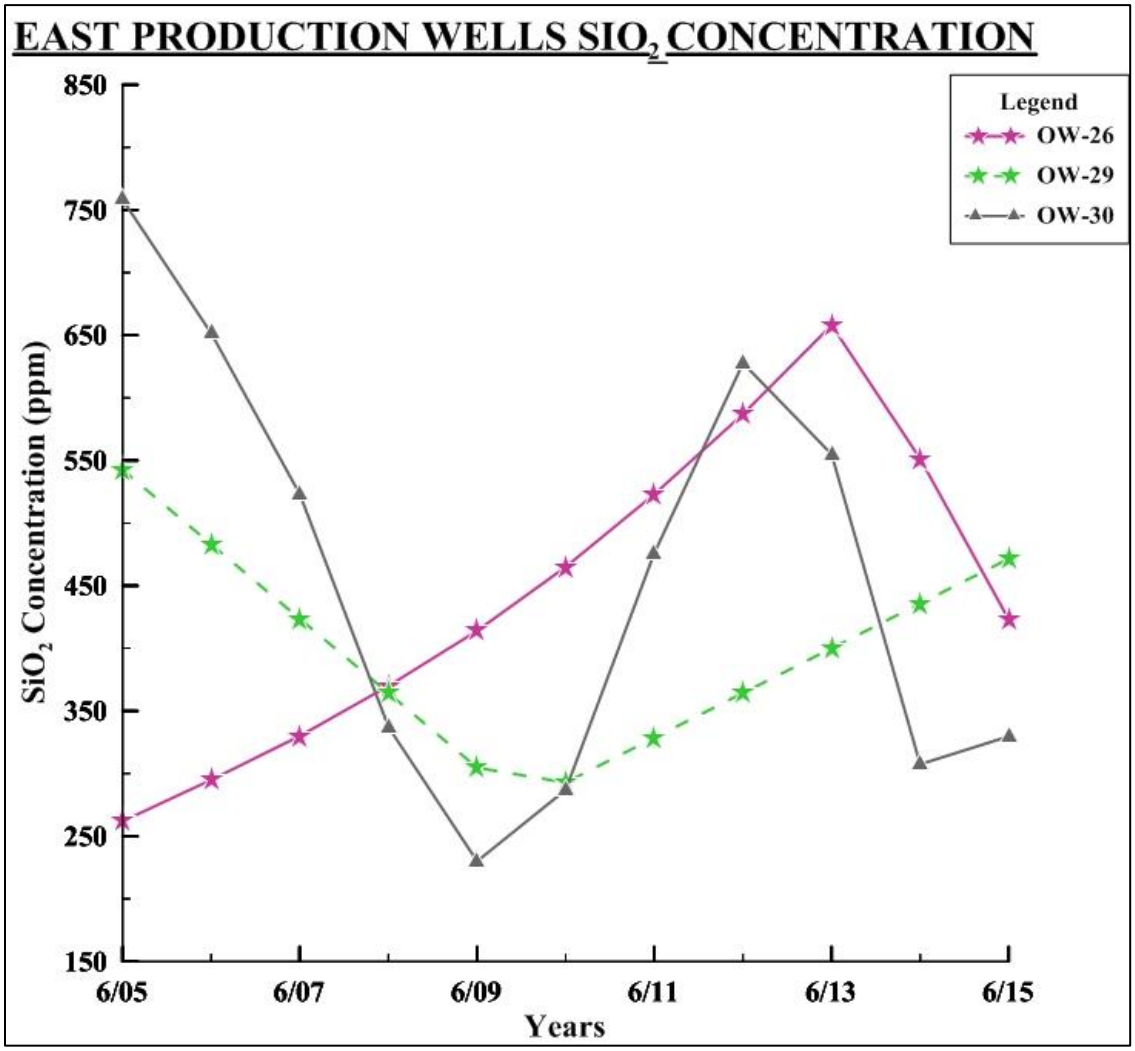

Figure 4.14 East field production wells' Silica concentrations (OW-26, 29 and 30)

SiO_2's concentration in OW-26 rose from 2005-2013 at a rate of 49.5 ppm/yr before dropping to the end of the study period at a rate of 117.419 ppm/yr.

OW-29's SiO_2 concentrations experienced a two-phase decline between 2005 and 2010 at a rate of 49.932 ppm/yr before increasing at a rate of 35.730 ppm/yr from 2010 to 2015.

OW-30's concentrations of SiO_2 dropped at a rate of 132.059 ppm/yr over the 2005-2009 interval before increasing in two phases at a rate of 132.567 ppm/yr in 2009-2012 period. The two-phase decline of 2012-2014 of a rate of 160.136 ppm/yr preceded the rise in SiO_2 by 22.285 ppm in 2014-2015.

OW-30's decline rates rose whereas its incline rates dropped with the same decline and increment rates in 2005-2009 and 2009-2012 respectively.

4.1.6.3 Magnesium Concentrations

The plot did not display an overall trend: OW-26 was stable, OW-29 was rising then declined whereas OW-30 displayed repeated cycles. The range was 0-0.629 ppm and the average concentration was 0.001-0.342 ppm/yr.

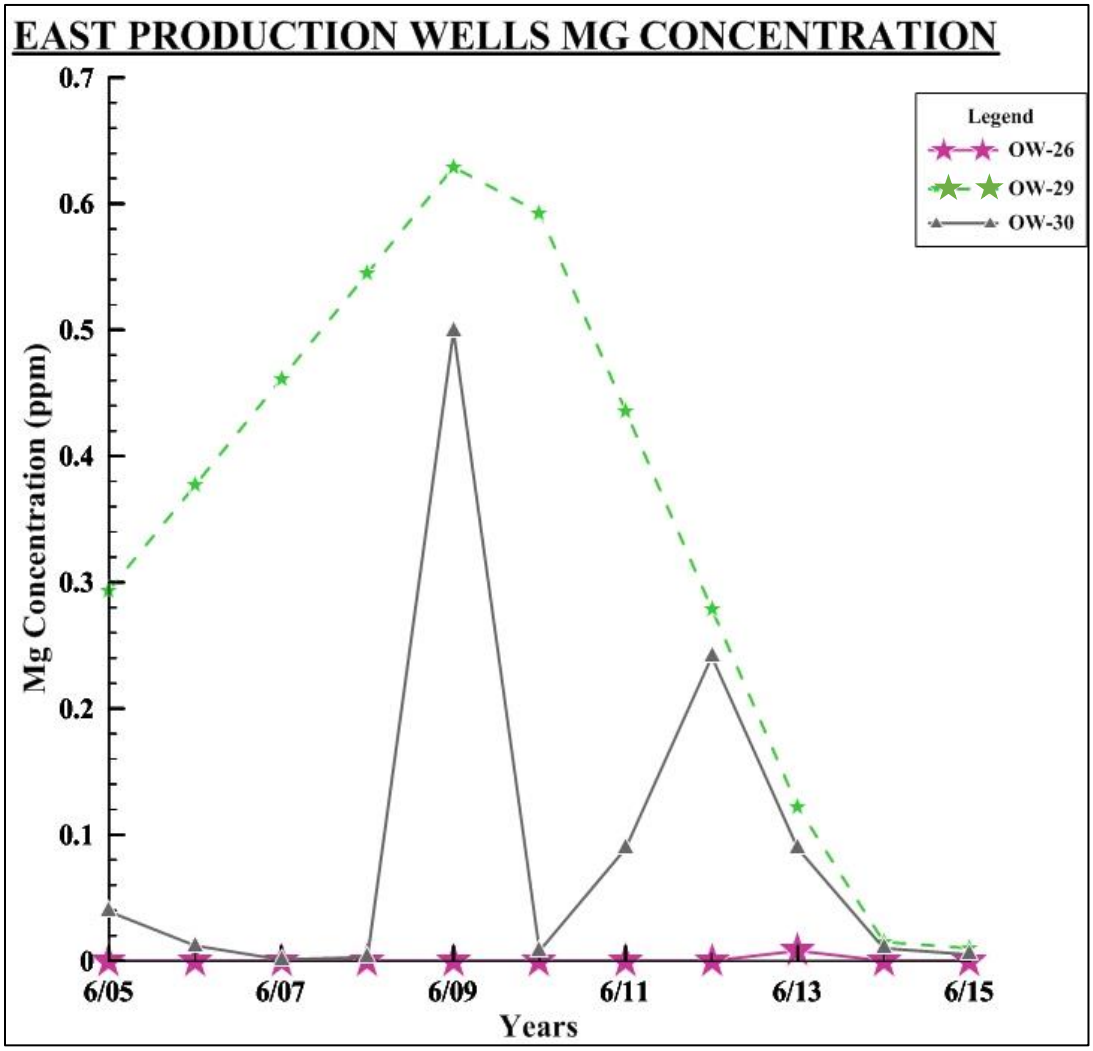

Figure 4.15 Magnesium concentrations in East field production wells (OW-26, 29 and 30)

The highest concentration was in OW-29 (0.629 ppm in 2009 and 0.01 ppm in 2015) followed by well OW-30 (0.499 ppm in 2009 and lowest value of 0.001 ppm in 2007) and lastly, well OW-26 (0.008 ppm in 2013 and lowest value of 0 ppm in 2005-2012 and 2014-2015). Hence, the order of production wells of decreasing Mg concentration was as follows: 29>30>26.

OW-29 and 30 recorded their highest values in 2009 and OW-26 and 29 recorded their lowest values in 2015. In 2013-2014, all the production wells declined and appeared stable in 2014-2015 with OW-29 and 30 recording the same values and displaying the same trend in 2014 and 2015.

OW-26's Mg concentration started with a stability phase of 0 ppm from 2005 to 2012 then increased by 0.008 ppm between 2012 and 2013. Concentration then declined by the same amount over 2013-2014 period and maintained the stable concentration of 0 ppm afterwards.

Mg concentration of OW-29 rose between 2005 and 2009 at a rate of 0.084 ppm/yr only to decline at a rate of 0.123 ppm/yr in two phases over 2009-2014 interval before finally stabilizing at 0.01 ppm.

OW-30's Mg concentration dropped between 2005 and 2007 at a rate of 0.019 ppm/yr then increased between 2007 and 2009 in two phases at an average rate of 0.258 ppm/yr. The value dropped by 0.491 ppm over 2009-2010 period before increasing at a rate 0.117 ppm/yr in the 2010-2012 interval and dropping at a rate of 0.079 ppm/yr in 2012-2015.

OW-26 had the same increment and decline rates with OW-30 increment rates dropping and its decline rates rising then dropping.

Production geothermal wells which displayed decline towards the end of their study periods were:

North-east field: OW-709 which had a decline in enthalpy, OW-713 which had a gradual decline in enthalpy and SiO_2 and a rise in Mg values and OW-728 which had a decline in SiO_2.

East field: OW-26 which had a decline trend in WHP, enthalpy and SiO_2 and OW-30 which also had a decline trend in WHP.

Thus, out of the total seven production wells, five possible production wells indicated possible declining trends in their future performance.

4.1.7 Correlations of Production wells and Parameters

Correlation of Olkaria production geothermal wells

Using correlation coefficients, each of the parameters of the production geothermal wells was evaluated in order to determine if any similarities exist among them. They are illustrated in the tables that follow.

WHP

Table 4.1 Correlation coefficients of production wells WHP

	26	29	30	709	713	720	728
26	1.0000						
29	0.9991	1.0000					
30	0.9969	0.9976	1.0000				
709	0.9857	0.9863	0.9866	1.0000			
713	0.9857	0.9864	0.9867	1.0000	1.0000		
720	0.9855	0.9862	0.9864	1.0000	1.0000	1.0000	
728	0.9858	0.9865	0.9867	1.0000	1.0000	1.0000	1.0000

The table revealed strong correlations of production well: 26 with 29 and 30; 29 with 30; 709 with 713, 720 and 728; 713 with 720 and 728 and 720 with 728.

ENTHALPY

Table 4.2 Correlation coefficients of production wells enthalpy

	26	29	30	709	713	720	728
26	1.0000						
29	0.8416	1.0000					
30	0.8750	0.9903	1.0000				
709	0.8645	0.9788	0.9640	1.0000			
713	0.8799	0.9176	0.9505	0.8812	1.0000		
720	0.9102	0.9731	0.9809	0.9460	0.9550	1.0000	
728	0.8706	0.9857	0.9749	0.9710	0.8849	0.9758	1.0000

Strong correlations existed in production well: 29 with 30, 709, 720 and 728; 30 with 720 and 728; 709 with 728 and 720 with 728.

CHLORIDE

Table 4.3 Correlation coefficients of production wells Cl concentrations

	26	29	30	709	713	720	728
26	1.0000						
29	0.1581	1.0000					
30	0.7660	0.3245	1.0000				
709	0.8378	-0.2659	0.6919	1.0000			
713	0.5152	-0.4087	0.3943	0.7268	1.0000		
720	0.1797	-0.5023	0.1156	0.4242	0.3171	1.0000	
728	0.7649	-0.3469	0.4499	0.8364	0.5948	0.4553	1.0000

Cl concentrations revealed strong correlations in production well: 26 with 709 and 709 with 728.

SILICA

Table 4.4 Correlation coefficients of production wells SiO_2 concentrations

	26	29	30	709	713	720	728
26	1.0000						
29	0.3915	1.0000					
30	0.3066	0.7667	1.0000				
709	-0.4184	-0.0707	0.3241	1.0000			
713	-0.4631	-0.0682	-0.0007	-0.0774	1.0000		
720	-0.4960	-0.1711	0.0410	-0.0199	0.7133	1.0000	
728	-0.4976	0.1810	0.1604	0.3227	0.0963	-0.0774	1.0000

From the table, correlations were observed in production well: 29 with 30 and 713 with 720.

MAGNESIUM

Table 4.5 Correlation coefficients of production wells Mg concentrations

	26	29	30	709	713	720	728
26	1.0000						
29	0.9997	1.0000					
30	0.9999	0.9997	1.0000				
709	1.0000	0.9997	0.9999	1.0000			
713	1.0000	0.9997	0.9999	1.0000	1.0000		
720	1.0000	0.9997	0.9999	1.0000	1.0000	1.0000	
728	1.0000	0.9997	0.9999	1.0000	1.0000	1.0000	1.0000

The table revealed correlations in production well: 26 with 709, 713, 720 and 728; 709 with 713, 720 and 728; 713 with 720 and 728 and 720 with 728.

From the correlation tables, OW-26 showed a moderate correlation with OW-709 in Cl and Mg; OW-29 showed a strong correlation with OW-30 in WHP, enthalpy and SiO_2; OW-709 showed a

moderate correlation with OW-713 in WHP and Mg and very strong correlation with OW-728 in WHP, enthalpy, Cl and Mg; OW-713 showed a strong correlation with OW-720 in WHP, SiO_2 and Mg and moderate correlation with OW-728 in WHP and Mg and OW-720 showed a strong correlation with OW-728 in WHP, enthalpy and Mg.

The correlations of the chosen parameters for study were interpreted with respect to the geology based on Figure 4.16.

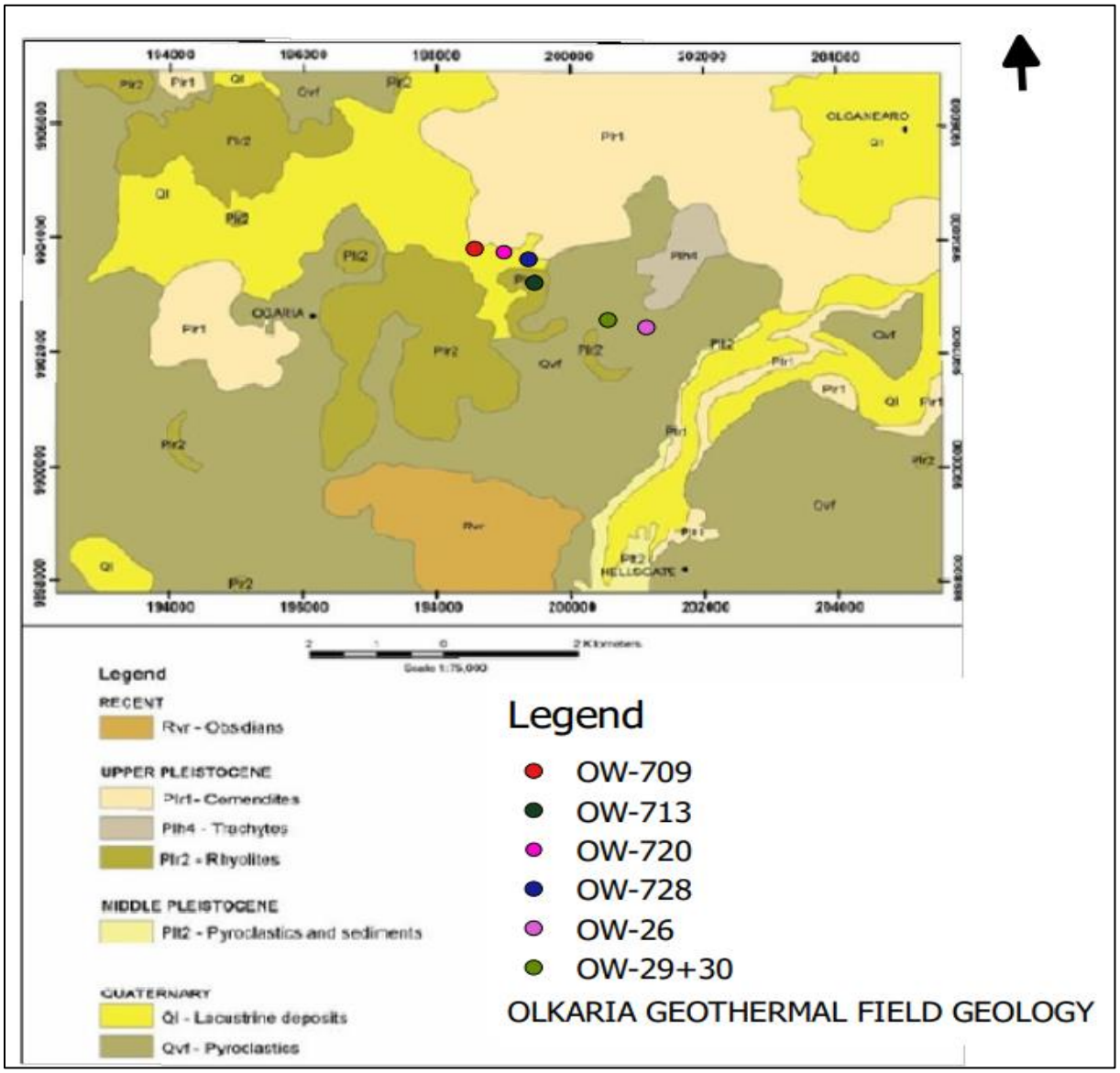

Figure 4.16 Distribution of Production geothermal wells in Olkaria Geothermal Field

The WHP correlations were restricted to production geothermal wells in the same sector which were affected by the same processes such as extensive boiling and cold influx in the East

production field and boiling, hot reinjection and SiO_2 scaling in the North-east field. The enthalpy correlations were as a result of the present up flow zones around OW-709, 720, 728, 29 and 30 and locations of cold inflow with low correlations at OW-26. The Cl values showed correlations for specific wells indicative that Cl dissolution and recharge likely occurred at specific points in the field (along Olkaria fault) whereas the SiO_2 correlations were present in OW-29 and 30 and OW-713 and 720 due to the hot up flow locations which enabled the dissolution of more SiO_2 into the fluid and the occurrence of boiling phases in these production wells that cause scaling. Mg correlations were indicative of cold influx that has been linked to recharge along Ololbutot fault.

Correlation of Parameters of Olkaria production wells

Based on the values of the coefficients, each physical and geochemical parameter was compared to the others and between the two groups to determine if any correlation existed as shown in the table below. WHP displays moderate correlation with enthalpy whereas enthalpy displays moderate correlation to Mg.

Table 4.6 Correlation coefficients of physical and geochemical parameters

	WHP	ENTHALPY	CHLORIDE	SILICA	MAGNESIUM
WHP	1.0000				
ENTHALPY	0.6314	1.0000			
CHLORIDE	-0.0704	-0.0222	1.0000		
SILICA	-0.1554	-0.1094	0.1966	1.0000	
MAGNESIUM	0.2256	0.5535	0.1590	-0.1942	1.0000

4.1.8 Future production of Geothermal Wells

During the monitoring of geothermal wells, one of the important tools that is used is pressure and its relation to production. Pressure can provide estimates for the future performance of geothermal wells (Requejo, 1996). Changes in reservoir pressure cause the mass flow and rate to change (Hidayat, 2016) with production wells declining in productivity attributed to a drop in pressures (Bodvarsson and Pruess, 1987). Hence, the key parameters for evaluation of decline of geothermal wells are pressure and productivity represented by WHP and flow rate respectively. From objective two, none of the North-east field production wells displayed a decline in WHP whereas in the East field, a declining trend in WHP was observed in OW-26 from 2014 and in OW-30 from 2013. Subsequently, investigations of the productivity using the steam flow rate were carried out to validate the declining trend.

4.1.8.1 Steam Flow Rate against Time

From figure 4.17, OW-26 commenced the start of the study period with an increase in production for a period of one year before subsequently dropping from 2006 to 2008. This was then followed by a two-phase increment to 2010 where the production started declining until the end of the study period. Based on the plot, the production in the interval 2014-2015 is higher than that recorded at the start of the study period and the declining production in the last year coincides with the fall in WHP in the same period hence validating its declining status.

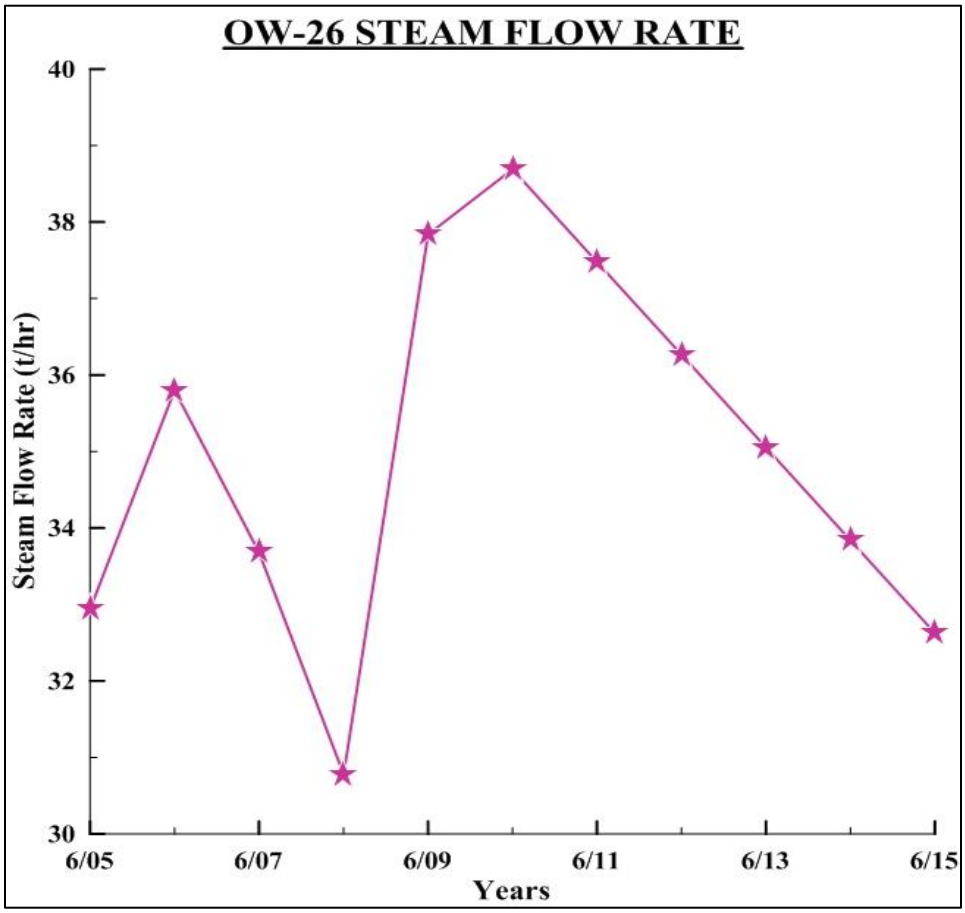

Figure 4.17 Steam Flow Rate plot of WHP declining production geothermal well OW-26

OW-30 commenced the study period with a drop in production lasting one year before undergoing an increment between 2006 and 2007. The 2007-2008 period was characterized by a small decline in production which was followed by a rise to 2013. Between 2013 and 2014, the production well had a drop in production before subsequently rising to the end of the study period. The 2014-2015 period recorded almost twice as high production as the start of the study period and the rise in production in the last year coupled with a declining WHP is indicative of recovery of the

production well hence the rise in steam flow rate as a result of mass flow increment. This indicated that OW-30 was not declining in production.

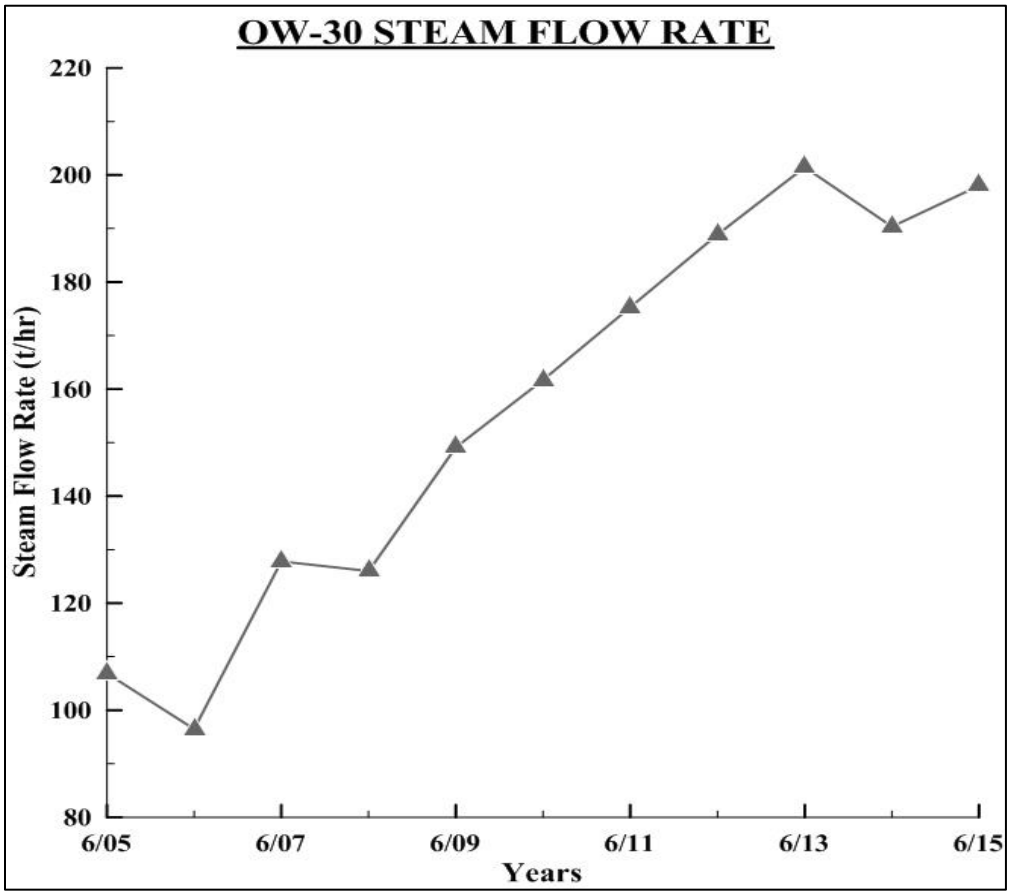

Figure 4.18 Steam Flow Rate plot of WHP declining production geothermal well OW-30

4.1.8.2 Decline curve and decline rate determination

Decline curve determination

The decline curve was determined by plotting production rate (Q) versus time represented by cumulative production (Np). Decline curve determination was based on two models: the exponential model and the harmonic model as shown in the following figures. The exponential production decline curve was represented by a semi-log plot whereby the production was converted into log values and plotted against the cumulative production of OW-26 over the one year period. The model is described as exponential due to the fact that the decline production equation is raised in terms of the power of ***e*** and the rate of change is high. Based on figure 4.18, the curve was linear and displayed a declining trend evidenced by the drop in cumulative

production and logs of the recorded intervals. Additionally, the decline appeared to be uniform between the observation points.

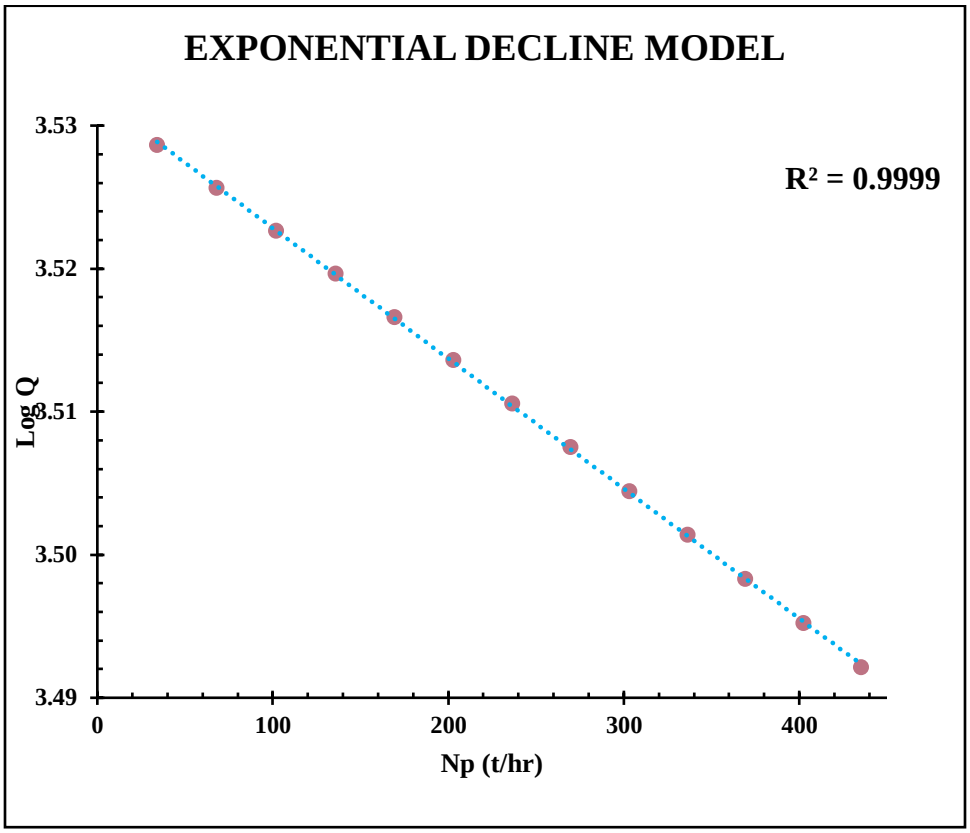

Figure 4.19 Exponential production decline curve for OW-26

The harmonic production decline curve was represented using a log-log plot whereby both production and cumulative production were converted to their log values and plotted against each other. For any harmonic model, a log-log plot should result in a linear curve and hence used in comparative studies for decline curve determination. Based on figure 4.20, the curve was rather hyperbolic and the decline rate appeared to vary between the observation points. It also displayed a decline in both production and cumulative production over time. Based on the low log values of the production, this indicated that the production of the geothermal well was low and was dropping over time.

With reference to both models, the most linear curve was obtained from the exponential decline model. Secondly, the exponential model recorded a higher R^2 value (0.9999) as compared to R^2 value of 0.8858 in harmonic model making the former the most suitable for prediction.

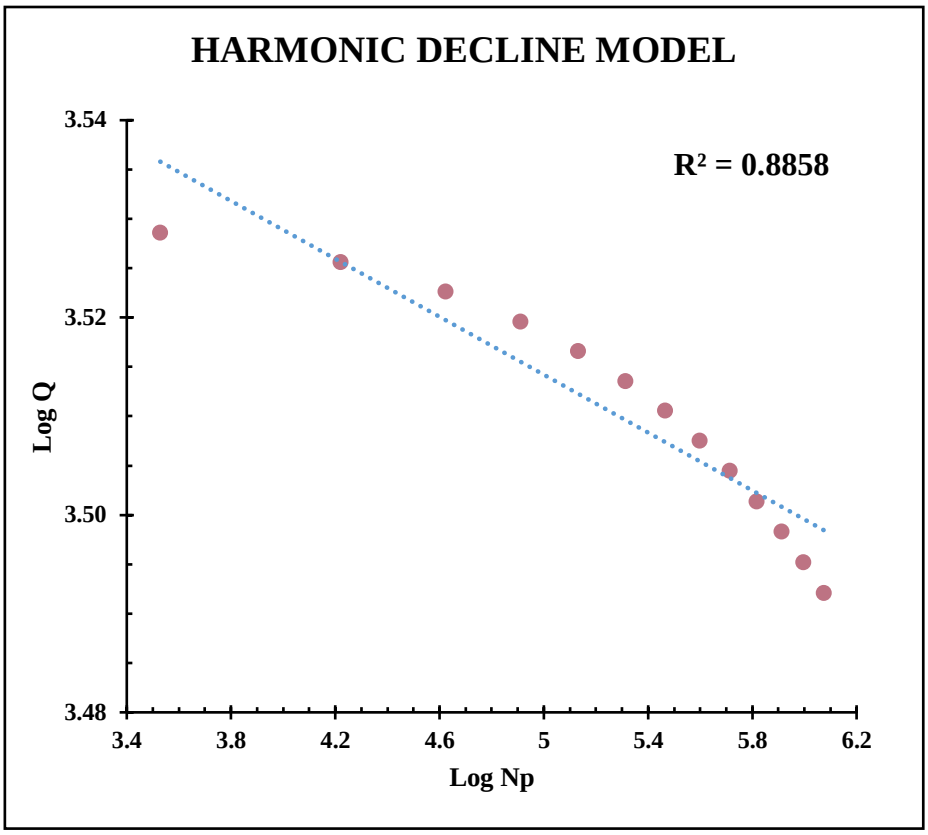

Figure 4.20 Harmonic production decline curve for OW-26

Decline rate determination

The effective monthly decline rate (De) was determined to be:

= (1/Loss ratio) *100% = (1/328.276) * 100% = 0.3046%

The nominal decline rate (D) was then determined as follows:

= -Ln (1-De) = -Ln (1-0.003046) = 0.3051% in a month = 3.6610 % a year

4.1.8.3 Prediction of future performance

The commercial limit for the production of steam from a geothermal well was arbitrarily taken as 10t/hr (Aguilar et al, 2016) and using the production of the OW-26 at the start of the study period and the monthly nominal decline rate, the production well was predicted to have a remaining production life of 401 months which is equal to 33 years and 5 months. Based on the initial date of June, 2014, the production well will have reached its commercial limit by November, 2047.

The most suitable choice of action would be to increase the amount of reinjected hot brine from the plant as soon as it is expelled and reduce the level of production within each of the production wells in the Olkaria East production field in order to prevent excessive boiling within the reservoir since the number of geothermal wells has increased. Maintaining the same levels of production with a higher number of production wells than it was previously, would increase the amount of fluid extracted and hence the drawdown resulting in frequent boiling phases.

The trends of steam flow rate of production geothermal wells was as shown in figure 4.21.

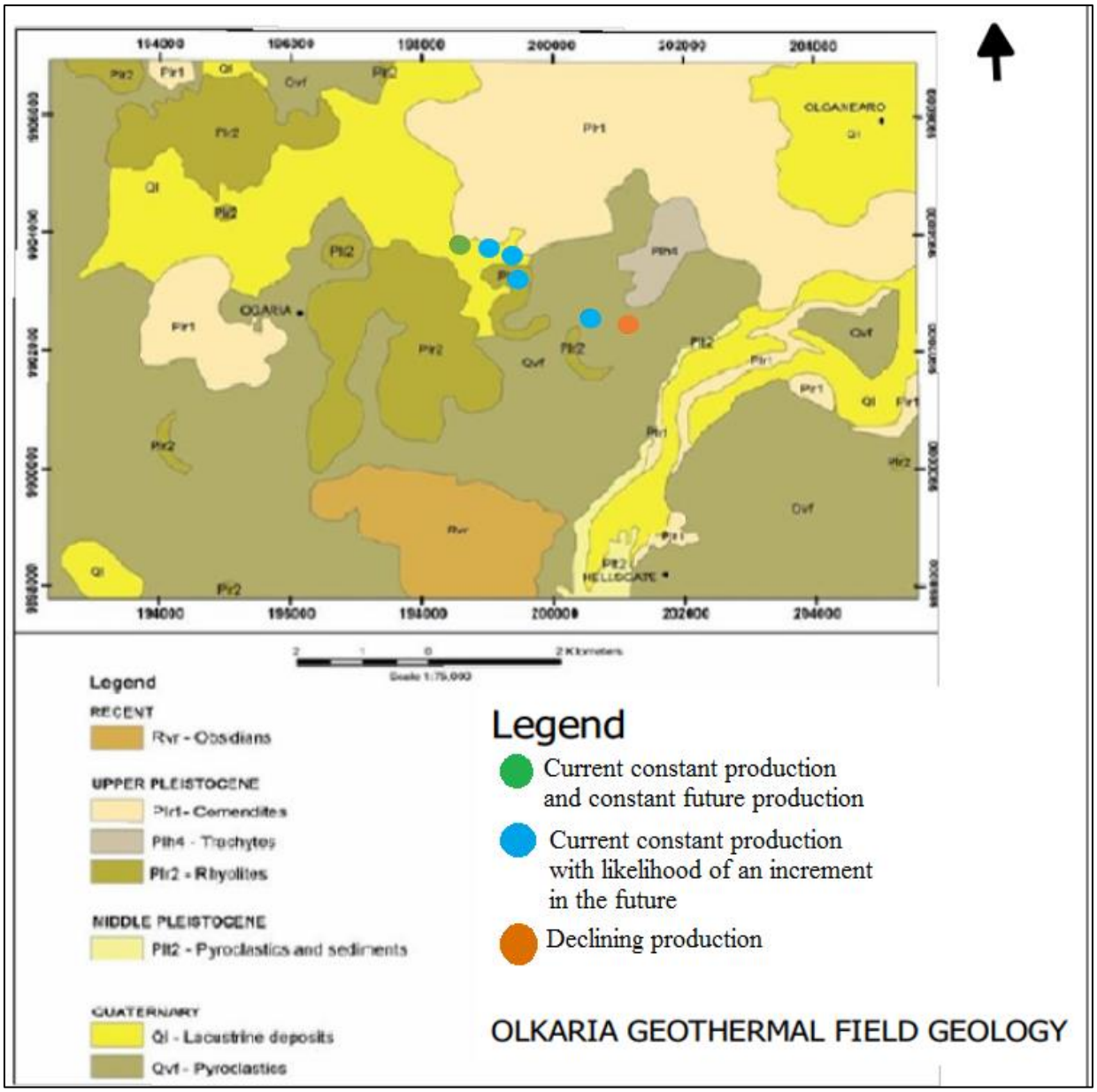

Figure 4.21 Performance trends of production geothermal wells

4.2 Discussions

4.2.1 Retired Geothermal wells

From the trends of OW-7+8, the reservoir underwent excessive boiling due to over production in 1985-1986 with the WHP rising by 2 bars due to the pressure associated with steam production and the temperatures exceeding the solubility limit for SiO_2 (340°C) causing its concentration to drop. This was followed by adiabatic cooling in 1986-1987 with the WHP dropping from 9.8 to 8.0 bars due to the release of the steam from the reservoir with cooling being sufficient to prompt the dissolution of Mg into brine. Another phase of boiling occurred in 1987-1988 due to the continuous exploitation and limited hot recharge. This was evidenced by the drop in SiO_2 and Cl concentrations since the amount of fluid in the reservoir dropped as a result of extraction hence limiting the amount of solutes that could be dissolved. Adiabatic cooling and an inflow of cooler fluids in 1988-1989 helped maintain the WHP but caused SiO_2 concentrations to drop as a result of precipitation.

Over 1989-1991, temperatures rose in the reservoir but the recharge by hot geothermal waters was insufficient causing the drop in concentrations and Cl concentration remaining constant. In 1991-1992, a drawdown caused the reservoir's rise in temperature and prompted hot recharge of geothermal water hence maintaining WHP and as boiling occurred, the solute concentrations rose with Mg remaining stable since its solubility was limited by the high temperatures. Adiabatic cooling followed in 1992-1993 with the reinjection later in the period raising WHP and causing SiO_2 to drop in values. Excessive boiling occurred again over 1993-1994 since the reinjected brine was not sufficient for the reservoir's recovery and the steam produced caused the WHP to rise. The reservoir cooled adiabatically afterwards over 1994-1995 with hot reinjection raising the WHP but not sufficient to raise the solubility of SiO_2.

Reinjection in 1995-1996 led to the dissolution of SiO_2 possibly due to increased pH and the WHP to drop with temperatures rising again in the reservoir in 1996-1997 but Cl values dropped since there was no hot up flow of geothermal waters which occurred later causing its concentrations to rise during the boiling episode over in 1997-1998 and the WHP rose because of high steam production. In 1998-1999, cold fluids flowed in due to the drawdown of the reservoir and helped maintain the WHP. A short intermediate phase of boiling occurred which resulted in adiabatic

cooling in 2000 and the temperatures were lowered enough to cause the dissolution of Mg into brine.

OW-13 trends in 1990-1991 inferred temperatures in the reservoir rose but the hot recharge was limited causing solute concentration to drop but the rise was not significant to start steam production causing the WHP to remain stable. Temperatures maintained Mg concentration and were still high not allowing its dissolution. A hot up flow of fluids and the boiling occurred in 1991-1992 followed by cold reinjection in 1992-1993 and temperatures rose again in 1993-1994 with Cl dropping as a result of no recharge of geothermal waters. Boiling occurred over in 1994-1995 and the limited hot up flow and high temperatures were evidenced by the drop in SiO_2 concentrations but the excessive steam production resulted in a rise in WHP. A possible influx of cold fluids in the later stages of boiling could have caused a slight drop in enthalpy that caused Mg to slightly rise.

The hot reinjection in 1995 prompted adiabatic cooling to occur and the rise of solute concentrations and as the volume rose in the reservoir, Mg concentration remained constant since the drop in temperatures was not sufficient to prompt further dissolution of Mg. This caused its overall concentration to drop since the concentration remained constant but the reservoir volume increased. Cold fluids flowed into the reservoir in 1996-1997 and caused SiO_2 to dissolve due to a rise in pH.

Between 1997 and 1998, a short intermediate phase of boiling occurred which caused adiabatic cooling to occur over 1997-2000 with the drop in temperatures causing SiO_2 to precipitate and explains why WHP dropped. Recovery of the reservoir caused WHP to become stable and SiO_2 concentrations to rise and as a result of cooling over time, Mg concentrations finally rose. In 2000-2001, temperatures rose in the reservoir with no recharge followed by adiabatic cooling and the cold recharge of the system from 2001-2003, helped to maintain WHP and caused SiO_2 to drop. Continuous cold recharge occurred over 2003-2005 causing WHP to rise and solute concentration to drop.

Both geothermal wells indicated that a rise in temperatures occurred over 1990-1991with hot up flow and boiling in 1991-1992 followed by cooler fluid recharge in 1992-1993 with temperatures rising in south-east as boiling occurred in the south-west over 1993-1994 and later extended to the south-east. Reinjection in 1995 affected the reservoir evidenced by the drop in enthalpy and caused

WHP and SiO_2 to rise possibly causing scaling. The rise in temperatures in the south-west occurred as an intermediate phase at OW-13 with extensive boiling occurring at OW-7+8 before adiabatic cooling commenced. Both demonstrated that the start of the study period commenced with boiling and ended with cooling of the reservoir.

4.2.2 Physical and Geochemical Trends of Production Geothermal Wells

The trends of the physical parameters of the production geothermal wells revealed that the North-east field trends were dominated by repeated cycles as a result of an abundance of different processes occurring in that section of the reservoir such as production, reinjection and recharge and whereas the East field had clear trends displaying a clear dominance of a particular process in the reservoir at different time periods. Additionally, the range of the parameters was higher in the East field as compared to the North-east field due to the extensive boiling in the reservoir caused by overproduction and limited recharge hence causing higher enthalpies and consequently, high steam production and thus higher WHPs. The rates of increment and decline tend to be higher in the North-east field possibly as a result of its lower levels of production hence giving it room to be able to increase or decrease at a higher rate as compared to the East field which is operating at its peak levels hence giving it less capability of drastically changing.

The chemical parameters of the North-east field also displayed repeated cycles further confirming the high variety of processes occurring in the reservoir while the East field production wells each displaying different trends to each other apart from the SiO_2 parameter where the repeated cycles were observed. The rising trends in Cl and declining trends in Mg indicated proximity to the hot up flow of Cl-rich fluids and boiling whereas the declining trends in Cl and rising trend in Mg were indicative of low geothermal fluid recharge and interaction of the production well to cold influx. Repeated cycles observed could be attributed to boiling, cold influx and scaling within the production wells.

Greater ranges are observed in the North-east field with respect to the Cl and SiO_2 concentrations favored by recharge of the reservoir and lower productivity of the section hence enabling the reservoir section to be able to dissolve more solids as compared to the peaking operations in the East field. As a result, their rates of change tend to be greater whereas the Mg concentrations and their rates were greater in the East field indicative of the higher influx of cooler waters into this

section of the reservoir. The overproduction caused high pressure drawdown prompting a hydraulic gradient which caused a flow of water to refill the reservoir.

Geothermal reservoirs globally are monitored through geothermal wells using physical or geochemical parameters or both. The research conducted bore similarities to several studies carried out in different reservoirs such as in: Krafla where decline was identified through use of well head conditions and dropping enthalpy values (Requejo, 1996) whereas Los Azufres and Cerro Prieto fields, Mexico used only the well head conditions to infer processes in the bottom of the production well (Aguilar et al, 2012). Bacon Manito and Geysers fields' decline was based on pressure (Requejo, 1996 and Sanyal et al, 2000) with chemical and temperature monitoring being applied in Reykjavik (Gunnlaugsson, 2008) while the Wayang Windu field was subjected to monitoring of its production and geochemical data to determine the trends, well processes, problems and interactions occurring within the reservoir (Aditya and Jantiur, 2013). Research conducted in Olkaria reservoir used various parameters to identify decline such as: Cl concentrations and trends (Karingithi, 2002), enthalpy and geochemistry (Ofwona, 2002), pressure and enthalpy (Ouma, 2008), pressure (Mariaria, 2012) pressure, temperature, enthalpy and Cl (Ouma et al, 2016).

Despite the similarities, differences in the methodology in identifying declining production wells were also observed. They included use of: mass flow in Bacon Manito (Requejo, 1996), steam delivery in Kamojang and production data and mass flow in Geysers (Ripperda and Bodvarsson, 1987 and Hidayat, 2016).

Apart from the usual parameters used to determine decline such as pressure, temperature/ enthalpy and Cl concentrations in the Olkaria reservoir, the research was able to incorporate use of two sensitive chemical parameters- SiO_2 and Mg and used the mentioned variables to determine the trends of operational production wells and their rates of change. Subsequently, use of the additional parameters enabled the inference of every possible process occurring in the reservoir (not only the most dominant), changes in the chemistry and recharge patterns hence determining the future performance of the production wells.

4.2.3 Sub-surface processes in the reservoir

North-East Production Field

Based on the trends exhibited by OW-709, 2005-2006 was characterized by adiabatic cooling after a phase of boiling with WHP rising. As the steam condensed back to the reservoir, it increased its volume and with temperatures still being relatively high, it ended up greatly diluting the already present concentration of Mg resulting in a drop in its concentration. An excessive boiling phase ran from 2006 to 2007 with production of steam raising the WHP but as a result of limited recharge of geothermal waters, the concentrations of Cl and SiO_2 rapidly declined.

Later on an influx of cooler waters commenced and raised Mg values becoming more evident the following year causing a sharp drop in enthalpy and concentrations of Cl and SiO_2. The recharge was sufficient to replace the water that had been discharged hence maintaining the WHP but the high influx which likely had a high Mg concentration increased the total volume of the reservoir waters and subsequently lowered the average Mg concentration causing it to decline. In 2008-2009, the production well was characterized by the occurrence of excessive boiling which was later followed by an influx of cool waters that raised Mg values. The influx helped to reduce the magnitude of the boiling between 2009 and 2010 and as temperatures continued to rise, Cl concentration dropped due to limited recharge of hot geothermal waters. Additionally, the drop in WHP prompted an influx of cool recharge that raised Mg values.

2010-2011 had the reservoir adiabatically cooling with the return of the condensed steam back to the reservoir lowering the average Mg concentration to a great extent. A drop in WHP caused cool recharge to occur afterwards before the reservoir started boiling in 2012-2013 exhibited by a sharp rise in WHP but lacked a recharge of hot geothermal waters however the following year as a result of limited recharge to the reservoir and continuous boiling, SiO_2 also dropped as a result of the high temperatures exceeding its solubility limit and the reservoir started producing steam hence the WHP rose. Later, an influx of cool waters took place raising the Mg concentrations greatly and likely prompted the adiabatic cooling and rise in WHP between 2014 and 2015 but with no further influx and increase in volume, Mg concentrations dropped.

OW-713 started with excessive boiling phase in 2005-2006 characterized with limited recharge of hot geothermal waters. An influx of cool waters raised Mg concentration with boiling still continuing the following year but characterized with hot up flow. Steam production and discharge

in 2007-2008 caused the volume to drop in the reservoir due to lack of geothermal water recharge and the concentrations of Cl and SiO_2 dropped and an inflow of cool water which raised Mg concentrations.

The influx prompted adiabatic cooling between 2008 and 2009 but due to the low temperatures attained, SiO_2 started precipitating and Mg concentrations rose even further. An intermediate phase of excessive boiling preceded the adiabatic cooling period between 2009 and 2010 with no hot up flow of geothermal waters but incorporation of cooled steam lowering the Mg amount present. A recharge followed afterwards and further lowered the overall concentration of Mg in the reservoir before there was a slight rise in temperatures that accompanied an adiabatic cooling phase and small influx of cool waters that helped to raise the Mg values in 2011-2012.

Excessive boiling occurred over 2012-2013 before adiabatic cooling took place with lacking geothermal waters and condensed steam reducing Mg values. Another boiling phase followed afterwards but had no steam production thus helped maintain WHP values in 2013-2014 with adiabatic cooling following afterwards allowing Mg to be incorporated into reservoir waters. The cooling continued between 2014 and 2015 allowing the WHP and enthalpy to remain constant but caused SiO_2 to precipitate whereas Mg concentration continuously rose.

OW-720 also commenced with boiling in the first year with temperatures exceeding solubility temperatures of 340°C thus causing SiO_2 to drop. This was followed by a bit of mixing that raised Mg values before adiabatic cooling occurred in 2006-2007 characterized by low geothermal water recharge. 2007-2008 had excessive boiling of the reservoir which exceeded solubility limits for SiO_2 causing its decline. The loss of steam in 2008-2009 caused a drop in WHP and prompted cool inflow later on that raised Mg concentration. The boiling phase continued but as a result of continuous steam loss and no hot up flow, the concentration of Cl also dropped in 2009-2010. Recovery occurred the following year thus their concentrations rose and the temperatures rose further leading to production of steam and rise in WHP.

The excessive boiling phase continued to 2011-2012 with the latter period having an influx raising Mg values followed by a cold recharge in 2012-2013 and hence a rise in Mg. An intermediate boiling phase preceded the adiabatic cooling observed in 2013-2014 but the cooling led to a drop in Mg. The period ended with an excessive boiling phase at a temperature of 340°C that maintained SiO_2 concentrations.

OW-728 had adiabatic cooling in 2005-2006 and dropped temperatures causing SiO_2 to precipitate but not enough to incorporate more Mg so concentration remained stable. A cold recharge followed afterwards before excessive boiling occurred in 2007-2008 and as a result of loss of fluid, a cold recharge occurred in 2008-2009 which raised the WHP further. In 2009-2010, there was a rise in reservoir temperatures but due to no hot up flow, the concentration dropped. Excessive boiling took over the following year with recharge in Cl and a drop in SiO_2 due to solubility limits being exceeded.

2011-2012 was still marked with boiling but an increment in the pH levels enabled more SiO_2 to be dissolved thus raising its value with the steam cap formation enabling the maintenance of WHP. A later influx of cool waters raised Mg values with the cool recharge in 2012-2013 that cooling steam and lowering WHP and Mg average concentrations. An intermediate excessive boiling phase preceded the 2013-2014 adiabatic cooling phase sufficient to dissolve more Mg so values rose. Another phase of excessive boiling occurred the following year but limited recharge led to a decline in concentration of SiO_2 and Cl and a maintenance of Mg values.

Based on the inferred processes, there was an occurrence of adiabatic cooling in OW-709 and 728 and a cold influx in OW-713 and 720 in 2005-2006 with excessive boiling in OW-709 and 713 in 2006-2007 and in OW-713, 720 and 728 in 2007-2008. An influx of cool waters in OW-709 and 720 in 2008-2009 was observed with boiling in OW-709, 720 and 728 and all production wells having a drop in Cl concentrations in 2009-2010. OW-720 and 728 experienced excessive boiling in 2010-2011 with a cool influx in OW-713 and 720 in 2011-2012. 2012-2013 was characterized by cold recharge in OW-720 and 728 and a drop in Cl concentrations in OW-709 and 713. 2013-2014 was preceded by an intermediate boiling phase in OW-713, 720 and 728 and hence adiabatic cooling in the mentioned production wells while 2014-2015 had OW-709 and 713 adiabatically cooling whereas the rest were excessively boiling.

East Production Field

OW-26 was characterized with excessive boiling within the reservoir between 2005 and 2007 with the high steam production causing an increment in the WHP and the limited recharge of geothermal waters leading to a decline in Cl values. As a result of no influx of cooler waters, the Mg concentration remains constant. Maximum temperatures were attained in the reservoir in 2007-2008 hence causing the enthalpy and WHP to remain constant with no further production of steam.

Consequently, this was followed by adiabatic cooling of the reservoir in 2008-2009 only for excessive boiling to occur again between 2009 and 2012.

An influx of cool waters in 2012-2013 reduced the intensity of the boiling in this time period causing the WHP to drop as steam was cooled and Mg concentrations to go up. In 2013-2014, the reservoir boiled excessively but was marked with the first increment of Cl concentration due to recharge by geothermal waters with SiO_2 declining as a result of the temperatures exceeding 340°C. Mixing within the reservoir also took place helping to stabilize the WHP in the reservoir and raise Mg values. Another cool influx occurred towards the end of the study period condensing the steam present and hence lowering the WHP but the drop in temperature was not sufficient to dissolve more Mg into the reservoir fluid.

OW-29 also started off with excessive boiling between 2005 and 2006. The boiling appeared to be occurring at maximum temperatures hence maintained the enthalpy values but as a result exceeded the solubility limits of SiO_2 hence causing its decline. A later cool inflow caused the Mg value to rise. Another episode of mixing in 2006-2007 reduced the intensity of boiling hence dropping the WHP but maintaining the enthalpy and Mg hence rises in concentration.

Excessive boiling resumed in the reservoir in 2007-2013 characterized as follows- a cool influx causing Mg values to rise between 2007 and 2009, no mixing in 2009-2010 hence the Mg values dropped and a rise in SiO_2 in 2010-2013 as a result of an increment in pH which enabled the fluid to dissolve more SiO_2. This was followed by adiabatic cooling the following year and excessive boiling in 2014-2015.

OW-30 shows that the reservoir was adiabatically cooling in 2005-2006 after an excessive boiling phase which led to a drop in SiO_2 values as a result of their precipitation and a drop in Mg since the temperatures did not cool enough to dissolve more Mg. Excessive boiling spans the reservoir from 2006-2010 characterized as follows: 2006-2007 with limited up flow of geothermal waters causing Cl and SiO_2 values to decline, 2007-2009 having limited recharge of geothermal waters and a later influx of cool waters raising Mg values and 2009-2010 attaining possible maximum temperatures hence maintaining enthalpy values and a recharge to the reservoir that raises Cl and SiO_2.

An influx in 2010-2011 reverted the reservoir to normal boiling processes maintaining the constant enthalpy and WHP, raising Mg values and dropping Cl values due to limited hot up flow. A higher influx occurred in 2012-2013 which lead to the overall dilution of the Mg causing concentrations to drop. 2013-2014 was preceded by an intermittent excessive boiling phase which prompted the adiabatic cooling and led to the precipitation of SiO_2 with the decline of Mg due to increment of volume of the reservoir as a result of condensed steam. Finally the reservoir boiled in its last year of the study period.

Based on these inferences, excessive boiling occurred in 2005-2006 for OW-26 and 29, 2006-2007 for OW-26 and 30, 2007-2009 for OW-29 and 30, 2009-2010 for all three production wells and 2010-2012 for OW-26 and 29. Additionally, limited recharge of geothermal waters was observed in 2006-2009 and 2010-2012 for OW-26 and 30, an inflow of cool waters in 2007-2009 for OW-29 and 30 and 2012-2013 for OW-26 and 30 and adiabatic cooling occurring in 2013-2014 for OW-29 and 30.

The trends exhibited by the North-east production wells were generally steady but were characterized by intermittent sharp trends; majorly observed in SiO_2 and Mg concentrations for extensive periods. The trends in East production wells were dominated generally by a rising trend for the WHP, enthalpy and Cl parameters whereas SiO_2 was fluctuating and Mg displayed general sharp trends. Any changes within the reservoir were reflected immediately in the parameters that are interrelated since changes in the physical aspects of the reservoir immediately affect the chemistry of the Olkaria reservoir.

The parameters under study were the physical and geochemical parameters. The physical parameters included: Well Head Pressure and Enthalpy whereas the geochemical parameters included: Chloride, Silica and Magnesium concentrations.

Changes within a reservoir such as drawdown are indicated by WHP and enthalpy. These physical parameters cause changes in the geochemistry of the reservoir. These changes are caused by the occurrence of certain sub-surface processes such as boiling, adiabatic cooling, influx of cold fluids and reinjection (Barragán et al, 2016).

Boiling is caused by exploitation and is characterized by the formation of two phases as the liquid part of the reservoir is converted into steam which is associated with higher enthalpies. It is

associated with a rise in enthalpy, SiO_2, Cl and pH and a drop in Mg concentration and WHP (Marini, 2004; Thorhallson, 2012 and Gunnlaugsson et al, 2014). It is associated with corrosion which destroys equipment, cooling and SiO_2 scaling which causes clogging of equipment. Generally, for high enthalpy systems, boiling tends to occur around 300°C while adiabatic cooling which follows an episode of boiling is associated with a drop in enthalpy and a rise in solute concentration; that is SiO_2 and Cl due to steam loss (Kemboi, 2015). Cold recharge and reinjection cause SiO_2 and Cl concentrations and enthalpy to drop and Mg and WHP and pressure to rise. Pressure rises when there is a recharge to the system but due to the recharge fluid having lower temperatures than the geothermal brine, the overall temperature of the fluid will drop. When pressure falls as a result of extraction, volume in the reservoir drops and due to the contact with hot rocks, the heat acquired is distributed throughout a limited volume causing temperatures to rise (Burgos, 1999; Sigfusson and Gunnarsson, 2011 and Barragán et al, 2016).

With respect to Olkaria Geothermal Field, the WHP values are usually associated with both the steam and brine phase extracted from the reservoir which are subjected to separation on route to the plant where steam is the only utilized component. The field has been subjected to frequent boiling phases occurring around 500-700m depth (Bodvarsson and Pruess, 1987) which was caused by overproduction and consequently affected the concentration of elements in the reservoir together with the hot up flowing brine in zones of permeability such as faults and fractures. The dominance of the Na-Cl waters in the field can be attributed to the dissolution of the Na component of the peralkaline rocks by the geothermal fluids as it flows through the strata whereas the Cl concentrations have been attributed to dissolution of the anions from amphiboles found in trachytes and halogens common in rhyolites which make the dominant component of the lithology of the Olkaria Geothermal Field reservoir. The SiO_2 values also are attributed to the lithology of the rocks in the area that are dominantly silicate whereas Mg values are present as a result of cooler influx into the reservoir and likely originate from the mafic rocks making up the geothermal field such as basalt.

Geothermal fields' decline has been attributed to the factors of cooling, corrosion and scaling. With respect to Olkaria geothermal field, all the production geothermal wells suffered from episodes of cooling as a result of mixing or adiabatic cooling whereas OW-713, 728 and 30 were the only ones to suffer from scaling.

Based on the study of the retired geothermal wells, OW-13 clearly indicated how the behavior of the parameters' trends could infer the decline of production wells. Generally, the optimum operational WHP was 5 bars whereby any decline in pressure would indicate a drop in the supply of pressure by steam required to turn turbines. Additionally, a drop in enthalpy was an indication of decline which would subsequently result in drop in Cl and SiO_2 concentrations. The drop in enthalpy could be attributed to excessive cooling or mixing which would cause a rise in Mg values.

4.2.4 Statistical correlation of production geothermal wells and parameters

Olkaria geothermal wells

The correlation coefficients revealed that there existed similarities between production wells depending on the parameters used. In the determination of the extent of similarity, production wells displaying correlations in two or more variables were identified.

Based on this, OW-26, 709 and 713 showed similarity to a moderate extent with OW-709, 713 and 728 respectively; a strong similarity existed between wells OW-29, 713 and 720 with OW-30, 720 and 728 respectively. The greatest similarity was observed in wells in the North-east field between OW-709 and OW-728. Conclusively, none of the wells displayed complete similarity to each other with the closest similarity observed in four variables between OW-709 and 728. Additionally, OW 728 tend to correlate to all the other wells in the North-east field.

The correlations observed in the production wells revealed that WHP was controlled by the prevailing sub-surface processes occurring in the same field whereas the enthalpy values were dependent on the proximity of the production wells to hot up flow zones and cold influx. The geochemistry on the other hand could likely be controlled by the recharge fault system controlling both the hot brine and the cold recharge along Ololbutot fault.

Physical and Geochemical parameters

The correlation coefficients revealed that between the two physical parameters of WHP and enthalpy, a moderate correlation exists whereas the relationship between WHP and geochemical parameters shows a low to negative correlation. Enthalpy displayed a negative correlation with the geochemical parameters apart from Mg. Cl had low correlation to the other geochemical parameters whereas SiO_2 had a negative correlation to Mg.

4.2.5 Declining Production Geothermal Wells

Production of electricity in a geothermal power plant is dependent on the supply of steam. Decline within the geothermal reservoir is caused by a number of factors such as production, scaling, influx of cool waters, changes in enthalpy, bleeding, drilling of make-up wells, seismicity and skin effect/well damage hence focus is placed on monitoring any declines in pressure and production (Requejo, 1996).

Production and exploitation cause pressure drawdown due to extraction of mass from the reservoir which results in a drop in the steam supplied resulting in a loss in production. The over extraction of steam especially of shallow production wells has been associated with the rapid depletion of the steam zone and the drop in steam supply. Scaling on the other hand occurs when there is a fall in pressure and temperature with the latter affecting the chemistry or cold recharge. SiO_2 scaling is quite common with SiO_2's concentration being able to rise with increase in temperatures. A drop in temperatures commonly caused by cooling usually reduces the solubility of SiO_2 in the fluids hence prompting its precipitation to get rid of the excess concentration in the reservoir. The SiO_2 commonly precipitates within the walls of the geothermal wells hence reducing its outlet dimensions and reducing the amount of flow to the surface.

Influx of cool waters commonly occurs due to reinjection or fluid mixing. Due to withdrawal during production, fluids in the reservoir require replacement but dependence on the natural recharge is not possible since the rate of recharge is infinitesimal to the rate of a producing geothermal well. As a result, fields usually inject brine back into the reservoir from the plant but the fluid is usually at lower temperatures and continuously cools with time hence if there is a rather direct or rapid route of flow to the reservoir without the fluid being heated to the reservoir temperatures, the fluid ends up cooling the reservoir.

On the other hand, as the geothermal fluid is flowing in the sub-surface or through faults, it can also interact with percolated rain water or groundwater and the mixing between these waters not only alters the chemistry but also lowers the temperature of geothermal brine. Enthalpy changes are attributed to inflow of cool waters into the reservoir or the change in the feed zones of exploitation from high enthalpy shallow steam dominated zones to deep liquid dominated ones which are associated with lower temperatures.

Bleeding of steam and brine and damage within geothermal wells results in decline in supply to the plant whilst maintaining constant pressure in the field while the increase in the number of make-up wells also contributes to decline since the steam supply being acquired from the reservoir is now divided by a higher number of outlets thus causing a geothermal well to record lower values than it previously was.

Seismicity is a common phenomenon in rift valleys and hence can be an important factor in geothermal energy production especially when fields occur in such an area. Seismic activity is responsible for formation of faults, activation or alteration of existing ones in a bid to release pressure. Well damage usually results in the loss of fluids from the reservoir through compromised well set-ups and it causes pressure drawdowns as production wells are forced to over extract from the reservoir to maintain supply to the plant and damage to the well tends to increase with a decline in production.

Olkaria Geothermal Field is susceptible to cold recharge which occurs as a result of numerous boiling phases. The boiling tends to result in steam production which upon release and cooling causes a drop in water levels in the reservoir prompting a hydraulic gradient to occur and trigger the influx of cooler waters from reinjected wells or nearby water sources to maintain levels in the reservoir. The cold influx as a consequence cools fluids in the reservoir and causes temperatures to drop hence enthalpy values usually fall. Enthalpy is also likely to fall due to the drilling of deeper production wells in the field which harness the brine component of the reservoir which has lower enthalpy values. Seismicity is also a likely factor to affect production in Olkaria Geothermal Field since the field is characterized by numerous faults and some micro-activities.

Additionally, the faults are the dominant conduits for transport of fluids in the Olkaria Geothermal Fluid hence the Kenyan Rift Valley is susceptible to seismic activity. From the SiO_2 trend graphs, some of the production wells demonstrated scaling during their production history and occurs when the production well has cooled extensively to temperatures of 140°C due to adiabatic cooling and cold recharge and considering the high values of SiO_2 concentration in the North-east field and two of its production wells having displayed periods of scaling, the Olkaria Geothermal Field is quite vulnerable to scaling especially in collaboration with the frequent cold influxes and dropping enthalpy values.

Pressure and production are interrelated such that a drop in pressure reflects conditions in the reservoir whereby a drop in steam production usually results from pressure drawdown and consequently results in a drop in production. Drops in pressure can be caused by production or mass flow since extraction of fluid causes pressure drawdown while an increment in mass flow cools the steam within a boiling reservoir which subsequently causes pressure to fall (Aguilar et al, 2012). The pressures in OW-709, 713, 720 and 728 in Olkaria North-east production field and OW-29 in Olkaria East production field did not display a decline as a result of the maintenance of constant production levels and balance between withdrawals from the reservoir and the reinjection and recharge taking place. Additionally, these production geothermal wells are located in zones of up flow which indicates a constant recharge of geothermal waters and dissolution of elements into the reservoir fluid.

From the steam flow rate graphs, OW-30 recorded almost five times the steam flow rate of OW-26 and had a rising trend validating that the production well did not display any decline and the drop in pressure was attributed to increase in mass flow which indicated that the production well was recovering. A decline in both WHP and steam flow rate was identified only in OW-26 which appeared to have been declining in production for the last five years of the study period with the slow rate of decline not causing an immediate drop in pressure. The drawdown which started towards the end of the study period could have been attributed to adiabatic cooling and influx of cool waters within an extensively boiling reservoir.

In order to determine the decline rate, data was normalized pertaining to the flow rate using back pressure equation and the prevailing pressure in the well head (Aditya and Jantiur, 2013) in order to determine the actual trend of decline (Reyes et al, 2006). The equation entailed using values of 40 bars for the static pressure, 6 bars for the standard flowing pressure (Mutinda, 2009) and 5 bars for the standard flowing WHP (Mariaria, 2012).

The steam flow rate was plotted using decline curves which are an important tool for reservoir monitoring and the basis for estimating future production using past data either by linear or harmonic functions based on the assumption of a smooth decline of a geothermal well's mass flow. In determination of decline curves for prediction, the model could either be exponential with a constant rate of decline or harmonic whose rate tends to change over time (Hidayat, 2016). Based on the curves plotted, the harmonic model was rather hyperbolic rather than linear whereas the

exponential model was more linear and had a higher R^2 value. The determination of decline rates is usually based on the Arps method (Requejo, 1996). The 3.66 % annual decline rate indicated that the production well is gradually declining.

Prediction of the future performance of a production well/field is important to enable the effective management of a production field and provide an estimate of the future production (Hidayat, 2016). Based on the exponential predictive formulae, OW-26 has 33 years and 5 months to go (as from June 2014) before it has attained its economic limit and due to the increasing number of make-up and production wells in the Olkaria Geothermal Field.

OW-26's decline could be attributed to limited recharge and overproduction over the years which has caused frequent boiling. The observed decline rate and the remaining long production life of the geothermal well has been possible as a result of the frequent hot reinjections that helped maintain production. Olkaria East production field had reported 3.7 % decline as a result of the geothermal wells over withdrawal and inflow of cooler fluids (Ouma, 2008) which is almost similar to the determined decline rate.

These trends in Olkaria geothermal field were also observable in other geothermal fields in the world such as the Geysers field and Larderello had been characterized by drastic drops in pressure as a result of overproduction and drilling of make-up wells with reinjection helping to reduce those declines (Ungemach and Antics, 2010) while Los Azufres' overproduction resulted in a rise in enthalpy due to boiling. Cl concentration rose but as the liquid fraction decreased, the concentration started dropping. Reinjection measures carried out reduced the enthalpy (Barragán et al, 2016). Berlin geothermal field, El Salvador had a marked increase in Cl concentration due to recovery and boiling (Montalvo and Axelsson, 2000) and the Wairakei field, New Zealand production caused drop in pressure and a boiling phase that led to the development of a zone of steam. Enthalpy dramatically rose with the Cl values drop caused by cold influx and drop of temperature in the reservoir (Pratama, 2015). The reinjection temperatures were above 180°C in order to prevent scaling that is associated with drop in temperatures of geothermal fluid.

Decline curve analysis has been applied to various geothermal fields such as: Kamojang which had a 20% decline attributed to location of make-up wells near production wells and scaling (Sasradipoera et al, 2000) and the Geysers which had a 1.2% decline due to over-extraction (Sanyal et al, 2000).

CHAPTER FIVE: CONCLUSIONS AND RECOMMENDATIONS

5.1 Conclusions

Generation of electricity from geothermal resources is highly dependent on two factors- pressure and constant supply of steam. When a production well suffers from pressure drawdown, steam production also falls and as such if the geothermal well undergoes continuous decline, it will consequently become unsuitable for steam supply. When production wells are no longer capable of supplying an optimum amount of steam, they are removed from the supply channel and termed as retired. Instead of shutting these retired geothermal wells permanently, they are converted into reinjection or monitoring wells to aid in replacing extracted fluid and keeping track of reservoir conditions respectively.

Based on the five parameters studied (WHP, enthalpy, Cl, SiO_2 and Mg), the retired geothermal wells' trends displayed repeated cycles apart from Mg whose concentration is likely controlled by cool influxes into the reservoir. The retired geothermal well OW-7+8 recorded the highest values in WHP and Mg whereas the rest of the parameters were highest in retired geothermal well OW-13 with both Mg and WHP being characterized by stable phases. The retired geothermal wells were characterized by boiling with temperatures exceeding 340°C, adiabatic cooling, SiO_2 scaling and cool influx.

The retired geothermal wells trends of repeated cycles in the five parameters were also observed in the North-east production wells with the former having higher values in all the parameters excluding Mg. The sub-surface processes observed in the retired geothermal wells were all observed in OW-728 with all the production wells boiling and OW-720 and 728 exceeding temperatures of 340°C and adiabatically cooling. SiO_2 scaling and intermediate boiling phases were observed in OW-713 and 728. The retired geothermal wells' similarity with the East field was its repeated cycles in SiO_2 with the former recording higher WHPs, Cl and SiO_2 concentrations. The North-east field production wells had higher enthalpy due to the frequent boiling phases while the higher Mg values was as a result of the higher influx of cooler waters. The similar processes observed were boiling, adiabatic cooling and cool influx. Temperatures exceeded 340°C in all East production wells apart from OW-30 which was characterized by SiO_2 scaling and an intermediate boiling phase.

The North-east production wells had OW-709 recording the fourth highest values in all the parameters except Cl while OW-728 recorded the third highest values in enthalpy, SiO_2 and Mg. The same order of hierarchy was observed in both enthalpy and SiO_2 with no production wells being characterized by the same processes. All the production wells boiled, adiabatically cooled and had cool influx. All the parameters for all the production wells displayed repeated cycles which were similar to the trends in SiO_2 for the East production wells. They also had higher values in Cl and SiO_2 indicative of more recharge in the North-east field. The East production wells had higher values in WHP and enthalpy than North-east field due to excessive boiling while Mg was higher due to the cool influx. The production wells displayed different trends to each other in the same parameter with OW-29 recording the highest values in enthalpy, Cl and Mg while OW-26 recorded the third highest values in WHP and enthalpy. OW-30 was characterized by repeated cycles in its trends with all production wells boiling, adiabatically cooling and having cool influx.

Boiling phases in both fields have resulted in pressure drawdowns. The frequent drawdowns are responsible for the dominant behavior of repeated cycles in the trend rather than an expected general trend. High enthalpy values observed in Olkaria Geothermal Field are attributed to the shallow depth magmatic intrusions but it records declines often. The drops in enthalpy are caused by additional geothermal wells being drilled which cause further division of output and overall individual drop in enthalpy, influx of cooler fluids and the tapping of lower sections of the reservoir associated with lower enthalpy.

Geochemistry had irregularities caused by the ongoing production which extracts fluid from the reservoir, presence of a two-phase reservoir whereby both phases affect the concentration of solutes and multiple feed zones whose temperatures and solute content vary. Hot up flow of Cl-rich geothermal fluids occurs along Olkaria fault which transects these two fields and recharges the geothermal reservoir. The Cl concentration of the Eastern sector is further affected by frequent boiling which is caused by the reservoir's contact with hot volcanic rocks. A dominant declining trend in Cl concentrations is a direct result of the cooler influx into the reservoir further validated by the rise in Mg. The geology of the reservoir and field consist of trachytes, basalts and rhyolites and the volcanism is dominantly silicic. These indicate high SiO_2 content but as a result of the influx of cooler waters into the reservoir, the concentrations tend to drop as a result of decrease in solubility and the scaling within the plant equipment.

Mg and WHP of production wells had very strong correlations while Cl had weak to strong correlations. Strong correlation was also observed in enthalpy while weak to average correlations were present in SiO_2. Negative correlations were observed in Cl and SiO_2.

Two production wells in the East field had a drop in WHP with OW-30 having an increase in steam flow rate hence only OW-26 was declining. Exponential curve was used to assess the decline which was valued at 0.30% equivalent to 3.66% a year. This means that currently, the production well has 27 years and 1 month (as per October 2020) until its production life hits its economic limit in November, 2047.

Conclusively, the trend graphs were able to reveal the changes in the values and concentrations of key parameters and from the general trends aid in the identification of potential declining production wells. Based on the comparison of the trends of different geothermal wells on the same graph, it was possible to validate no two production wells are identical hence their future productive life would differ. The trends collectively were able to identify the sub-surface processes occurring during their production history and was able to hence answer the question of the rise in decline in 1998 in Olkaria Geothermal Field. This can be attributed to substantial cooling as a result of cold influx and adiabatic cooling after an intermediate boiling phase.

From the sub-surface processes, major challenges to the Olkaria Geothermal Field were seen to be cold influx and SiO_2 scaling which can be mitigated through the constant use of hot reinjected brine whereas the decline in the production wells is likely caused by overproduction and the inflow of cooler waters. From the trends of the production wells, declining production wells can be identified and subsequently from decline curves, the future production and rate of decline of the production wells can be determined using normalized steam flow rate and Trend analysis.

5.2 Recommendations

The production wells have been characterized by frequent phases of boiling during their chosen study periods as a result of overproduction and large pressure drawdowns. In order to reduce these, production needs to be managed in a way that the amount of fluid being extracted is reduced to the optimum requirement needed for production of electricity in a day's span.

As a result of withdrawals from the reservoir, geothermal fluid needs to be replaced. It is herein recommended that this be carried out through reinjection in order to maintain fluid levels and more importantly, the reservoir pressures.

Monitoring of production wells is key in the management of the geothermal field as a whole so to prolong its production life, monitoring of both the physical, production and chemical parameters should be carried out repeatedly in order to be able to identify any indications of decline within a production well(s) which can then be subjected to further scrutiny to evaluate whether any problems will arise. This will subsequently help to address any issues arising in its early stages.

Occasionally, production wells tend to suffer from scaling associated with the cooling of the fluids which causes the precipitation of substances like SiO_2 or $CaCO_3$. In order to reduce the decline of the steam supply of the production well, examination of the well equipment and cleaning of the production wells through dosing should be carried out.

From predictions made of declining production wells' future performance, make up wells need to be drilled in order to prolong the life of the declining production well but if the geothermal well has been in production for its projected life span of 30 to 40 years, then it could be approaching retirement. This then prompts the need to drill new make-up wells to supply the needed steam for the plant.

REFERENCES

Abebe, T. 2000. Geological limitations of a geothermal system in a continental rift zone: example of the Ethiopian rift valley. [Internet]. Available from: https://www.geothermal-energy.org/pdf/IGAstandard/WGC/2000/R0030.PDF [1-4-2019

Aditya, H. and Jantiur, S. 2013. Production decline analysis of dry steam wells in Wayang Windu field. **SGP-TR-198**. [Internet]. Available from: https://pangea.stanford.edu/ERE/pdf/IGAstandard/SGW/2013/Hernawan.pdf [15-06-2019].

Agonga, O. 1992. Geothermal geology: stratigraphy and hydrothermal alteration of well OW-716, Olkaria geothermal area, Kenya. **10**. [Internet]. Available from: https://orkustofnun.is/gogn/unu-gtp-report/UNU-GTP-1992-10.pdf [12-7-2019].

Aguilar, A.A., Barragán, R.M. and Arellano, V. 2016. Analysis of production-decline data: case of geothermal wells as renewable energy. *IOSR Journal of Engineering*, **6**(10), pp. 32-40.

Aguilar, A.A., Montalvo, G.I., Gómez, V.A., Verma, M.P. and Morales, G.B. 2012. Declining productivity in geothermal wells as a function of the damage effect. *Geofisca international*, **51**(4), pp. 339-348.

Allen, D.J., Burgess, W.G. and Darling, W.G. (1989). Geothermics and hydrology of the southern part of the Kenya rift with emphasis on the Magadi-Nakuru area. *BGS report SD/89/10*. **68**. 67 pp.

Ambusso, W.J and Ouma, P.A. 1991. Thermodynamic and permeability structure of Olkaria North-east geothermal field: Olkaria fault. *Geothermal council transactions*, **15**, pp. 237-242.

Atkilt, G. 2001. Soil survey to predict characteristics relevant to land management (Naivasha, Kenya). MSc. thesis. University of Iceland.

Axelsson, G., Arnaldsson, A., Ármannsson, H., Árnason, K., Einarsson, G., Franzson, H., Frdriksson, T., Gudmundsson, G., Gylfadóttir, S., Halldórsdóttir, S., Hersir, G., Mortensen, A., Thordarson, S., Jóhannesson, S., Bore, C., Karingithi, C., Koech, V., Mbithi, U., Muchemi, G., Mwarania, F., Opondo, K. and Ouma, P. 2013. Updated conceptual model and capacity estimates for the Greater Olkaria Geothermal System, Kenya. **SGP-TR-198**. [Internet]. Available from: https://www.researchgate.net/publication/288324333_UPDATED_CONCEPTUAL_MODEL_AND_CAPACITY_ESTIMATES_FOR_THE_GREATER_OLKARIA_GEOTHERMAL_SYSTEM_KENYA [9-05-2019].

Baker, B.H. and Wohlenberg, J. 1971. Structural evolution of the Kenya rift valley. *Nature*, **229**, pp. 538-542.

Baker, B.H., Williams, L.A.J., Miller, J.A. and Fitch, F.J. 1971. Sequence and geochronology of the Kenya rift volcanoes. *Tectonophysics*, **11**, pp. 191-215.

Barragán, R.M., Arellano, V.M. and Nieva, D. 2016. Analysis of geochemical and production well monitoring data- a tool to study the response of geothermal reservoirs to exploitation. [Internet]. Available from: https://www.intechopen.com/books/advances-in-geothermal-energy/analysis-of-

geochemical-and-production-well-monitoring-data-a-tool-to-study-the-response-of-geotherm [24-08-2019].

Bodvarsson, G.S. and Pruess, K. 1987. East Olkaria geothermal field, Kenya. History match with production and pressure decline data. *Journal of Geophysical research*, **92** (B1), pp. 521-539.

Burgos, M.I.M. 1999. Geochemical interpretation of thermal fluid discharge from wells and springs in Berlín geothermal field, El Salvador. **7**. [Internet]. Available from: https://www.semanticscholar.org/paper/GEOCHEMICAL-INTERPRETATION-OF-THERMAL-FLUID-FROM-IN-In%C3%A9s-Burgos/e86c114580935d4a9434d03174834393ac1eb5c5 [4-10-2019].

Çakin, A. 2003. Environmental effects of geothermal applications. Case study: Balçova geothermal field. MSc. thesis. İzmir Institute of Technology.

Clarke, M.C.G., Woodhall, D.G., Allen, D. and Darling, G. 1990. Geological, volcanological and hydrogeological controls of the occurrence of geothermal activity in the area surrounding Lake Naivasha, Kenya. Ministry of Energy. 95 pp.

Coghlan, A. 2018. A little book of R for time series: release 0.2. [Internet]. Available from: https://silo.tips/download/a-little-book-of-r-for-time-series [15-9-2019].

Gehringer, M. and Lokshav, M. 2012. Geothermal handbook: Planning and financing power generation: Energy Section Management Assistance Program. **002/12**. [Internet]. Available from:https://www.esmap.org/file/DocumentLibrary/FINAL_Geothermal%20Handbook_TR002-12_Reduced.pdf [23-09-2020].

GENZL. 1992. Reservoir review and simulation of the Kamojang field relating to production decline and steam supply for an additional 1x55 MWe unit. PERTAMINA. Internal report.

GIBB Africa Ltd. 2014. 140MW Olkaria V geothermal power plant in Greater Olkaria area in Naivasha sub-county, Nakuru County: Environmental and Social Impact Assessment. [Internet]. Available from: http://www.eib.org/attachments/compalints/eia_1104-olkaria-v-full-esia-brief-report.pdf [18-10-2020].

Gunnlaugsson, E. 2008. Importance of chemistry in geothermal exploration and utilization. [Internet]. Available from: https://orkustofnun.is/gogn/unu-gtp-sc/UNU-GTP-SC-06-15.pdf [28-03-2019].

Gunnlaugsson, E., Ármannsson, H., Thorhallsson, S. and Steingrímsson, B. 2014. Problems in geothermal operation- scaling and corrosion. [Internet]. Available from: https://orkustofnun.is/gogn/unu-gtp-sc/UNU-GTP-SC-18-19.pdf [2-10-2019].

Haizlip, J. 2016. Best practices in geothermal operations and maintenance- Reservoir monitoring and management. [Internet]. Available from: https://geothermal.org/Annual_Meeting/PDFs/O&M_Workshop_2016/Reservoir_Monitoring_&_Management.pdf [15-6-2019].

Haukwa, C.B. 1984. Recent measures within Olkaria East and West fields. Kenya Power Company. Internal report. 13 pp.

Hidayat, I. 2016. Decline curve analysis for production forecast and optimization of liquid dominated geothermal reservoir. *Earth and environmental science,* **42**, 11 pp.

International Finance Corporation. 2013. Success of geothermal wells: A global study. [Internet]. Available from: https://www.ifc.org/wps/wcm/connect/topics_ext_content/ifc_external_corporate_site/sustainability-at-ifc/publications/publications_gpn_geothermal-wells [16-7-2020].

Johnson, O.W. and Ogeya, M. 2018. Risky business: developing geothermal power in Kenya. [Internet]. Available from: https://www.sei.org/wp-content/uploads/2018/10/181025b-gill-johnson-kenya-geothermal-transrisk-db-1810g-1.pdf [24-08-2019].

Karanja, J. and Ngare, I. 2016. Climate change resilient geothermal production in Eburru and Olkaria, Nakuru County, Kenya. *Imperial journal of interdisciplinary research,* **2**(12), pp. 971-978.

Karingithi, C.W. 2000. Geochemical characteristics of the Greater Olkaria geothermal field, Kenya. **9**. [Internet]. Available from: https://orkustofnun.is/gogn/unu-gtp-report/UNU-GTP-2000-09.pdf [10-05-2019].

Karingithi, C.W. 2002. Hydrothermal mineral buffers controlling reactive gases concentration in the Greater Olkaria geothermal system, Kenya. MSc thesis. University of Iceland.

Kemboi, E. 2015. Evaluation of groundwater hydrogeochemical characteristics and mixing behavior in Olkaria geothermal systems, Naivasha Kenya. [Internet]. Available from: http://agid.theargeo.org/reports/Kenya/Evaluation%20of%20Groundwater%20Hydrogeochemical%20Characteristics%20and%20Mixing%20Behaviour%20in%20Kenya.pdf [6-10-2019].

Kenya power and lightning company. 2009. Environmental and impact assessment of the proposed Kisumu-Lessos-Olkaria transmission line upgrading project. [Internet]. Available from: https://www.ketraco.co.ke/opencms/export/sites/ketraco/projects/downloads/Olkaria-Lessos-Kisumu/Olkaria_Lessos_Kisumu_ESIA_VolI_report_22Dec09_Part1.pdf [10-5-2019].

Koech, V.K. 2011. Initial conditions of wells OW 905A, OW 907A, OW 913A and OW 916A and a simple natural state model of Olkaria domes geothermal fields, Kenya. **17**. [Internet]. Available from: https://orkustofnun.is/gogn/unu-gtp-report/UNU-GTP-2011-17.pdf [6-5-2019].

Kollikho, P. and Kubo, B. 2001. Olkaria geothermal gaseous emissions and their effects to the environment- a flower trail case study. KenGen technical proceedings. 57-64 pp.

Lagat, J.K. 1995. Borehole geology and hydrothermal alteration of well OW-30, Olkaria geothermal field, Kenya. **6**. [Internet]. Available from: https://orkustofnun.is/gogn/unu-gtp-report/UNU-GTP-1995-06.pdf [18-6-2019].

Lagat, J.K. 2004. Geology, hydrothermal alteration and fluid inclusion studies of Olkaria domes geothermal field, Kenya. MSc. thesis. University of Iceland.

Lichoro, C.M. 2009. Joint 1-D inversion of Tem and MT data from Olkaria domes geothermal area, Kenya. **16**. [Internet]. Available from: https://www.researchgate.net/publication/267769000_JOINT_1-D_INVERSION_OF_TEM_AND_MT_DATA_FROM_OLKARIA_DOMES_GEOTHERMAL_AREA_KENYA [21-6-2019].

Lukman, A.P. 2003. Regional impact of climate change and variability of water resources- case study, Lake Naivasha basin, Kenya. MSc thesis. International institute for aerospace survey and earth science.

Mabwa, E.S. 2010. Olkaria III geothermal power generation project-Kenya. [Internet]. Available from: https://www.geothermal-energy.org/pdf/IGAstandard/WGC/2010/0244.pdf [9-5-2019].

Mariara, J. M. 2012. Response of Olkaria east field reservoir to production. **SGP-TR-194**. [Internet]. Available from: https://pangea.stanford.edu/ERE/pdf/IGAstandard/SGW/2012/Mariaria.pdf [22-03-2019].

Mariita, N.O. 1986. Schlumberger vertical soundings: techniques and interpretations with examples from Krisuvik and Glerardalur, Iceland and Olkaria, Kenya. [Internet]. Available from: https://orkustofnun.is/gogn/unu-gtp-report/UNU-GTP-1986-05.pdf [10-7-2019].

Marini, L. 2004. Geochemical techniques for the exploration and exploitation of geothermal energy. [Internet]. Available from: http://www.appliedgeochemistry.it/doc/Geochemistry_Marini.pdf [1-10-2019].

Marshall, A.S., Hinton, R.W. and Macdonald, R. 1998. Phenocrystic fluorite in peralkaline rhyolites, Olkaria, Kenya Rift Valley. *Mineralogical Magazine*, **62**(4), pp. 477-486.

Mbithi, U.K. 2011. Initial conditions of wells OW-906A, OW-908, OW-910A and OW-914 and a simple natural state model of Olkaria domes geothermal field, Kenya. **22**. [Internet]. Available from:https://orkustofnun.is/gogn/unu-gtp-report/UNU-GTP-2011-22.pdf [13-7-2019].

Mertz and McLellan-Virkir. 1979. Status report on steam production. The Kenya power company Ltd., Olkaria geothermal project report.

Montalvo, F. and Axelsson, G. 2000. Assessment of chemical and physical reservoir parameters during six years of production-reinjection at Berlin geothermal field (El Salvador). [Internet]. Available from: https://www.researchgate.net/publication/267852312_ASSESSMENT_OF_CHEMICAL_AND_PHYSICAL_RESERVOIR_PARAMETERS_DURING_SIX_YEARS_OF_PRODUCTION-REINJECTION_AT_BERLIN_GEOTHERMAL_FIELD_EL_SALVADOR [10-6-2020].

Muchangi, J. and Kagweni, M. 2014. Hell's Gate facing death. *The star newspaper*.

Muchemi, G.G. 1982. Stratigraphy and hydrothermal alteration of well OW-601 Olkaria geothermal field, Kenya. [Internet]. Available from:https://orkustofnun.is/gogn/unu-gtp-report/UNU-GTP-1985-06.pdf [10-7-2019].

Muchemi, G.G. 2000. Conceptual model of Olkaria geothermal field. KenGen. Internal report.

Muga, J.A. 2012. Geochemical evidence of cold fluid incursion into the Olkaria well reservoir, Naivasha, Rift valley- Kenya. MSc thesis. University of Nairobi.

Mukeu, P. and Langat, R. 2016. Olkaria (Kenya) geothermal project case study. *GRC Transactions*, **40**, pp. 85-90.

Mungania, J. 1999. Geological report of well OW-714. Kenya Power Company. Internal report.

Mutia, T. 2010. CDM projections for Kenya: towards a green geothermal economy- the case of Olkaria and Menengai geothermal power projects. **21**. [Internet]. Available from: https://orkustofnun.is/gogn/unu-gtp-report/UNU-GTP-2010-21.pdf [9-5-2019].

Mutinda, P.N. 2009. An overview of geothermal energy in Kenya. MSc. Thesis. University of Nairobi.

Mwangi, M.N. 1982. Two-dimensional interpretation of schlumberger soundings and head-on data with examples from Eyjafjordur Iceland and Olkaria Kenya. [Internet]. Available from: https://orkustofnun.is/gogn/unu-gtp-report/UNU-GTP-1982-09.pdf [11-7-2019].

Mwarania, F.M. 2014. Reservoir evaluation and modelling of the Eburru geothermal system, Kenya. MSc. thesis. University of Iceland. 67 pp.

Naylor, W.I. 1972. The geology of Eburru and Olkaria geothermal prospects. Kenya Power Company. Project report. 58 pp.

Odongo, M.E. 1993. A geological review of Olkaria geothermal reservoir based on structure. [Internet]. Available from: https://www.geothermal-energy.org/pdf/IGAstandard/NZGW/1993/Odongo.pdf [20-6-2019].

Ofwona, C.O. 2002. A reservoir study of Olkaria east geothermal system, Kenya. MSc. Thesis. University of Iceland.

Ofwona, C.O. 2005. Resource assessment of Olkaria I geothermal field, Kenya. [Internet]. Available from: https://www.semanticsholar.org/paper/Resource-Assessment-of-Olkaria-I-Geothermal-Field%2C-Ofwona/887039fbbfc1654e826dcbbf43635a320ea1d492 [16-10-2020].

Ofwona, C.O. 2011. Reservoir response to twenty-eight years of production at Olkaria I, Kenya. **SGP-TR-191**. [Internet]. Available from: https://pangea.stanford.edu/ERE/pdf/IGAstandard/SGW/2011/ofwona.pdf [22-03-2019].

Ogola, P.F.A. 2004. Appraisal drilling of geothermal wells in Olkaria domes (IV), Kenya-baseline studies and socioeconomic impacts. **13**. [Internet]. Available from: https://orkustofnun.is/gogn/unu-gtp-report/UNU-GTP-2004-13.pdf [6-5-2019].

Ogoso-Odongo, M.E. 1986. Geology of Olkaria geothermal field. *Geothermics*, **15**, pp. 741-748.

Okoo, J.A. 2013. Borehole geology and hydrothermal alteration mineralogy of well OW-39A, Olkaria geothermal project, Naivasha, Kenya. **24**. [Internet]. Available from: https://orkustofnun.is/gogn/unu-gtp-report/UNU-GTP-2013-24.pdf [21-03-2019].

Omenda, P.A. 1994. Geological control on the reservoir characteristics of Olkaria west geothermal field, Kenya. **19**. [Internet]. Available from: https://pdfs.semanticscholar.org/f5ed/b04fea2256bde2d265e27fcba9a4d0131d5c.pdf?_ga=2.90475482.1724713644.1566804676-996987484.1566804676 [3-5-2019].

Omenda, P.A. 1998. The geology and structural controls of the Olkaria geothermal system, Kenya. *Geothermics*, **27**(1), pp. 55-74.

Omenda, P.A. 2000. Anatectic origin for comendite in Olkaria geothermal field, Kenya rift: geochemical evidence for syenitic protholith. *African journal of science and technology*: Science and Engineering series. **1**, pp. 39-47.

Omenda, P.A. and Simiyu, S. 2015. Country update report for Kenya 2010-2014. [Internet]. Available from: https://www.geothermal-energy.org/pdf/IGAstandard/WGC/2015/01019.pdf [8-5-2019].

Onacha, S.A. 1989. An electrical resistivity study of the area between Mt. Suswa and the Olkaria geothermal field, Kenya. MSc. thesis. University of Nairobi.

Opondo, K.M. 2007. Corrosive species and scaling in wells at Olkaria, Kenya and Reykjanes, Svartsengi and Nesjavellir, Iceland. MSc. thesis. University of Iceland.

Ouma, P.A. 1992. Steam gathering system for the NE-Olkaria geothermal field, Kenya-preliminary design. **9**. [Internet]. Available from: https://orkustofnun.is/gogn/unu-gtp-report/UNU-GTP-1992-09.pdf [9-7-2019].

Ouma, P.A. 2008. Geothermal exploration and development in the Olkaria geothermal field. [Internet]. Available from: https://orkustofnun.is/gogn/unu-gtp-sc/UNU-GTP-SC-15-1207.pdf [22-03-2019].

Ouma, P.A., Koech, V. and Mwarania, F. 2016. Olkaria geothermal field reservoir response after 35 years of production (1981-2016). [Internet]. Available from: http://theargeo.org/fullpapers/Olkaria%20Geothermal%20Field%20reservoir%20response%20after%2035%20%20years%20of%20production.pdf [24-08-2019].

Pratama, H. 2015. The evolution of liquid dominated geothermal reservoir under exploitation and sustainability: A review. 4th ITB Geothermal workshop. [Internet]. Available from: https://researchgate.net/publication/313161141_THE_EVOLUTION_OF_LIQUID_DOMINATED_GEOTHERMAL_RESERVOIR_UNDER_EXPLOITATION_AND_SUSTAINABILITY_A_REVIEW [22-7-2020].

Razzano, F. and Cei, M. 2015. Geothermal power generation in Italy 2010-2014 update report. [Internet]. Available from: https://pangea.stanford.edu/ERE/db/WGC/papers/WGC/2015/01075.pdf [7-7-2019].

Regalado, J.R. 1981. A study of the response to exploitation of the Svartsengi geothermal field, SW Iceland. [Internet]. Available from: https://orkustofnun.is/gogn/unu-gtp-report/UNU-GTP-1981-07.pdf [16-6-2019].

Requejo, R.A. 1996. Monitoring of production decline and pressure drawdown in geothermal reservoirs using decline curves analysis method. **14**. [Internet]. Available from: https://orkustofnun.is/gogn/unu-gtp-report/UNU-GTP-1996-14.pdf [16-03-2019].

Reyes, J.L.P., Li, K. and Horne, R.N. 2006. A new decline curve analysis applied to the Geysers geothermal field. *GRC Transactions*. **30**. 9 pp.

Ripperda, M. and Bodvarsson, G.S. 1987. Decline curve analysis of production data from the Geysers geothermal field. **SGP-TR-109**. [Internet]. Available from: https://www.researchgate.net/publication/242134941_Decline_Curve_Analysis_of_Production_Data_from_the_Geysers_Geothermal_Field [22-03-2019].

Sanyal, S.K., Butler, S.J., Brown, P.J., Goyal, K. and Box, T. 2000. An investigation of productivity and pressure decline trends in geothermal steam reservoirs. [Internet]. Available from: http://www.geothermex.com/files/Sanyal_2000-5.pdf [9-6-2020].

Sasradipoera, D.S., Sujata, I. and Komaruddin, U. 2000. Evaluation of steam production decline rends in the Kamojang geothermal field. [Internet]. Available from: http://www.geothermal-energy.org/pdf/IGAstandard/WGC/2000/R0540.PDF [22-03-2019].

Shackleton, R.M. 1986. Precambrian collision tectonics in Africa in Coward M.P. and Ries A.C. ed. *Collision tectonics. Geological society special publications*, **19**, pp. 329-349.

Shterev, D. 1994. Assessment of the Olafsfjordur low temperature geothermal field, N-Iceland. **12**. [Internet]. Available from: https://orkustofnun.is/gogn/unu-gtp-report/UNU-GTP-1994-12.pdf [14-7-2019].

Sigfusson, B. and Gunnarsson, I. 2011. Scaling prevention experiments in the Hellisheidi power plant, Iceland. **SGP-TR-191**. [Internet]. Available from: https://pangea.stanford.edu/ERE/pdf/IGAstandard/SGW/2011/sigfusson.pdf [5-10-2019].

Sikes, H.L. 1935. Notes on the hydrology of Lake Naivasha. *Journal of East Africa Uganda natural history society*, **13**, pp. 74-89.

Simiyu, S.M. and Keller, G.R. 2000. Seismic monitoring of the Olkaria geothermal area, Kenya rift valley. *Journal of Volcanology and geothermal research*, **95**, pp. 197-208.

Simiyu, S.M., Omenda, P.A., Keller, G.R. and Anthony, E.Y. 1995. Geophysical and geological evidence for the occurrence of shallow magmatic intrusions in the Naivasha sub-basin of the Kenya rift. *AGU meeting*, **F657** (V21A-2).

Sombroek, W.G., Braun, H.M.H. and Pour, B.J.A. van der. 1982. Exploratory soil map and agro-climatic zone map of Kenya. Kenya soil survey. **E1**. [Internet]. Available from: http://library.wur.nl/WebQuery/wurpubs/487553 [5-5-2019].

Stănășel, O. 1996. Assessment of production characteristics of geothermal fluids and monitoring of corrosion and scaling Oradea, Romania and Seltjarnarnes, Iceland. **16**. [Internet]. Available from: https://orkustofnun.is/gogn/unu-gtp-report/UNU-GTP-1996-16.pdf [17-6-2019].

Thorhallsson, S. 2012. Common problems faced in geothermal generation and how to deal with them. [Internet]. Available from: https://www.researchgate.net/publication/265063576_Common_problems_faced_in_geothermal_generation_and_how_to_deal_with_them [5-10-2019].

Truesdell, A.H., D'Amore, F. and Nieva, D. 1984. The effects of localized boiling on fluid production at Cerro Prieto. *GRC Transactions*, **8**, pp. 223-229.

Ungemach, P. and Antics, M. 2010. The road ahead toward sustainable geothermal development in Europe. [Internet]. Available from: https://www.researchgate.net/publication/288712132_The_road_ahead_toward_sustainable_geothermal_development_in_Europe [10-6-2020].

United Nations Development Program. Sustainable Development Goals [Internet]. Available from: https://www.undp.org/content/undp/en/home/sustainable-development-goals.html [31-08-2019].

Wamalwa, R. 2015. The initial-state geochemistry as a baseline for geochemical monitoring at Olkaria domes, Kenya. *GRC Transactions*, **39**, pp. 255-258.

Wamalwa, R.N. 2017. Evaluation of the geothermal energy potential of the Olkaria geothermal field Kenya, based on geochemical data- a numerical model. Ph.D. thesis. University of Nairobi.

Wamalwa, R.N., Waswa, A.K., Nyamai, C.N., Mulwa, J. and Ambusso, W.J. 2016. Evaluation of the factors controlling concentration of non-condensable gases and their possible impact on the performance of geothermal systems: case study of Olkaria wells in the Kenyan rift valley. *International journal of geosciences***,** **7**, pp. 257-279.

Wambugu, J.M. 1996. Assessment of Olkaria-North-east geothermal reservoir, Kenya based on well discharge chemistry. **20**. [Internet]. Available from: https://orkustofnun.is/gogn/unu-gtp-report/UNU-GTP-1996-20.pdf [8-7-2019].